



TECHNICKÁ UNIVERZITA V LIBERCI  
Fakulta textilní



# Multifunkční bavlněná textilie s celulózou plněnou nano TiO<sub>2</sub>

## Disertační práce

*Studijní program:* P3106 – Textile Engineering  
*Studijní obor:* 3106V015 – Textile Technics and Materials Engineering  
*Autor práce:* **Bandu Madhukar Kale**  
*Vedoucí práce:* prof. Ing. Jiří Militký, CSc.





# Multifunctional Cotton Fabric with Nano TiO<sub>2</sub> Loaded Cellulose

## Dissertation

*Study programme:* P3106 – Textile Engineering  
*Study branch:* 3106V015 – Textile Technics and Materials Engineering  
*Author:* **Bandu Madhukar Kale**  
*Supervisor:* prof. Ing. Jiří Militký, CSc.



## Prohlášení

Byl jsem seznámen s tím, že na mou disertační práci se plně vztahuje zákon č. 121/2000 Sb., o právu autorském, zejména § 60 – školní dílo.

Beru na vědomí, že Technická univerzita v Liberci (TUL) nezasahuje do mých autorských práv užitím mé disertační práce pro vnitřní potřebu TUL.

Užiji-li disertační práci nebo poskytnu-li licenci k jejímu využití, jsem si vědom povinnosti informovat o této skutečnosti TUL; v tomto případě má TUL právo ode mne požadovat úhradu nákladů, které vynaložila na vytvoření díla, až do jejich skutečné výše.

Disertační práci jsem vypracoval samostatně s použitím uvedené literatury a na základě konzultací s vedoucím mé disertační práce a konzultantem.

Současně čestně prohlašuji, že tištěná verze práce se shoduje s elektronickou verzí, vloženou do IS STAG.

Datum:

Podpis:

## DECLARATION

I hereby declare that the material in this thesis, herewith I now submit for assessment for PhD defence is entirely my own work. I have taken precautionary measures to ensure that the work is original and does not to the best of my knowledge breach any copyright law, and hasn't been extracted from the work of others save and to the extent that such work has been cited and acknowledged within the text of this work.

The core theme of the thesis is **Multifunctional cotton fabric with nano TiO<sub>2</sub> loaded cellulose** and contains 5 original papers published in peer reviewed impact factor journals, 1 book chapter and 5 papers presented in international conferences. The ideas, development and writing up of all the papers in the report were the principal responsibility of me, the candidate working within the Department of Material Engineering, under the supervision of prof. Ing. Jiří Militký, CSc, EURING.

Name: Mr. Bandu Madhukar Kale, M.Sc.

Signature:

Student Number: T13000168

Liberec, March 2017



## TABLE OF CONTENT

<b>DECLARATION</b> .....	iv
<b>ACKNOWLEDGEMENTS</b> .....	viii
<b>ABSTRACT</b> .....	ix
<b>ABSTRAKT</b> .....	xi
<b>LIST OF FIGURES</b> .....	xiii
<b>LIST OF TABLES</b> .....	xvi
<b>LIST OF ABBREVIATIONS</b> .....	xvii
<b>LIST OF UNITS</b> .....	xviii
<b>CHAPTER 1 INTRODUCTION</b> .....	1
1.1 Background .....	1
1.2 Research problem .....	2
<b>CHAPTER 2 AIM AND OBJECTIVES</b> .....	5
<b>CHAPTER 3 LITERATURE REVIEW</b> .....	6
3.1 Cotton .....	6
3.2 Functional fabric .....	6
3.3 Self-cleaning materials .....	7
3.4 Antibacterial cotton fabric .....	9
3.5 Antifungal cotton fabric .....	11
3.6 Stiff cotton fabric .....	12
3.7 Functional nanoparticles .....	13
3.7.1 Titanium dioxide .....	15
3.7.2 Uses of Titanium dioxide .....	16
3.7.3 Photoinduced hydrophilicity by generation of light induced surface .....	18
3.7.4 Mechanism of self-cleaning and antimicrobial by Titanium dioxide .....	20
3.7.5 Methods to apply Titanium dioxide .....	21

3.8 Starching .....	21
3.9 Cellulose.....	23
3.10 Cellulose-TiO <sub>2</sub> coating.....	24
3.11 Solvents for cellulose dissolution .....	25
<b>CHAPTER 4 EXPERIMENTAL .....</b>	<b>28</b>
4.1 Materials.....	28
4.2 Cellulose coating .....	29
4.2.1 Cellulose dissolution .....	29
4.2.2 Dispersion of TiO <sub>2</sub> nanoparticles in cellulose solution.....	29
4.2.3 Padding.....	30
4.3 Dyeing with reactive dyes .....	31
4.4 Characterization and measurements .....	32
<b>CHAPTER 5 RESULTS AND DISCUSSION .....</b>	<b>41</b>
5.1 Morphology of cellulose and cellulose-TiO <sub>2</sub> coated cotton fabric .....	41
5.2 Photocatalytic degradation of orange II under UV light.....	43
5.3 Wine stain degradation .....	44
5.4 Durability of cellulose coated cotton fabric for self-cleaning ability .....	46
5.5 Rubbing effect on wine stain degradation.....	47
5.6 Stiffness.....	48
5.6.1 Stiffness of cellulose coated cotton fabric in Urea-Thiourea-NaOH.....	48
5.6.2 Stiffness of cellulose-TiO <sub>2</sub> coated cotton fabric in 60% Sulfuric acid .....	51
5.7 Durability of stiffness against washing of cellulose-TiO <sub>2</sub> coated cotton fabric ....	52
5.8 Antibacterial activity of cellulose-TiO <sub>2</sub> coated cotton fabric.....	53
5.9 Evaluation of Antifungal activity of cellulose-TiO <sub>2</sub> coated cotton fabric .....	57
5.10 Investigation the effect of cellulose-TiO <sub>2</sub> coating and strong solvent on cellulose structure by X-ray diffraction patterns .....	59
5.10.1 Effect of cellulose-TiO <sub>2</sub> coating and 60% Sulfuric acid on structure of cellulose .....	59
5.10.2 Effect of NaOH-Urea-Thiourea solvent system on cellulose structure .....	62
5.11 Colour strength and related parameter.....	65
5.12 Evaluation of fastness properties.....	67

5.13 Mechanical properties .....	70
5.14 Air and water vapor permeability .....	71
<b>CHAPTER 6 CONCLUTIONS</b> .....	<b>73</b>
6.1 Morphology and X-ray diffraction .....	73
6.2 Photocatalytic self-cleaning .....	73
6.3 Stiffness.....	74
6.4 Antibacterial and antifungal activity.....	74
6.5 Mechanical and comfort properties .....	74
6.6 Dyeing.....	74
<b>CHAPTER 7 APPLICATIONS AND FUTURE WORK</b> .....	<b>75</b>
<b>REFERENCES</b> .....	<b>78</b>
<b>LIST OF PUBLICATIONS</b> .....	<b>90</b>

## ACKNOWLEDGMENTS

First and foremost, I would like to express my sincere respect and appreciation to my supervisor Prof. Ing. Jiri Militky, CSc. EURING, for his inspiration, guidance and giving me an opportunity to work under his kind supervision. I want to say special thanks to Prof. Ing. Jakub Wiener, PhD for his time-to-time suggestions and help during my entire research work. He has been encouraging and supportive throughout my entire time at Technical University of Liberec, and I would like to thank doc. Rajesh Mishra, PhD for his kind help and support during my entire study. In the absence of financial support, this research would not have been possible; I, therefore, thank Ing. Jana Drasarova, Ph.D (Dean of the Faculty of Textile Engineering); Ing. Gabriela Krupincova, PhD (Vice-Dean for Science and Research), Ing. Pavla Tesinova, PhD (Vice-Dean for international affairs) and Dr. Blanka Tomkova (HOD, Department of Materials Engineering) for their kind support, conference attendance and mobility funds where necessary such that this work may be done and progresses to another level.

For crystal structure analysis, there was a need of X-ray diffraction (XRD) patterns and I am grateful to Prof. Youjiang Wang, Dr Thomas Oomman, Dr David Tavakoli and Prof. Karl Jacob for providing chemicals, testing facility and their help during my internship stay at School of Material Science and Engineering Georgia Institute of Technology, Atlanta, USA.

I would like to say a big thank you to my work colleagues in the department especially Samson Rwawiire and Abdul Jabbar who we always shared the perils of doctoral research. I would also like to thank Ing. Hana Cesarová Netolická, Kateřina Štruplová, Ing. Hana Musilová, Bohumila Keilová, Martina Čimburová and Jana Grabmüllerová for their regular help and support. I want to say special thanks to Dr Anasuya Sahoo for her constant support and guidance in my personal and professional carrier.

Finally yet importantly, where I am today is only because of the prayers of my parents and best wishes of brothers, sisters, uncles, aunts, sister in-laws, nieces and nephew.

Bandu Madhukar Kale

## **ABSTRACT**

Cotton is a leading textile fibre due to its unique properties such as hydrophilicity, biodegradability, durability, good dyeability, and relatively low cost. However, now a day's people want cotton fabric to be smart, which can give comfort according to weather conditions. Self-cleaning, antibacterial, antifungal and permanently stiff textiles are becoming important due to market demand, and broad research is being done in this areas. Nanoparticles such as Titanium dioxide (TiO<sub>2</sub>), Zinc oxide (ZnO), Copper oxide (CuO), Silver (Ag), Carbon nanotubes (Singlewalled carbon nanotubes (SWCNTs), Multiwalled carbon nanotubes (MWCNTs) show excellent functional activity towards light. Nano TiO<sub>2</sub> is the most environment-friendly and relatively cheap among all other nano particles. TiO<sub>2</sub> can be applied on different substrates such as activated carbon, stainless steel and glass. Researchers have coated TiO<sub>2</sub> on cotton fabric by various methods such as in-situ suspension polymerization with nano TiO<sub>2</sub>-acrylatecopolymer and functionalizing cotton fabric with nano sized TiO<sub>2</sub>. However, they do not claim that fabric is stable against washing.

In this thesis, a new route to make cotton fabric self-cleaning and permanently stiff by coating cellulose-TiO<sub>2</sub> on its surface is demonstrated. Cellulose solution was prepared by dissolving 10% cellulose in aqueous sulphuric acid (60%) or Sodium hydroxide-Urea-Thiourea solvent system. TiO<sub>2</sub> with different concentrations (1, 3, 5 and 10 % TiO<sub>2</sub> on the weight of cellulose) was dispersed in cellulose solution and coated on the surface of cotton fabric by padding machine. The surface morphologies of pure cotton fabric, cellulose and cellulose-TiO<sub>2</sub> coated cotton fabric were observed on scanning electron microscope (SEM). Simulation method was developed to quantify amount of cellulose II by using X-ray diffraction patterns on Mercury software. Effect of cellulose coating on dyeing was investigated with Reactive dyes.

Self-cleaning ability of cellulose-TiO<sub>2</sub> coated cotton fabric was investigated with Orange II dye and wine stain under UV light. Antibacterial and antifungal activity was studied according to international standards. Results revealed that samples coated with more than 3% TiO<sub>2</sub> showed strongest inhibition efficiency against Staphylococcus aureus (SA), Methicillin resistant Staphylococcus aureus (MRSA) bacteria's. Antifungal testing results showed that the photo-catalytic activity of titanium dioxide nanoparticles allows a disinfection of cotton fabric from fungal colonization. The amount of cellulose II in cotton fabric increased slightly after solvent treatment. However, breaking strength also increased by cellulose coating. Air and water vapor permeability were hardly affected. The stiffness of cellulose coated cotton fabric increased substantially. Degradation of orange II dye was increased with increasing TiO<sub>2</sub>

concentration and irradiation time. The samples coated with 1, 3 and 5% TiO<sub>2</sub> were stable against washing up to 20 washing cycles for both self-cleaning and stiffness properties. However, 10% TiO<sub>2</sub> coated sample does not show similar stability against washing due to poor dispersion of TiO<sub>2</sub> in cellulose solution.

**Keywords:** Cotton fabric, cellulose, self-cleaning, stiffness, antibacterial, antifungal, Titanium dioxide.

## ABSTRAKT

Bavlna je díky svým jedinečným vlastnostem jako je hydrofilita, biodegradabilita, trvanlivost, dobrá barvitelnost a relativně nízká cena významným textilním materiálem. Dnes však lidé očekávají od bavlněné tkaniny i další vlastnosti, díky nimž poskytuje bavlna komfort podle počasí. Vzhledem k požadavkům trhu roste význam samočisticích, antibakteriálních, antimykotických a nemačkových textilií, které jsou předmětem rozsáhlého výzkumu. Nanočástice jako TiO<sub>2</sub>, ZnO, oxid měďnatý, Ag nebo uhlíkové nanotrubic (SWCNTs nebo MWCNTs) vykazují vynikající funkcionalizační aktivitu na světle. Nanočástice oxidu titaničitého jsou nejšetrnější k životnímu prostředí a ve srovnání s ostatními nanočásticemi i relativně levné. TiO<sub>2</sub> lze aplikovat na různé substráty jako je aktivní uhlí, nerezová ocel nebo sklo. Výzkumníci aplikují TiO<sub>2</sub> na bavlněné tkaniny různými způsoby, jako je in situ suspenzní polymerace s nano TiO<sub>2</sub>-akrylátovým kopolymerem a funkcionalizace bavlněné tkaniny nanočásticemi TiO<sub>2</sub>. Nicméně tyto tkaniny nejsou odolné v praní.

Tato práce se zabývá přípravou samočisticí ztužené bavlněné tkaniny potažené celulózu a TiO<sub>2</sub>.. Celulóзовý roztok se připraví rozpuštěním 10% celulózy ve vodném roztoku 60% kyseliny sírové a nebo v rozpouštěcí směsi z hydroxidu sodného, močoviny a thiomčoviny. TiO<sub>2</sub> o různých koncentracích (1, 3, 5 a 10% TiO<sub>2</sub> z hmotnosti celulózy) se disperguje v roztoku celulózy a nanese na povrch bavlněných tkanin klocováním. Povrchová morfologie čisté bavlněné tkaniny a bavlněné tkaniny povrstvené celulózu a celulózu s TiO<sub>2</sub> byla pozorována rastrovacím elektronovým mikroskopem (SEM). Pro kvantifikaci celulózy II byla vyvinuta simulační metoda s použitím rentgenové difrakce na softwaru Mercury. Vliv celulóзовého povrstvení na barvitelnost byl zkoumán pomocí reaktivních barviv.

Samočisticí schopnost bavlněné tkaniny potažené celulózu a TiO<sub>2</sub> byla zkoumána pomocí barviva Orange II a skvrn od vína pod UV světlem. Antibakteriální a protiplísňový účinek byl testován podle mezinárodních norem. Výsledky ukázaly, že vzorky potažené více než 3% TiO<sub>2</sub> vykazovaly nejsilnější inhibiční účinek na bakterie *Staphylococcus aureus* (SA) a methicillinu rezistentní *Staphylococcus aureus* (MRSA). Protiplísňové testy ukázaly, že fotokatalytická aktivita nanočástic oxidu titaničitého umožňuje dezinfikovat bavlněnou tkaninu od kolonií plísní. Množství celulózy II v bavlněné tkanině se po ošetření rozpouštědlem mírně zvýšilo. Celulóзовý povlak také zvýšil pevnost do přetrhu bavlněné tkaniny. Prodyšnost a paropropustnost prakticky nebyly ovlivněny. Tuhost bavlněné tkaniny potažené celulózu se podstatně zvýšila. Degradace barviva Orange II se zvyšuje s rostoucí koncentrací TiO<sub>2</sub> a dobou ozařování. Pokud jde o tuhost i samočisticí vlastnosti, vzorky potažené 1, 3 a 5% TiO<sub>2</sub> byly

odolné v praní do 20 pracích cyklů. Nicméně vzorek potažený 10% TiO<sub>2</sub> nevykazoval podobnou stabilitu v praní v důsledku špatné dispergovatelnosti TiO<sub>2</sub> v roztoku celulózy.

**Klíčová slova:** bavlněná tkanina, celulóza, samočištění, tuhost, antibakteriální, protiplísňový, oxid titaničitý



## LIST OF FIGURES

Figure 1	Figure 1. Cotton bolls ready for harvest	6
Figure 2	Figure 2. Functional fabric	7
Figure 3	Lotus effect	8
Figure 4	Functional nanomaterials a) Copper oxide b) Titanium dioxide c) Zinc oxide d) Silver oxide e) Single-walled carbon nanotube f) Multi-walled carbon nanotube	14
Figure 5	Forms of Titanium dioxide	15
Figure 6.	Schematic illustration of various processes occurring after photoexcitation of pure TiO <sub>2</sub> with UV light	17
Figure 7	Schematic representation of photo-induced hydrophilicity. Electrons reduce the Ti(IV)–Ti(III) state and thereby the oxygen atoms will be ejected (creation of oxygen vacancies). Oxygen vacancies will increase the affinity for water molecules and thereby transforming the surface hydrophilic	19
Figure 8	Mechanism of self-cleaning, antibacterial and antifungal by TiO <sub>2</sub>	20
Figure 9	Representative partial structure of amylose	22
Figure 10	Representative partial structure of amylopectin	22
Figure 11.	Chemical structure of cellulose	24
Figure 12	Graphical representation of cellulose-TiO <sub>2</sub> coating.	25
Figure 13	Chemical structure of (a) Cellulose xanthate (b) Cellulose carbamate (c) Cellulose acetate and (d) Methyl cellulose	26
Figure 14	Chemical structure of (a) Ionic liquid and (b) N-methyl morpholine N-oxide	27
Figure 15	Cotton fabric used for study	28
Figure 16	Dissolution and dispersion of TiO <sub>2</sub>	29
Figure 17	Padding machine	30
Figure 18	TS5130 Vega-Tescan Scanning Electron Microscope	32
Figure 19	PANalytical X'Pert <sup>3</sup> X-ray powder diffractometer	33
Figure 20	Method to analyze photocatalytic degradation of stain by ImageJ	35
Figure 21(a)	Device TH-7	36
Figure 21(b)	Hysteresis loop of bending from device TH-7	37

Figure 22.	Scheme and photography of bending sample on device TH-7	37
Figure 23	SEM images of (a, c) uncoated cotton fabric and (b, d) cellulose-coated cotton fabric	41
Figure 24	SEM photographs of TiO <sub>2</sub> - cellulose coated cotton fabric a) Control, b) 0% TiO <sub>2</sub> , c) 1 % TiO <sub>2</sub> , d) 3% TiO <sub>2</sub> , e) 5 % TiO <sub>2</sub> , f) 10% TiO <sub>2</sub>	42
Figure 25	Degradation of Orange II under UV-visible light irradiation on cellulose-TiO <sub>2</sub> coated samples	43
Figure 26	Evaluation of orange II degradation by ImageJ	44
Figure 27	Scanned pictures of (a) Control (b) only cellulose coated and (c) TiO <sub>2</sub> -cellulose coated cotton fabric after irradiation of red wine stain under UV light	45
Figure 28	Effect of TiO <sub>2</sub> concentration on wine stain degradation	45
Figure 29	Effect of washing on stain degradation	46
Figure 30	Scanned images of wine stain degradation of rubbed samples after 15 minutes of UV irradiation	47
Figure 31	Evaluation of rubbing effect on wine stain degradation after 15 min of UV irradiation by ImageJ	48
Figure 32	Stiffness of uncoated and coated samples	49
Figure 33	Effect of cellulose concentration on stiffness of cotton fabric	50
Figure 34	Durability of only cellulose coated cotton fabric against washing	50
Figure 35	Stiffness of control, Solvent treated (Sol. Tr.), Starched, only cellulose (0% TiO <sub>2</sub> ) and cellulose-TiO <sub>2</sub> coated cotton fabric.	52
Figure 36	Durability of stiffness against washing	53
Figure 37(a)	Antibacterial activity against Staphylococcus aureus bacteria	54
Figure 37(b)	Antibacterial activity against Methicillin-resistant Staphylococcus aureus	55
Figure 38	Antifungal activity of (a) Control (b) 1% TiO <sub>2</sub> (c) 3% TiO <sub>2</sub> (d) 5% TiO <sub>2</sub> and (e) 10 % TiO <sub>2</sub> coated cotton fabric	58
Figure 39	X-ray diffraction patterns of cellulose-TiO <sub>2</sub> coated cotton fabric	60
Figure 40	Diffraction pattern of Control (red curve) and solvent (without cellulose) treated (blue curve) cotton fabric	60

Figure 41	Diffraction pattern of control cotton fabric fitted with simulated pattern	61
Figure 42	Diffraction pattern of 60 % H <sub>2</sub> SO <sub>4</sub> treated cotton fabric fitted with simulated pattern	61
Figure 43	X-ray diffraction pattern and analysis of original (Black) and regenerated (Red) cellulose pulp.	63
Figure 44	X-ray diffraction pattern and analysis of control (black) and solvent treated cotton fabric (Red).	63
Figure 45	Diffraction pattern of control cotton fabric fitted with simulated pattern.	64
Figure 46	Diffraction pattern of solvent treated cotton fabric fitted with simulated pattern	64
Figure 47	Breaking strength of control, Solvent treated (Sol. Treat.) and coated cotton fabrics.	70
Figure 48 (a)	Effect of cellulose-TiO <sub>2</sub> coating on air permeability of cotton fabric	71
Figure 48 (b)	Effect of cellulose coating on water vapor permeability of cotton fabric	72
Figure 49	Cellulose-TiO <sub>2</sub> coated cotton fabric self-cleaning applications	75
Figure 50	Stiff fabric applications	76
Figure 51	Antibacterial and antifungal applications of cellulose-TiO <sub>2</sub> coated cotton fabric	77

## LIST OF TABLES

Table 1	Amount of cellulose coating on 4 g of cotton fabric	31
Table 2	Observation of antibacterial activity by AATCC 100	56
Table 3	Quantitative evaluation of bacterial reduction	57
Table 4	Evaluation of antibacterial testing by AATCC 147	57
Table 5	Estimated of cellulose fractions	64
Table 6	Spectrophotometric analysis of dyed sample	66
Table 7	Washing and Rubbing Fastness properties assessment of dyed samples	68
Table 8	Perspiration Fastness assessment of dyed samples	69
Table 9	Mechanical properties	71

## **LIST OF ABBREVIATIONS**

AATCC	American Association of Textile Chemists and Colorists
ASTM	American Standard Testing Methods
CB	Conduction Band
CFU	Colony-forming unit
CIE	Commission Internationale de l'Elclairage
DP	Degree Of Polymerization
EC	Escherichia Coli
FWHM	Full Width Half Maximum
ISO	International Organization for Standardization
KP	Klebsiella Pneumonia
QAC	Quaternary Ammonium Compounds
MRSA	Methicillin-resistant Staphylococcus aureus
MWCNT	Multiwalled Carbon Nanotubes
PVA	Polyvinyl Alcohol
PW6	Pigment White 6
ROS	Reactive Oxygen Species
SA	Staphylococcus Aureus
SEM	Scanning Electron Microscopy
SWCNT	Singewalled Carbon Nanotubes
UV	Ultra Violet
VB	Valence Band
XRD	X-Ray Diffraction

## LIST OF UNITS

Nomenclature	Unit
Air Permeablity	l/m <sup>2</sup> /s
Bacterial/fungal concentration	CFU/ml
Breaking force	N
Cellulose content	%
Colour intensity (IamgeJ)	counts
Elongation	%
Modulus	Mpa
Porosity	%
Relative colour strength	%
Stiffness	N.m
Thickness	mm
Water vapor permeability	%

# CHAPTER 1

## INTRODUCTION

### 1.0 Prologue

This chapter briefly describes the interest in the use of functional nanoparticles coating on cotton. It goes further by revealing the statement of the problem.

### 1.1 Background

Cotton fibre is one of the most common natural and leading textile fibre due to its unique properties such as hydrophilicity, biodegradability, durability, good dyeability, and relatively low cost [1]. Despite the excellent properties of cotton fabrics, some characters like the inherently hydrophilic property, impotent antimicrobial activity, low strength and poor sensitivity to the UV light, confine their wide applications, especially in some high-end areas for medicine, personal healthcare, functional textile and self-cleaning [2-4]. Therefore, value addition to cotton by functionalization has generated considerable academic and industrial attention, not only due to their potential use in physical, thermal, biological and medical protection, but also to meet the constantly evolving demand from consumers for advanced materials. Self-cleaning fabric materials are a research area that has accumulated huge interest over the years. The original idea of self-cleaning textiles envisioned a scenario where tablecloths and men's suits shrug off coffee, tea, wine and other stains; or where large awnings, tents and other architectural structures stay spotlessly clean without requiring any washing or cleaning. Due to the remarkable developments made in this field during the last few decades, the concept of self-cleaning widened to include apparel that cleanses itself of body odour, curtains that rid themselves of tobacco odours to stay 'ever fresh', and hospital sheets that disinfect themselves to reduce the incidence of cross infections[5].

A strategy that is commonly adopted for the purpose of self-cleaning is to modify the textile surface with photocatalytic nanoparticles such as Titanium dioxide (TiO<sub>2</sub>) and Zinc oxide (ZnO) [6, 7]. TiO<sub>2</sub> as a cheap, nontoxic, highly efficient, stable, and ecologically friendly photo catalyst, has been proved to be an excellent catalyst in the degradation of organic pollutants [8]. Cotton fabric is widely used in the apparel and household fields because of its good hygroscopicity, moisture regain and heat-resistant quality [9]. However, because of its poor stiffness and crease recovery, its application is restricted in some situations. As a differential fabric, stiff cotton fabric is important to many industries, such as applications to suit jackets, curtains and luggage. For comfort in hot environment people prefer to have some distance

between skin and cloth and that why most of the Asian and African countries use stiff cotton fabric due to high temperature. Starch is mainly being used to make cotton fabric stiff. However, it does not give permanent effect. Cellulose is not soluble in water so it can replace starch if it is coated on the surface.

Antibacterial activity is very interesting and demanding properties of cotton fabrics [10-13]. In recent years, the commercial market for antibacterial fibers has grown rapidly due to the increased need of consumers. Polymeric materials, such as cotton, wool and flax, provides an excellent substrate for bacteria growth because they are contaminated easily with microorganisms under the appropriate environmental conditions [14]. Microbial proliferation eventually causes damage to the fiber materials and induces human infections [15]. Nano particles like TiO<sub>2</sub>, ZnO, CuO, Ag, carbon nanotubes etc. show excellent antibacterial activity. TiO<sub>2</sub> is most environment-friendly [16] among all other nano particles and shows multifunctional ability, that's why it was selected for coating with cellulose. There are several methods and techniques researchers have introduced to make cotton fabric functional by coating nanoparticles on the surface, in-situ polymerization, depositing nanoparticles on the surface etc. However, these methods lacking in durability. To overcome with this problem, the new route has been introduced herein to make cotton fabric multifunctional by coating cellulose-TiO<sub>2</sub> nanoparticles on the surface of cotton fabric.

## **1.2 Research Problem**

Self-cleaning and permanently stiff textiles are becoming important due to market demand, and broad research is being done in this area [5, 17, 18]. TiO<sub>2</sub> can be applied on different substrates such as activated carbon, stainless steel and glass [19]. TiO<sub>2</sub> shows extraordinary photocatalytic activity since it has a high sensitivity to light [20]. Nano TiO<sub>2</sub> has the ability to decompose dye pollutant such as Acid Orange [21], Methylene Blue [22], C.I. Acid Blue-9 [23], Methyl Orange [24, 25], Ethyl violet dye [26], C.I. Reactive Red 2 [27] and photocatalytic decomposition of some air pollutants [28]. Recently some researches have coated TiO<sub>2</sub> on cotton fabric by in-situ suspension polymerization with nano TiO<sub>2</sub>-acrylate copolymer [29] and functionalizing cotton fabric with nano sized TiO<sub>2</sub> [30]. However, durability is major concern with these methods.

Starching is commonly used for increasing stiffness of cotton fabric by applying starch [31, 32] to them. Application of starch is widely used for increasing the bending rigidity of collars and sleeves of men's shirts and the ruffles of girl's petticoats. However, that notwithstanding,



the stiffness arising from starching isn't permanent due to the fact that when the fabrics are washed, starch dissolves in water [33] therefore leading to loss of fabric stiffness, and hence a need to reapply starch after each washing cycle. Cellulose is insoluble in water, therefore coating fabrics with cellulose leads a lasting and permanent stiffness effect unlike starch which is soluble in water whose stiffness is temporary [34]. In recent years, researchers have been trying to make cotton fabric self-cleaning and antibacterial in different ways such as: antibacterial finishing of cotton by microencapsulation[12], by synthesizing Photo bactericidal porphyrin-cellulose nanocrystals [35], Treating cotton fabric by SBA-15-NH<sub>2</sub>/polysiloxane hybrid containing tetracycline [36], plasma treatment and ZnO/Carboxymethyl chitosan composite finishing [37], self-cleaning by copper (II) porphyrin/ TiO<sub>2</sub> visible-light photocatalytic system [20], coating with nano TiO<sub>2</sub>-acrylate copolymer [29], Nano TiO<sub>2</sub> coating after treatment of cotton fabric with carboxylic acids such as oxalic, succinic, and adipic acids [38], functionalizing cotton fabric with p-BiOI/ n-TiO<sub>2</sub> heterojunction [39], bleaching and cationized cotton using nanoTiO<sub>2</sub> [10]. However, these methods do not give durable ability to kill bacteria's.

Research elsewhere has utilized various cellulose coated substrates for various applications such as high oxygen barrier and targeted release properties cellulose [34, 40], extension of the shelf life of rainbow trout fillets [41], bioactive composite coating [42], wood coatings [43] for active packaging [44] etc. Cellulose does not melt before decomposition and is insoluble in common organic solvents. Cellulose is a highly stable compound and its stability is primarily attributed to strong intra- and intermolecular hydrogen bonding leading to a remarkably stable fibrillar structure [45]. Solvents like 60% Sulfuric acid (H<sub>2</sub>SO<sub>4</sub>) [46], Ionic Liquid [47, 48], N-Methylmorpholine N-oxide (NMMO)[49], Sodium hydroxide-carbon disulfide (NaOH-CS<sub>2</sub>) [50], Dimethyl acetate/ Lithium chloride (DMAc/ LiCl) [51] can readily dissolve cellulose. Thus, there is a scope for cellulose coating on cotton fabric after dissolution since both the molecules are same and there will be exchange of hydrogen bonding for permanent change. Due to interlinkage between coated cellulose and cotton cellulose, coated cellulose will not be washed away unlike starch. Hypothesis is that cellulose can carry nanoparticles and hold for long duration after coating with help of hydrogen bonding between coated cellulose and cotton fabric cellulose.

Coating with cellulose-TiO<sub>2</sub> addresses four main uses: self-cleaning, antibacterial, antifungal and stiffness. For coating cellulose-TiO<sub>2</sub>, Urea-Thiourea-NaOH solvent system and 60 % H<sub>2</sub>SO<sub>4</sub> solution were selected for cellulose dissolution. Urea-Thiourea-NaOH solvent system dissolves cellulose directly at -12°C [52] and 60 % H<sub>2</sub>SO<sub>4</sub> is powerful and has the ability to

breakdown cellulose chains directly. The Degree of Polymerization of cellulose decreases after dissolution in 60% H<sub>2</sub>SO<sub>4</sub> [46]. This report, therefore, presents the findings of the investigation of the microstructural, self-cleaning, antimicrobial, stiffness and comfort properties of cellulose-TiO<sub>2</sub> coated cotton fabric for possible applications.

## CHAPTER 2

### AIM AND OBJECTIVES

Overall aim of this study is to develop a cellulose-TiO<sub>2</sub> coated cotton fabric and its characterization for organic stain degradation, inhibition efficiency against bacteria's, disinfection of cotton fabric from fungal colonization, stiffness, mechanical properties, X-ray diffraction, durability of cellulose-TiO<sub>2</sub> against washing and comfort properties such as air and water vapor permeability for multifunctional applications. Orange II dye and wine have been selected for investigation of self-cleaning properties and ImageJ software has been used to analyze stain degradation under UV light. The bacteriae such as Escherichia coli (EC), Klebsiella pneumonia (KP), Staphylococcus aureus (SA), Methicillin resistant staphylococcus aureus (MRSA) have been used to study antibacterial activity of coated fabric. X-ray diffraction patterns based simulation model was used to understand the effect of solvent on the structure of cellulose.

The specific objectives are as follows,

- a) investigation of morphology of cellulose-TiO<sub>2</sub> coated cotton fabric
- b) investigation of photocatalytic self-cleaning ability by degradation of orange II dye and wine stain under UV light.
- c) evaluation of antibacterial and antifungal properties of cellulose-TiO<sub>2</sub> coated cotton fabric
- d) investigation of stiffness, mechanical and comfort properties of cellulose coated cotton fabric
- e) effect of cellulose coating on dyeing, colour strength and related parameter with reactive dyes
- f) durability of cellulose-TiO<sub>2</sub> coated cotton fabric against washing.
- g) development of simulation method to quantify amount of cellulose I, II and amorphous content by X-ray diffraction.

## CHAPTER 3

### LITERATURE REVIEW

#### 3.0 Prologue

This chapter gives a broad overview of the field of research, background, underlying theories and up-to-date research that has been made in the field. The reader will familiarize him/herself to the experimental procedures which follow in the next section.

#### 3.1 Cotton

Cotton is a soft, fluffy staple fiber that grows in a boll, or protective case, around the seeds of the cotton plants of the genus *Gossypium* in the family of Malvaceae. The fiber (figure 1) is almost pure cellulose. Under natural conditions, the cotton bolls will tend to increase the dispersal of the seeds. The plant is a shrub native to tropical and subtropical regions around the world, including the Americas, Africa, and India. The greatest diversity of wild cotton species is found in Mexico, followed by Australia and Africa [53].



Figure 1. Cotton bolls ready for harvest [54]

#### 3.2 Functional cotton fabric

Cotton is one of the most abundant and widely used natural fibers on the Earth. Due its strong absorption capability, high specific surface, porous structure, biodegradability and less cost,

use of cotton has been extended from wear to technical textiles [55-57]. However, some characters like the inherently hydrophilic property, impotent antimicrobial activity, low strength and poor sensitivity to the UV light, confine their wide applications, especially in some high-end areas for medicine, personal healthcare, functional textile and self-cleaning [2-4]. Therefore, value addition to cotton by functionalization has generated considerable academic and industrial attention, not only due to their potential use in physical, thermal, biological and medical protection, but also to meet the constantly evolving demand from consumers for advanced materials (figure 2). Apart from the esthetic purpose of cotton, the value-added cotton materials have become a basis for many industrial and technical applications [58-62].

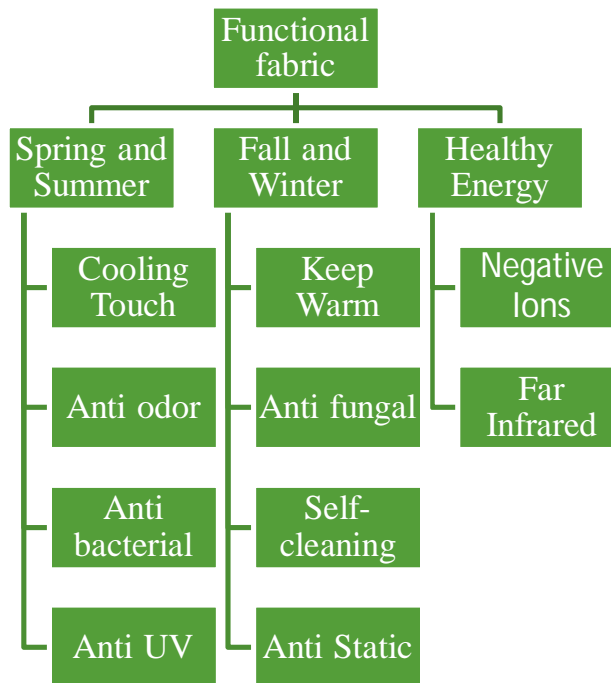


Figure 2. Functional fabric [63]

### 3.3 Self-cleaning materials

In 1975 discovered the botanists Barthlott and Neinhuis from the University of Bonn the self-cleaning capability of the Lotus flower [64]. The scientists observed that Lotus flowers get rid of mud and dirt while unfolding their leaves in the morning [65]. So they examined the leave surface structure of the Lotus with a scanning electron microscope discovering a not as expected smooth but a very rough structure (10<sup>-9</sup> nano and 10<sup>-6</sup> micro). This rough structure

is responsible for the super hydrophobic ability of the leaves. The leaf's surface has a double layer structure first it is covered by little pimples (papillae) whereupon a layer of hydrophobic wax lies. The wax prevents raindrops from getting into the pimples interspaces resulting in only 2% – 3% of the drops surface being in contact with the leaf. Additional is the contact angle at which a liquid or vapor meets a solid surface responsible for the water-repellent.

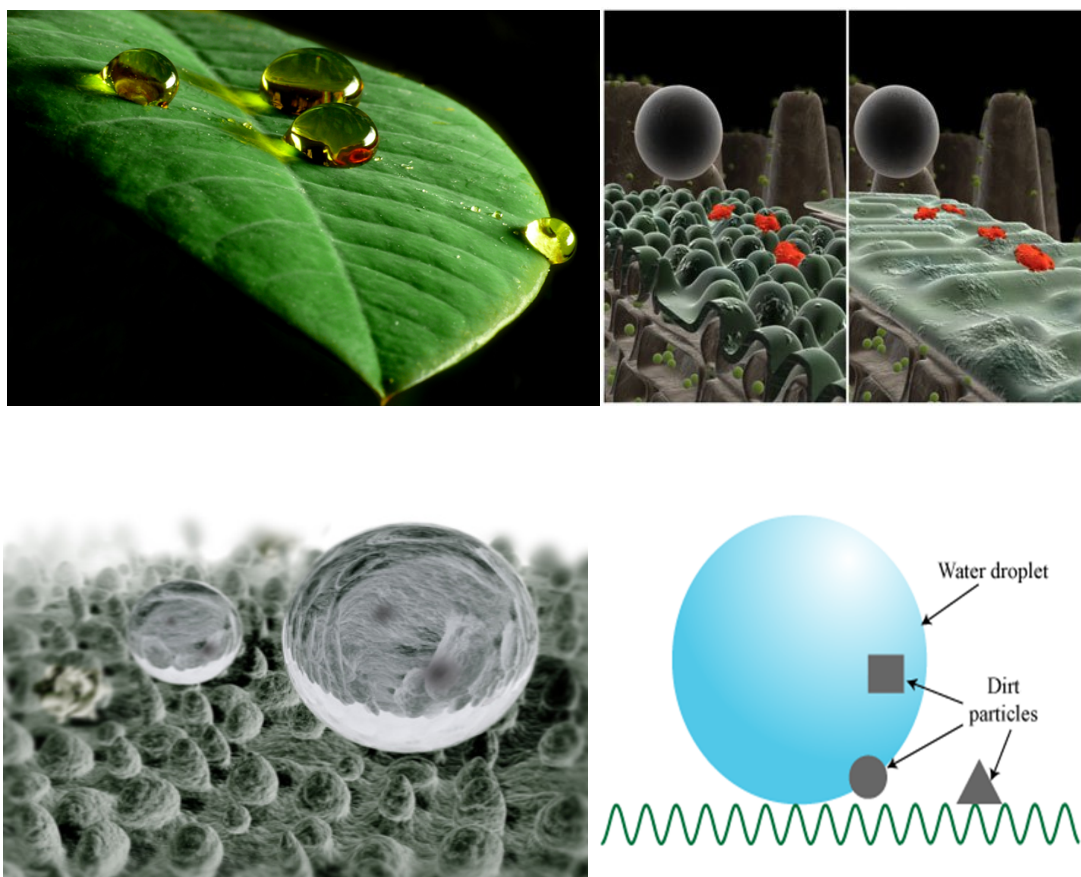


Figure 3. Lotus effect [66]

The smaller the contact angle ( $<90^\circ$ ), the flatter the droplets and the wetter the surface (figure 3). The larger the contact angle ( $>90^\circ$ ) the less the area of contact between the liquid or vapor and the solid interface, leading to a closer to dry surface. The Lotus pimples create a contact angle of over  $150^\circ$  [67]. These effects reduces the strength of adhesion and vests the lotus flower with a super hydrophobic surface. As the Lotus effect has been introduced into Bionics it has found its way to commercial use. Today we can find the Lotus effect in the textile industry producing hydrophobic cloth. Other fields of use include glass, plastics, painted surfaces,

metals and ceramics and equipped with a hydrophobic ability these products outpace competitors [68].

After understanding the phenomenon, scientists start thinking how one can mimic this "Lotus effect" (figure 3) and apply Lotus effect to our daily technology. For example, raincoats and umbrella will perform much better if one can apply Lotus effect [67]. In addition, paints incorporating the Lotus effect could keep houses and buildings clean and dry. Self-cleaning textiles are becoming important due to market demand, and broad research is being done in this area. With the increase of environment protection awareness recently, issues of the environmental pollution have become major concerns. Among these issues, the water consuming and release of wastewater during washing of materials is very important. Self-cleaning materials have attracted increasing attention. For example, the self-cleaning cotton fabrics with a life cycle of 25–50 times of washing are a class of new products classified as intelligent fabrics. About 14 million meters/year of such kind of fabrics are demanded in European Union market [69]. There is an even larger potential market in the area of Asia and Pacific. One benefit of using these self-cleaning fabrics is the resource savings on cleaning such as water and chemicals. On the other hand, the lifetime of the fabrics can be prolonged because the continuous self-cleaning of fabrics decreases the washing times of them. Such an innovation was made by depositing thin films of photoactive component on the surface of fabric. At present, the main photoactive component of self-cleaning fabrics is nano TiO<sub>2</sub> [70].

### **3.4 Antibacterial cotton fabric**

Bacterial resistance to antibiotics is a significant public health challenge, as infections caused by antibiotic-resistant bacteria claim the lives of nearly 23,000 people each year in the United States alone [71]. Recently, textiles with antiviral activity or antibacterial activity have become extremely important in the health protection of human body. The antibacterial activity of textiles can be obtained through the antibacterial finishing of textile using antibacterial agents or by incorporating them into synthetic fibers during extrusion [72]. A single pathogen, Methicillin-resistant staphylococcus aureus (MRSA), is responsible for nearly half of these fatalities. MRSA has been linked to invasive diseases including pneumonia [73] and sepsis [74], that affect a diverse population of patients including individuals with a compromised immune system such as young children. While a powerful arsenal of antibiotics was once capable of treating Staphylococcus aureus (S. Aureus) based infections, clinical isolates of MRSA have emerged to numerous antibiotics, including agents of last resort such as linezolid



and vancomycin [75, 76]. Researcher elsewhere has developed the antibacterial textile materials by incorporating, coating, depositing, treating, functionalizing, modifying with nanomaterials such as Titanium dioxide, copper, silver etc nanoparticles. The number of antibacterial agents that are suitable for textile applications on the market has increased dramatically in the past decades.

The main antibacterial agents include metals or metal salts [77-79], quaternary ammonium compounds (QACs) [80, 81] polybiguanides, [82] N-halamine, [83] chitosan, [84, 85] and triclosan [86]. These antibacterial agents have expanded greatly the use of textiles in pharmaceutical, medical, engineering, agricultural and food industries. However, most of the antibacterial agents still have some disadvantages, which limit their applications greatly. For instance, the uptake and durability of metals in textiles are the two big problems of treatment for the metal antibacterial agents. Many heavy metals are even toxic to environment. The QACs also have some inherent weakness, such as leaching from the textiles, incompatibility with the anion surfactant [87]. Dow Corning Company had produced one kind of QACs antibacterial finishing agent with alkoxysilanes (AEM 5700) for covalently binding onto the textile surface, imparting durable antibacterial activity [88]. However, the antibacterial activity of these durable QACs was also decreased or even expired because of the absorption of dirt, deadly microorganisms or complex formation between the positively charged QACs and the negatively charged anionic detergent during repeated laundering. In addition, the low antibacterial activity to epiphyte and the weak light tolerance influences the applications of polybiguanides greatly.

The bacterial resistance to triclosan has been well-documented and is of great concern. Triclosan has been banned in textiles and some other products by many countries because of its produced toxic polychlorinated dioxins upon exposure to sunlight. The chitosan tends to be environmentally friendly in the antibacterial applications. However, the antibacterial activity of chitosan is p<sup>H</sup> sensitive and limits to acidic conditions [89]. The chitosan also shows weak adhesion to cellulose fibers and is leached gradually from the fiber surface by repeated laundering. These disadvantages motivate researchers to actively explore new antibacterial agents and technologies for antibacterial textiles finishing. In addition, antibacterial efficiencies and durability, environmental friendliness, health, and safety are also important to the antibacterial agents. TiO<sub>2</sub> shows excellent photocatalytic activity towards light and has ability kill bacteria, fungi and clean the surface of material [16, 17, 90].



### **3.5 Antifungal cotton fabric**

Textile fabrics by virtue of their physicochemical characteristics and proximity to the human body are susceptible to microbial attack, as these provide large surface area and absorb moisture that aid microorganisms to grow, transfer and propagate infection. Ubiquitous microorganisms cover all surfaces in natural and artificial environments. Textiles are appealing materials for use in several medical applications, including hospital uniforms and linens; prosthetic valves; and wound dressings [91]. Microorganisms can cause problems in textile raw materials, process chemicals, during wet textile treatments, in textile and textile product warehouses during transportation, and even during the everyday usage of textile products [92]. Fungi produce at least three enzymes ('cellulase complex') of extra cellular activity during growth on exoglucanase or  $\beta$ -D-glucosydases cellulose, respectively to remove disaccharide units from the chain ends of endoglucanases or  $\beta$ -D-glucanohydrolases cellulose, respectively. And randomly break the  $\beta$ -1,4 bonds of cellulose chains; the third component is  $\beta$ -D-glucosidases, hydrolyzing cellobiose into glucose units, which are then used as a carbon source for fungal growth [93].

With the growing awareness about cleaner surroundings and healthy lifestyle, the demand for protective clothing has increased among consumers. This has created significant challenges for textile researchers and industrialists to address the issue through innovative ways. Consequently, the competitive and textile market is globally witnessing a rapid growth in the development of technical textiles and their end-uses that have generated many opportunities for the application of innovative finishes. Textiles with an antimicrobial finish and improved functionality find a variety of applications such as health, hygiene, and medical products, apart from healthy clothing. Among all textile finishes, antimicrobial finishing has become a very promising, high-growth research area due to their potential to provide quality and safety benefits to different kinds of textile materials [94].

Natural colorants from plant sources have been recently discovered as novel agents in imparting multifunctional properties to textiles such as antimicrobial, insect repellent, deodorizing, and UV protective besides imparting attractive shades. Application of natural colorants offers promise in developing antimicrobial textiles for aesthetic, hygienic, and medical applications owing to the presence of potent bioactive phytochemicals in their extracts. Substances and extracts isolated from different natural resources especially plants have always been a rich arsenal for controlling the fungal infections and spoilage. In the recent past, considerable research work has been undertaken on the application of natural dyes in coloration

and antimicrobial finishing of textiles around the globe and use of natural dyes for antimicrobial finishing of textiles has been widely reported [94].

On cotton fabric, fungal contamination starts on the cutting edge where the spores can easily reach the fibre's lumen. Hyphae sprout in the lumen and form a mycelium, which grows toward the fibre's wall, causing its degradation. The damage caused by microorganisms becomes visible with changes on the textile or fibre surface, mostly in the form of de-coloration and stains; in most cases, these changes are followed by a typically musty smell. De-coloration is mainly caused by chemical reactions between metabolites secreted by the microorganism and finishing agents or dyes in the textile material. In many cases, this leads to the production of pigment-like substances. One promising innovation is to impart these textiles with antimicrobial properties. Noble metals such as copper, gold, and silver have broad-spectrum antimicrobial activity. For example, silver has several effects on microorganisms, including impeding the electron transport system and preventing DNA replication [93].

### **3.6 Stiff cotton fabric**

Cotton fiber poor stiffness and crease recovery restricted its application in some situations. As a differential fabric, stiff cotton fabric is important to many industries, such as applications to suit jackets, curtains and luggage. Therefore, there are many reports on anti-crease finishing and stiffness finishing [9]. Starch, cyanaldehyde resin, urea formaldehyde resin, poly vinyl alcohol (PVA) and polyacrylate are widely used to improve stiffness of cotton fabric. The starch is being used for increasing the bending rigidity of collars and sleeves of men's shirts and the ruffles of girl's petticoats. However, such stiffness is not permanent, because starch dissolves in water during washing and the fabric loses its stiffness, resulting in the need to reapply starch after each laundering. Cotton fabric treated by starch slurry has poorer elasticity than the original fabric, and is not durable. Grafting of starch onto cotton fabric has been reported. Cotton fabric treated with PVA softens easily when exposed to heat, and is also not durable.

Cyanaldehyde resin and urea formaldehyde resin release formaldehyde, which is a health hazard, and the fabric strength decreases with these types of resin. In addition, the treated cotton fabric has a harsh feel, poor elasticity and high shrinkage rate. Polyacrylate is also applied to stiffness finishing of cotton. However, the finishing effect is inferior to that of cyanaldehyde resin. The treated cotton fabric is inelastic and has poor freezing resistance [95]. Currently, resin is always used as the stiffness agent for cotton fabric finishing. The stiffness agent is left

on the fabric; this increases health concerns. Thus, it is important to develop a finishing technique that can make cotton fabric stiff but leaves no auxiliary chemicals on the fabric to meet upmarket consumer demand [9].

### **3.7 Functional nanoparticles**

Recent years have witnessed the rapid development of inorganic nanomaterials for medical applications. Within the broad field of nanotechnology, which has developed rapidly over the last two decades, colloidal nanoparticles containing primarily inorganic components (herein inorganic NPs) have emerged as rich and versatile systems whose specific properties aid in medicine, be it as novel therapeutics or diagnostic tools [96]. Nanotechnology, a high-tech science and technology rapidly developed in the late 1980s, has been widely used in many fields such as raw material, chemical, textile, medicine, traffic, energy and so on. In recent years, many dyeing and finishing auxiliaries with special function and new textiles with high effective function have been produced due to the nanotechnology application in textile industry [97]. Because of this biocidal activity, metals have been widely used for centuries as antimicrobial agents in agriculture, healthcare, and industry in general.

Chemical structures of some nanoparticles which is being commonly used for functionality of material such as Titanium dioxide (TiO<sub>2</sub>), Zinc oxide (ZnO), Copper oxide (CuO), Silver (Ag), Carbon nanotubes (Singlewalled carbon nanotubes (SWCNTs) are shown in figure 4. Metal, oxide, or salt compounds based on copper and silver are among the most widely applied antimicrobial agents in this context. However, the use of these metals in industrial applications presents several challenges associated with the nature of the metal itself. Consequently, one of their first applications was in the form of salt-based additives, for instance as silver nitrate, avoiding its highly expensive metal form [97]. TiO<sub>2</sub> shows excellent photocatalytic activity towards light. TiO<sub>2</sub> is most environment-friendly among all other nano particles [16]. TiO<sub>2</sub> is being used to to apply on materials such as glass, ceramics, textile etc for self-cleaning application. It is even being used as a whitener. Nanoparticles of TiO<sub>2</sub> is stable in alkali and alkaline medium at room temperature that is why it is easy to process. Also TiO<sub>2</sub>nanoparticles has ability to kill bactrias and fungi. Due to these multiapplication approach it was selcted for coating on cotton fabric.

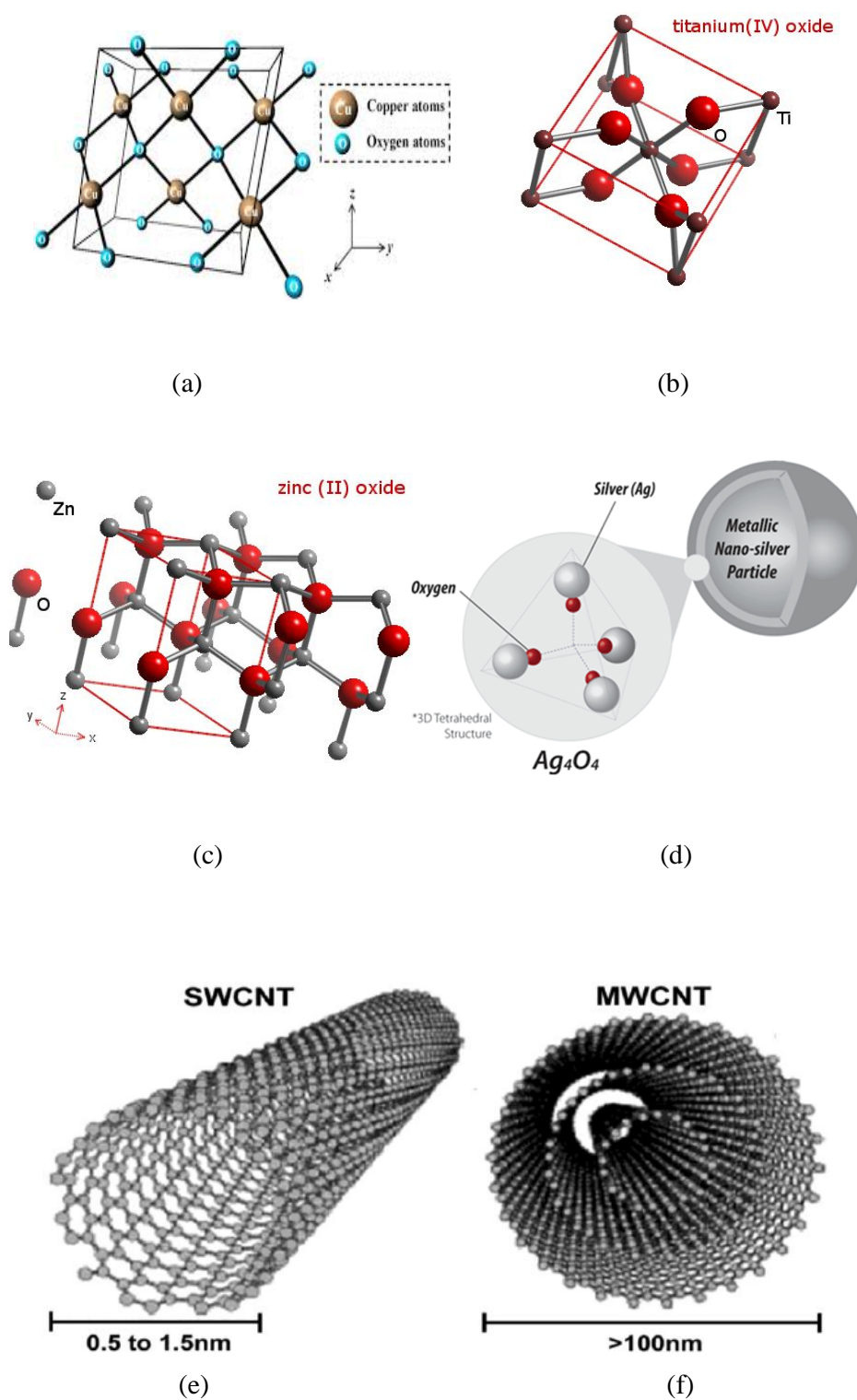


Figure 4. Functional nanomaterials a) Copper oxide b) Titanium dioxide c) Zinc oxide d) Silver oxide e) Single walled carbon nanotube f) Multi-walled carbon nanotube

### 3.7.1 Titanium dioxide

Titanium dioxide is the naturally occurring oxide of titanium. The chemical formula of titanium dioxide is TiO<sub>2</sub>. It is also known as titanium (IV) oxide or titania. When used as a pigment, it is called titanium white, Pigment White 6 (PW6), or CI 77891. It has a wide range of applications, from paint to sunscreen to food coloring [98]. When used as a food coloring, it has E number E171. World production in 2014 exceeded 9 million metric tons. Titanium dioxide (TiO<sub>2</sub>) exists as three different polymorphs; anatase, rutile and brookite [99].

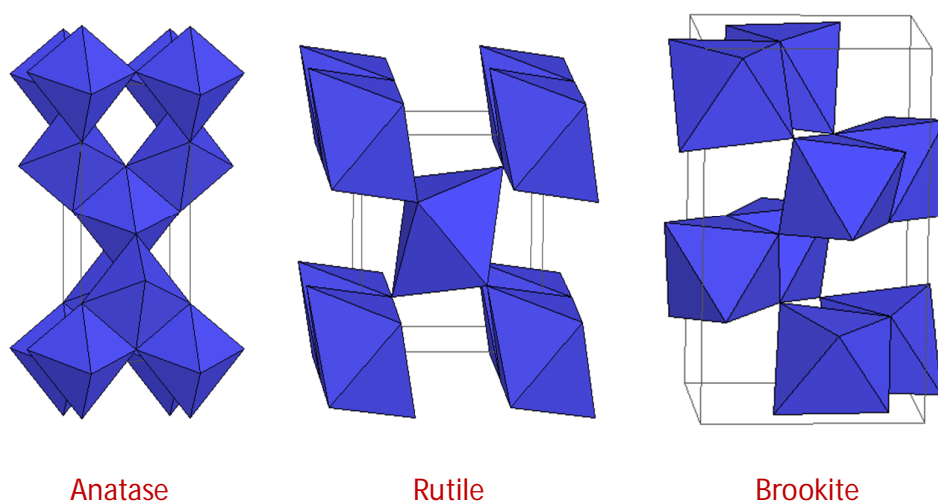


Figure 5. Forms of Titanium dioxide [100]

The primary source and the most stable form of TiO<sub>2</sub> is rutile. All three polymorphs can be readily synthesised in the laboratory and typically the metastable anatase and brookite will transform to the thermodynamically stable rutile upon calcination at temperatures exceeding ~600°C [101]. In all three forms, titanium (Ti<sup>4+</sup>) atoms are co-ordinated to six oxygen (O<sup>2-</sup>) atoms, forming TiO<sub>6</sub> octahedra. Anatase is made up of corner (vertex) sharing octahedra which form (0 0 1) planes (figure 5) resulting in a tetragonal structure. In rutile the octahedra share edges at (0 0 1) planes to give a tetragonal structure (figure 5), and in brookite both edges and corners are shared to give an orthorhombic structure (figure 5).

### **3.7.2 Uses of Titanium dioxide**

Titanium dioxide (TiO<sub>2</sub>) is the most widely used as a white pigment, for example in paints, food products, personal care products etc [98]. It has high brightness and a very high refractive index. The light passes through the crystal slowly and its path is substantially altered compared to air. If you have many small particles orientated in different directions, a high refractive index will lead to the scattering of light as not much light passes through. In lenses, high refractive index means high clarity and high polarising power. Titanium dioxide has a higher refractive index than diamond and there are only a few other substances that have a higher refractive index [102]. Cinnabar (mercury sulphide) is an example. Historically, cinnabar was used as a red pigment. In 2001, the first self-cleaning glass was brought onto the market. This type of glass is coated in a thin layer of transparent anatase. To make the coating, anatase is first combined with an organic complexing agent consisting of organic molecules which can act as ligands and bind to the titanium ion with co-ordinate bonds. This process is necessary to convert the titanium dioxide powder into a more soluble form so that it can be spread over the glass surface evenly. Once the coating is applied, the glass is heated to burn off the organic complexing agent, leaving the anatase coating.[103]

The cleaning process works in two phases;

- Photocatalytic breaking down of dirt.
- Washing off breakdown products when it rains.

The photocatalytic hydrophilic surfaces utilize sunlight/indoor light to decompose the dirt and other impurities [17]. TiO<sub>2</sub> based photocatalysts have gained considerable attention as TiO<sub>2</sub> exhibits significantly high physical and chemical stability, low cost, easy availability, low toxicity and excellent photo-activity [17]. In the presence of light of suitable energy (where, the energy of the excitation source is higher than the band-gap energy of the material), an electron ( $e^-_{CB}$ ) is excited from valence band of TiO<sub>2</sub> to the conduction band, generating a positive electron hole ( $h^+_{VB}$ ) in the valence band (figure 6). The photoexcited electron ( $e^-_{CB}$ ) can in turn recombine with the electron hole ( $h^+_{VB}$ ) and reduce the overall efficiency of the photoprocess. The charge carriers, which can escape the charge-annihilation reaction, migrate to the surface, where the photoexcited electrons can reduce atmospheric oxygen to generate superoxide radicals ( $\cdot O_2^-$ ) or hydroperoxyl radicals ( $HO_2\cdot$ ). The valence band hole can also oxidize surface adsorbed water or OH<sup>-</sup> and produce  $\cdot OH$ . These reactive oxygen species (ROS) can convert organic pollutants into CO<sub>2</sub> and water resulting in the cleaning of the surface. A major limitation in developing self-cleaning materials based on TiO<sub>2</sub> is the wide band gap of

the semiconductor, limiting its absorption to the UV region of sunlight, which comprises only 3–5% of the solar spectrum. Due to this wide band gap, utility of pure TiO<sub>2</sub> is restricted in fabrication of self-cleaning materials (e.g., glass and tiles) for outdoor application [17].

In photocatalysis, light of energy greater than the band gap of the semiconductor, excites an electron from the valence band to the conduction band (see figure 6). In the case of anatase TiO<sub>2</sub>, the band gap is 3.2 eV, therefore UV light ( $\leq 387$  nm) is required. The absorption of a photon excites an electron to the conduction band ( $e_{CB}^-$ ) generating a positive hole in the valence band ( $h_{VB}^+$ ) (Eq. 1).



Charge carriers can be trapped as Ti<sup>4+</sup> and O<sup>2-</sup> defect sites in the TiO<sub>2</sub> lattice, or they can recombine, dissipating energy. Alternatively, the charge carriers can migrate to the catalyst surface and initiate redox reactions with adsorbates. Positive holes can oxidize OH<sup>-</sup> or water at the surface to produce <sup>•</sup>OH radicals (Eq. (2)) which, are extremely powerful oxidants [104].

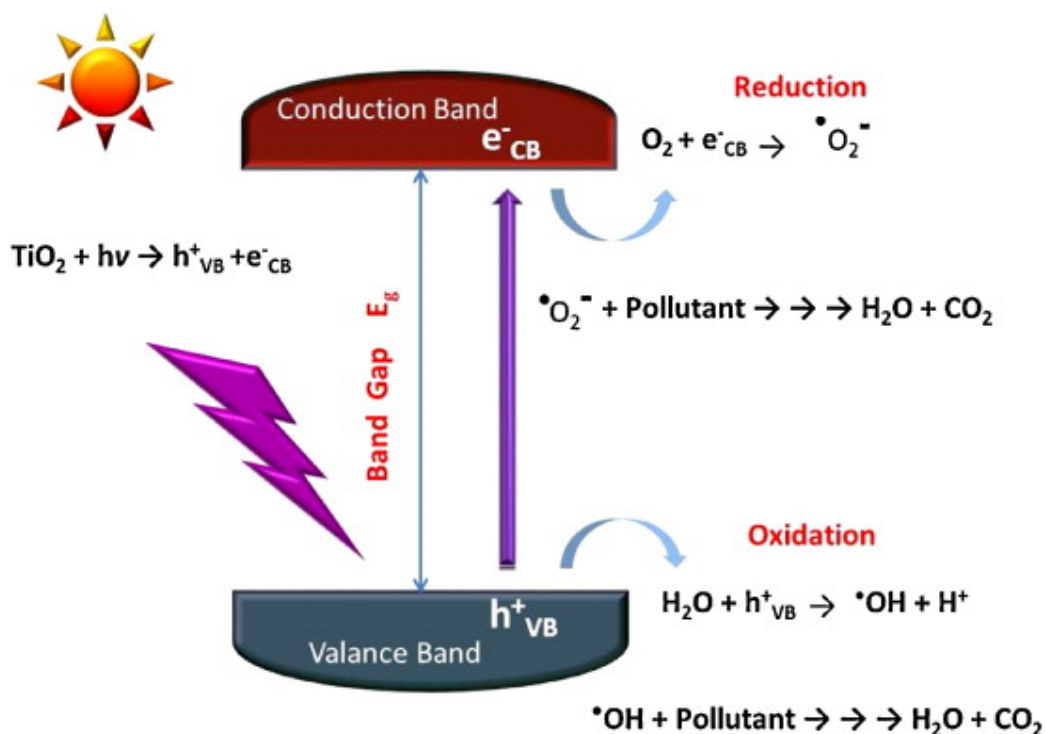
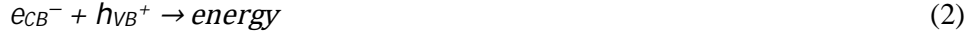


Figure 6. Schematic illustration of various processes occurring after photoexcitation of pure TiO<sub>2</sub> with UV light [104]



The hydroxyl radicals can subsequently oxidize organic species with mineralization producing mineral salts, CO<sub>2</sub> and H<sub>2</sub>O (Eq.( 5)).



Electrons in the conduction band can be rapidly trapped by molecular oxygen adsorbed on the titania particle, which is reduced to form superoxide radical anion ( $\cdot O^{2-}$ ) (Eq. (4)) that may further react with H<sup>+</sup> to generate hydroperoxyl radical ( $\cdot OOH$ ) (Eq. (6)) and further electrochemical reduction yields H<sub>2</sub>O<sub>2</sub> (Eq. (7)). These reactive oxygen species may also contribute to the oxidative pathways such as the degradation of a pollutant (Eqs. (8) and (9)).



### 3.7.3 Photo induced hydrophilicity by Generation of light induced surface vacancies

The initial and widely accepted mechanism for photo-induced hydrophilicity was proposed by Wang et al. which relies on the formation of surface defects upon UV light illumination [105]. Friction force microscopic studies suggested that UV irradiation resulted in a structural change at the TiO<sub>2</sub> surface thereby influencing the interfacial force along the solid–liquid boundary and consequently changing the contact angle. The surface of TiO<sub>2</sub> consists of five coordinated Ti atoms with the sixth position occupied by H<sub>2</sub>O or OH<sup>-</sup>. It is believed that UV irradiation creates oxygen vacancies at the two coordinated oxygen bridging sites at the surface, thereby



converting  $\text{Ti}^{4+}$  ions to  $\text{Ti}^{3+}$ . These defects can in turn increase the affinity for hydroxyl ions formed by dissociation of chemisorbed water molecules and thereby forming hydrophilic domains (figure 7). Moreover, crystal planes (1 1 0) and (1 0 0) of rutile  $\text{TiO}_2$  with bridging oxygen sites showed higher efficiency for hydrophilic conversion compared to the planes such as (0 0 1) without bridging oxygen sites [106]. Atomic force microscopic study of UV-illuminated rutile  $\text{TiO}_2$  single crystal showed that  $\text{TiO}_2$  surface consists of microscopic hydrophilic and oleophobic domains, which are believed to generate capillary flow channels for oil and water.

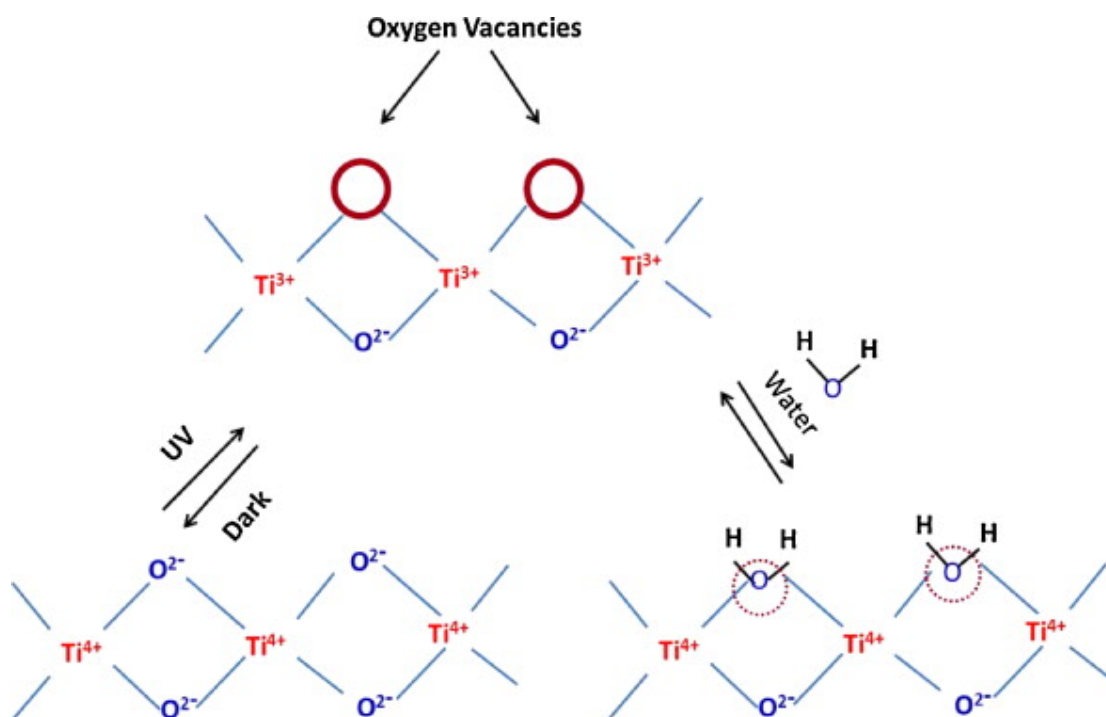


Figure 7. Schematic representation of photo-induced hydrophilicity. Electrons reduce the  $\text{Ti(IV)}\text{--Ti(III)}$  state and thereby the oxygen atoms will be ejected (creation of oxygen vacancies). Oxygen vacancies will increase the affinity for water molecules and thereby transforming the surface hydrophilic [17].

It was found that if the hydrophilic  $\text{TiO}_2$  material is stored in dark for a couple of days, the hydrophilic character gradually decrease due to slow replacement of the chemisorbed hydroxyl and water molecules by oxygen molecules from air. However, the hydrophilic nature of the surface can be retrieved by further UV illumination. Nakajima et al. demonstrated the photoinduced amphiphilic surface formation for polycrystalline anatase  $\text{TiO}_2$  thin films [107].

However, prolonged UV irradiation was shown to convert the surface into a hydrophilic–oleophobic one, which is considered to be due to variation in the rate of hydrophilic conversion of TiO<sub>2</sub> grains. Rutile TiO<sub>2</sub> exhibited photoinduced surface hardness correlated with the conversion of hydrophilic surface. This photo-induced change in surface hardness has been attributed to surface volume expansion resulting from the increase in distance between the adjacent Ti atoms arising from the dissociative adsorption of water molecules upon UV exposure.

### 3.7.4 Mechanism of self-cleaning, antibacterial and antifungal by TiO<sub>2</sub>

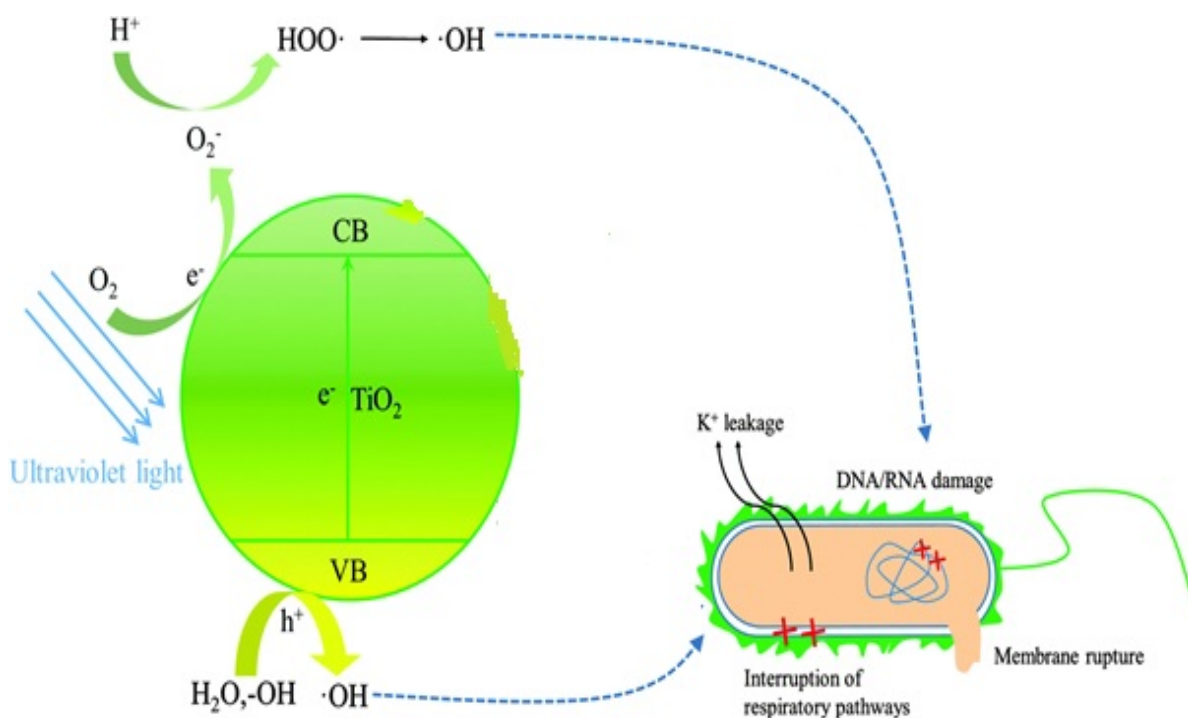


Figure 8. Mechanism of self-cleaning, antibacterial and antifungal by TiO<sub>2</sub> [108].

Figure 8 shows the mechanism of self-cleaning, antibacterial and antifungal by TiO<sub>2</sub> under UV light. The titanium dioxide, in contact with water and oxygen molecules adsorbs some radiation with an intensity of energy that is larger than the characteristic band-gap. Electrons promoted from valence to conduction band create free electrons and electron holes' pairs. These pairs produce reactive oxygen species like superoxide anions, hydroxyl radicals, and hydrogen peroxide molecules, which can oxidize organic compounds. These radicals can also

kill bacteria, viruses, fungi, and algae [109-113]. It is believed that the main cause of the biocidal effect of TiO<sub>2</sub> is a damage of the cell membrane[114] and its polyunsaturated phospholipids [115]. Titanium dioxide can be applied on various substrates like glass, stainless steel, textile materials, composites, activated carbon etc.

### **3.7.5 Methods to apply Titanium dioxide**

There are different methods to incorporate TiO<sub>2</sub> such as facile synthesis of casein-based TiO<sub>2</sub> nanocomposite[116], Platinum (IV) chloride modified TiO<sub>2</sub> and N-TiO<sub>2</sub> coatings for self-cleaning cotton fabrics[117], TiO<sub>2</sub> doped with SnO<sub>2</sub> thin films preparation by sol-gel method[118], Slightly carboxymethylated cellulose supported TiO<sub>2</sub> nanoparticles[119], finishing self-cleaning material on cotton fabric[120], coating of TiO<sub>2</sub> on cementitious materials[121]. Cellulose molecule is very stable in nature due to its strong inter and intra molecular hydrogen bonding. Solvents such as Ionic liquids[48], 60% sulfuric acid[46], Sodium Hydroxide-Carbon disulfide solvent system, can disturb hydrogen bonding and dissolve cellulose. Cellulose can be coated on cotton fabric by roller padding after dissolving in solvent. Sodium Hydroxide-Urea-Thiourea and 60% sulfuric acid were chosen to prepare the cellulose solution. TiO<sub>2</sub> nanoparticles were dispersed in the cellulose solution by stirring in order to coat on cotton fabric.

### **3.8 Starching**

Starch is the major carbohydrate reserve in plant tubers and seed endosperm where it is found as granules [122] each typically containing several million amylopectin molecules accompanied by a much larger number of smaller amylose molecules. By far the largest source of starch is corn (maize) with other commonly used sources being wheat, potato, tapioca and rice. Amylopectin (without amylose) can be isolated from 'waxy' maize starch whereas amylose (without amylopectin) is best isolated after specifically hydrolyzing the amylopectin with pullulanase [123]. Genetic modification of starch crops has recently led to the development of starches with improved and targeted functionality. Starch consists of two types of molecules, amylose (figure 9) normally 20-30% and amylopectin (figure 10) normally 70-80%. Both consist of polymers of  $\alpha$ -D-glucose units in the <sup>4</sup>C<sub>1</sub> conformation. In amylose these are linked - (1->4)-, with the ring oxygen atoms all on the same side, whereas in amylopectin about one residue in every twenty or so is also linked - (1->6)- forming branch-points. The relative proportions of amylose to amylopectin and - (1->6)- branch-points both depend on the source

of the starch, for example, amylomaizes contain over 50% amylose whereas 'waxy' maize has almost none (~3%) [124].

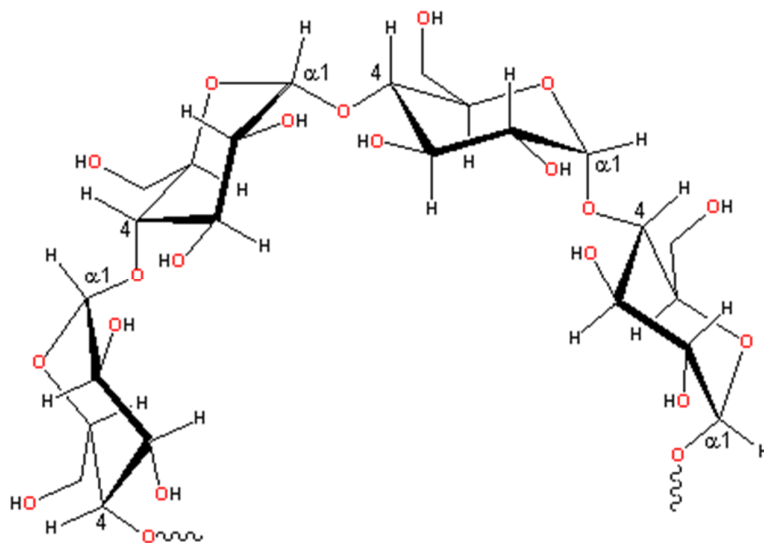


Figure 9. Representative partial structure of amylose

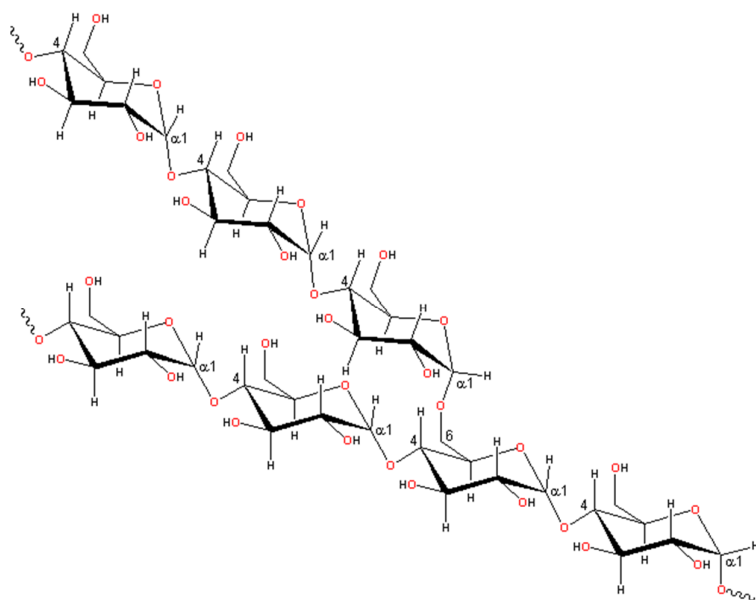


Figure 10. Representative partial structure of amylopectin

Starch is a versatile and cheap, and has many uses as thickener, water binder, emulsion stabilizer and gelling agent. Its form and functionality have recently been reviewed [125]. Starch is often used as an inherent natural ingredient but it is also added for its functionality. It is naturally found tightly and radially packed into dehydrated granules (about one water per glucose) with origin-specific shape and size (maize, 2-30  $\mu\text{m}$ ; wheat, 1-45  $\mu\text{m}$ ; potato, 5-100  $\mu\text{m}$ ). The size distribution determines its swelling functionality with granules being generally either larger and lenticular (lens-like, A-starch) or smaller and spherical (B-starch) with less swelling power. Granules contain 'blocklets' of amylopectin containing both crystalline (~30%) and amorphous areas. As they absorb water, they swell, lose crystallinity and leach amylose. The higher the amylose content, the lower is the swelling power and the smaller is the gel strength for the same starch concentration. To a certain extent, however, a smaller swelling power due to high amylose content can be counteracted by a larger granule size. Starch is widely used for increasing bending rigidity of collars and sleeves of men's shirts and the ruffles of girl's petticoats by applying starch to them [9]. However, stiffness is not permanent because during washing starch dissolves in water and fabric loses its stiffness, and results in need to reapply starch after each laundering.

### **3.9 Cellulose**

Cellulose can replace starch since it is insoluble in water and has similar kind of chemical structure like starch. Cellulose is the most abundant resource biosynthesized on earth with an annual production over  $7.5 \times 10^{10}$  tons, featuring sustainable, renewable, biodegradable, and carbon neutral [126, 127]. As a chemical raw material, cellulose and its derivatives have been widely utilized in many fields, such as papermaking, textile and pharmaceuticals [128, 129]. Generally, cellulose can be characterized as highly polymerized linear macromolecule consisting solely of 1-4-linked anhydro-d-glucose (figure 11). Particularly, the configuration at the anomeric carbon of glucose unit gives rise to a stretched chain conformation. Then, these chains are linked into flat sheets via hydrogen-bonds. The linear alignment of molecular chain enables the compact packing of numerous cellulose strands into crystalline fibrils, which makes it challenging to separate individual molecular chain and thus dissolve cellulose. Moreover, many other structural aspects have been identified, including the high molecular weight, the comparatively low flexibility of polymer chain, together with the hydrophobic surface attributed to the inferior solubility of cellulose in most solvents. Correspondingly, valorization of natural cellulose via physical and chemical conversion was severely restricted [130].

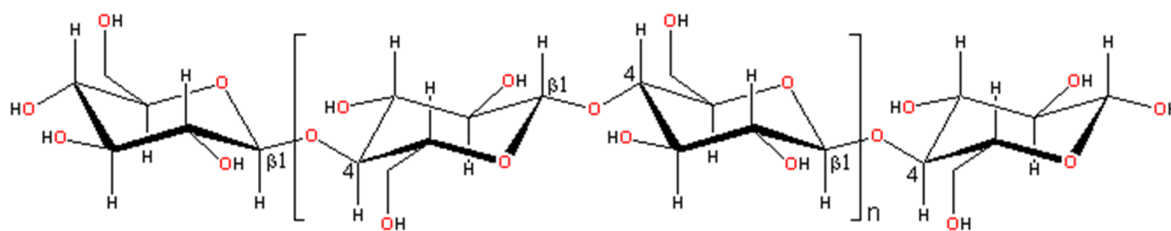


Figure 11. Chemical structure of cellulose

This natural polysaccharide has become one of the most used biomaterials due to its fascinating structural and physical properties and biocompatibility. These properties arise from the multiple hydrogen bonding interactions resulting in a semi crystalline polymer containing highly structured crystalline regions, which form materials with high tensile strength. Although Anselme Paven described applications of cellulose in 1838, the Hyatt Manufacturing Company produced the first cellulose-based thermoplastic material in 1870. This material was manufactured by treating cellulose with nitric acid to form cellulose nitrate and commercialized under the trade name “Celluloid” [131]. Cellulose is the substance that makes up most of a plant's cell walls. Since all plants make it, it is probably the most abundant organic compound on Earth. Aside from being the primary building material for plants, cellulose has many others uses. According to how it is treated, cellulose can be used to make paper, film, explosives, and plastics, in addition to having many other industrial uses. For humans, cellulose is also a major source of needed fiber in our diet.

In recent years, coating directly with cellulose, or its derivatives to achieve compatibility with the coated material, has been applied. Cellulose coating is being used for various applications such as high oxygen barrier and targeted release properties [40], extension of the shelf life of rainbow trout fillets [41], bioactive composite coating [42], wood coatings [43] for active packaging[44] etc., so cellulose can be coated on cotton fabric.

### 3.10 Cellulose-TiO<sub>2</sub> coating

Cellulose has ability to form strong intramolecular and intermolecular hydrogen bonding. However, it is possible when molecules are in one phase. After dissolution, cellulose molecules can come in one phase and form hydrogen bonding [132]. Using this theory it is possible coat cellulose on other cellulosic material. Since strong solvent being used to dissolve the cellulose, solvent molecules from cellulose solution try to interact with other cellulosic material and bring

it in one phase and form intermolecular hydrogen bonding. Due to this interchain linkage by hydrogen bonding, cellulose does not washed away with water. It is possible to disperse functional nanoparticles in cellulose solution and coat on cotton fabric so that cotton fabric becomes functional. figure 12 shows pictorial representation of this hypothesis.

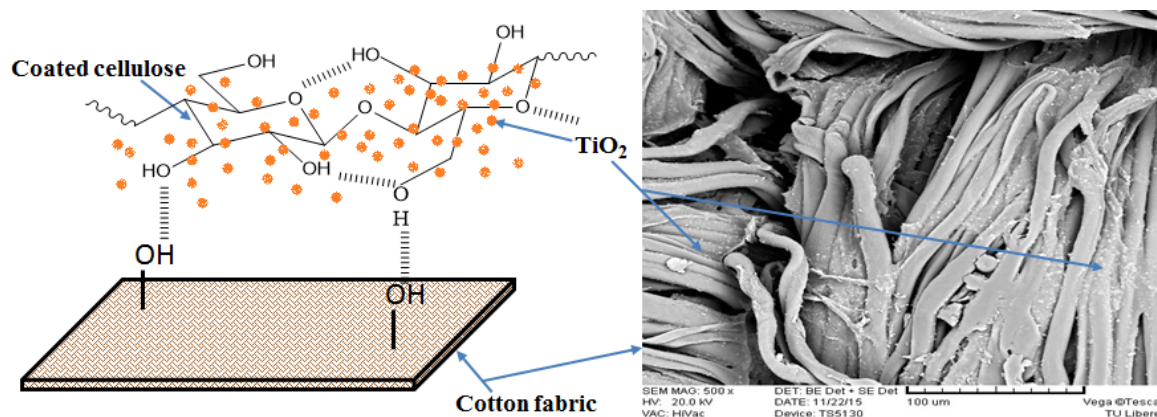


Figure 12. Graphical representation of cellulose-TiO<sub>2</sub> coating.

### 3.11 Solvents for cellulose dissolution

Cellulose has a 2-fold screw axis along the chain direction. The degree of polymerization (DP) of the macromolecule can vary from 100 to 20,000 depending on the sources [133]. Cellulose possesses a highly crystalline structure due to the presence of extensive intra- and intermolecular hydrogen bonding [132], which has been examined in great detail. Consequently this natural polymer is insoluble in water and typical organic solvents and can only be dissolved if the intra- and intermolecular hydrogen bonds are effectively disrupted. Cellulose dissolution processes can be broadly classified in two categories as will be discussed below.

#### (a) Cellulose dissolution with chemical modification

A well-known method of cellulose dissolution is by prior chemical modification of the macromolecule. The main objective of this procedure is to functionalize the hydroxyl groups so as to disrupt the intra- and intermolecular hydrogen bonds but with minimal chain degradation. Functionalization reactions of cellulose include nitration, xanthation (figure 13 (a)), esterification, (figure 13(c)) carbamation (figure 13 (b)) and etherification (figure 13 (d)).

Though the solubility of the derivatized cellulose depends on the type and degree of derivatization, most of the derivatives are soluble in common polar organic solvents like DMF, DMSO, dioxane etc.

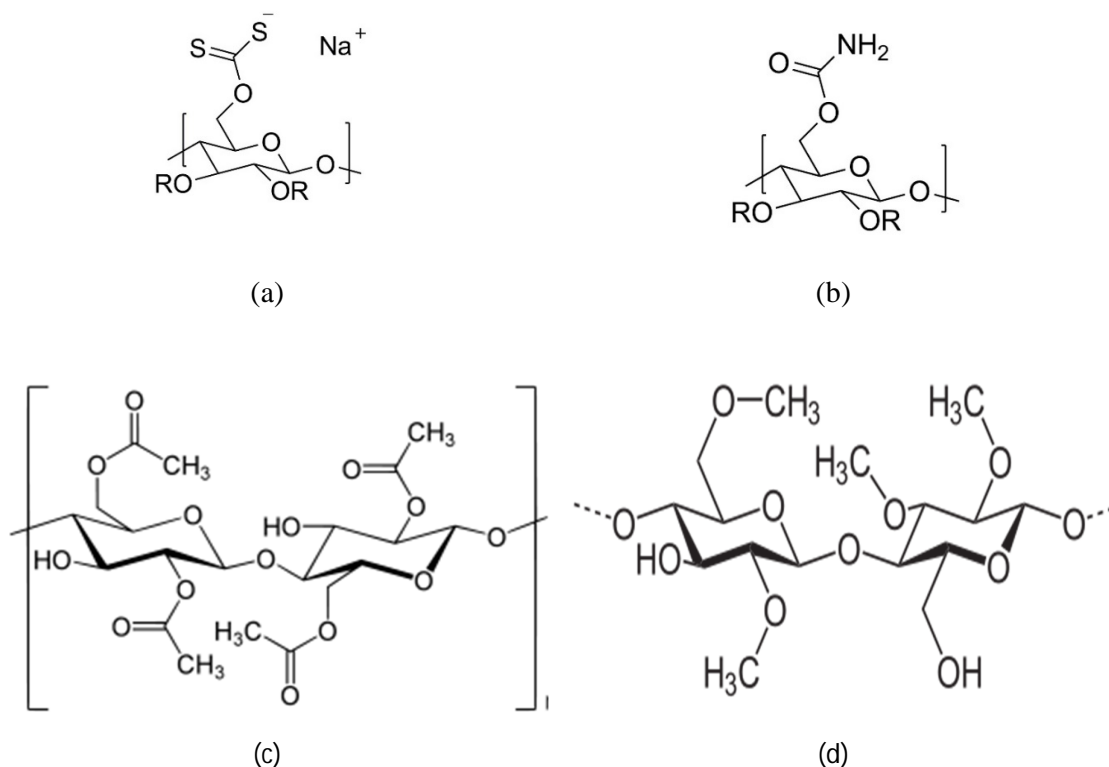


Figure 13. Chemical structure of (a) Cellulose xanthate (b) Cellulose carbamate (c) Cellulose acetate and (d) Methyl cellulose

#### **(b) Cellulose dissolution without chemical modification**

Solvents capable of dissolving cellulose without prior chemical modification are frequently described as non-derivatizing solvents. Such cellulose solvent systems are known to include ionic liquids (figure-14 (a)), organic solvents in the presence of an inorganic salt, amine oxides (figure 14 (b)), aqueous alkali solutions, aqueous complex solutions, and inorganic molten salt hydrates.



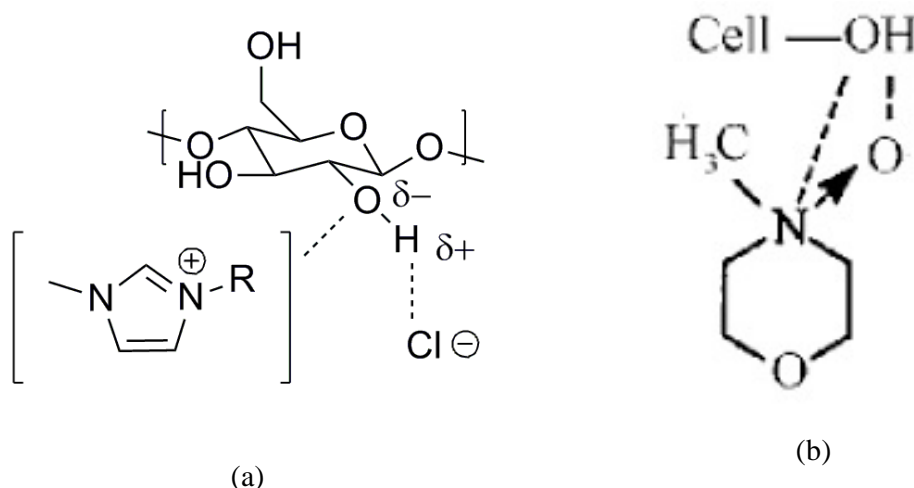


Figure 14. Chemical structure of (a) Ionic liquid and (b) N-methyl morpholine N-oxide

#### (c) NaOH-Urea-Thiourea-Water solvent system

It was found that NaOH/urea and NaOH/thiourea aqueous solutions can dissolve cellulose directly and quickly. Both solvent systems are inexpensive and less toxic, and good cellulose fibers can be prepared using simple technology. However, prepared dope with these two solvents is not stable. To overcome with this problem the NaOH-urea-thiourea solvent system was introduced [52]. NaOH-urea-thiourea solvent system can dissolve cellulose directly. The solvent system is of low toxicity and possesses higher solubility capacity for cellulose compared with NaOH/thiourea and NaOH/urea aqueous solutions. This simple technology is cheap and environmentally friendly that's why selected for cellulose coating.

#### (d) Aqueous sulfuric acid solution

Generally aqueous sulfuric acid is being used to prepare cellulose nanocrystals [134-137]. 60% sulfuric acid interacts with cellulose and try to breakdown the polymer chain. In the process of nanocrystal preparation in aqueous sulfuric acid solution, milled cotton linters were hydrolyzed by 64 % w/w sulfuric acid under vigorous stirring at 45 °C for 45 min (fibers/acid ratio 1:17.5 g/mL) [138]. Cellulose is in dissolved form after 30 min of mixing in aqueous sulfuric acid solution at low[139] temperature. The solvent 60% H<sub>2</sub>SO<sub>4</sub> is a powerful and has the ability to dissolve cellulose directly. The Degree of Polymerization of cellulose decreases after dissolution in 60% H<sub>2</sub>SO<sub>4</sub> [46] but it is not highly important for coating.

# CHAPTER 4

## EXPERIMENTAL

### 4.0 Prologue

The methods used to characterize the materials are herewith presented putting particular emphasis on the produced samples characterization methods.

### 4.1 Materials

Cotton plain weave fabric with the 0.28 mm thickness, 125.2 g/cm<sup>2</sup>, 97.3% porosity, density of 30warps/cm and 25 weft/cm was obtained from Tepna Nachod, Czech Republic (figure 15). TiO<sub>2</sub> nanoparticles (Degussa-P25) were purchased from Evonik industries with the average particle size of 50 nm. Vian Biocel V Mg-bisulfite softwood pulp was supplied by Lenzing Biocel Paskov A.S. Urea was purchased from Pentachem. Thiourea, sulfuric acid, and NaOH were purchased from Lachner, Czech Republic. Reactive Red 240, Blue 49, and Yellow 95 reactive dyes were purchased from Synthesia a.s. Sulfuric acid was purchased from Lach-ner, Czech Republic. Sodium carbonate was obtained from P-Lab a.s Czech Republic. The Orange II dye was used as a stain and it was obtained from Sigma Aldrich.

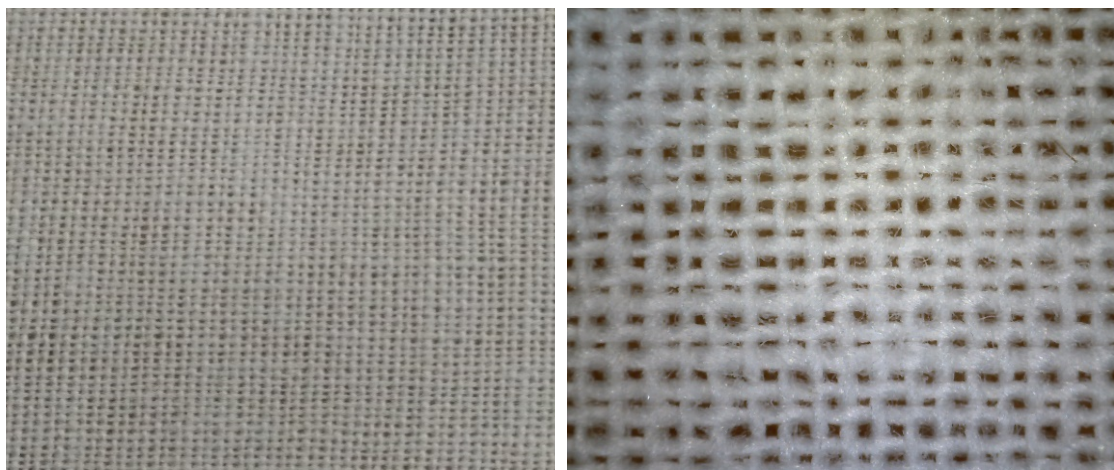


Figure 15. Cotton fabric used for study

## 4.2 Cellulose Coating

### 4.2.1 Cellulose dissolution

#### a) Dissolution in 60 % Sulphuric acid

Viscose fibers were used as a source of cellulose to prepare cellulose solution. 60 % of sulphuric acid solution was prepared by dissolving 60 g of sulphuric acid in 40 g of water. Prepared solution allowed to cool down at room temperature (20-25° C). 10 g of viscose fibers were dissolved in 90 g of 60 % Sulphuric acid solution at room temperature under continuous stirring for 30 min.

#### b) Dissolution of cellulose in Urea-Thiourea-NaOH Solvent system

The solvent system was prepared by mixing 8g of Urea, 6.5 g of Thiourea and 8g of NaOH in 77.5g of water by stirring. Various concentrations of cellulose pulp (0, 1, 3, and 5 %) were dissolved in the urea-thiourea-NaOH-water solvent system at -12° C by mechanical stirring.

### 4.2.2 Dispersion of TiO<sub>2</sub> nanoparticles in cellulose solution

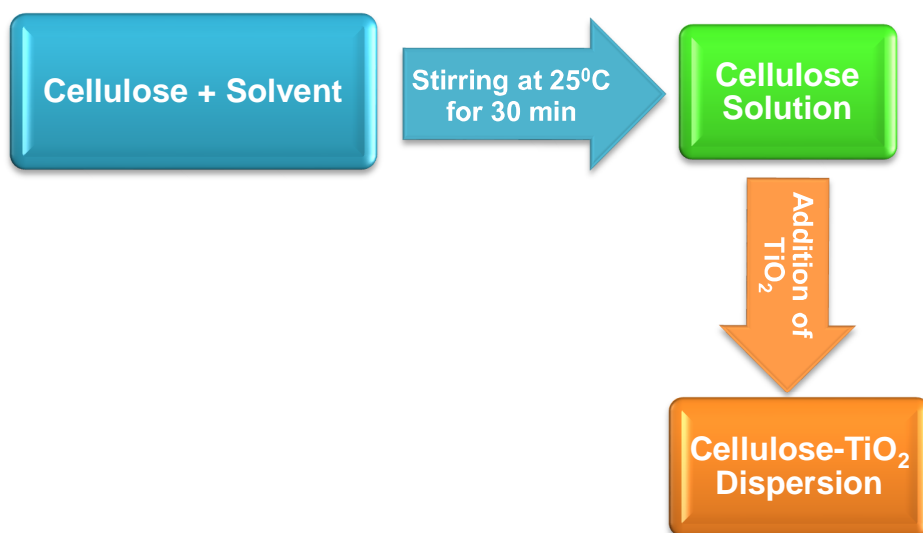


Figure 16. Dissolution and dispersion of TiO<sub>2</sub>

Cellulose solution was prepared by dissolving cellulose in direct solvents such as 60% Sulfuric acid and NaOH-urea-thiourea. Figure 16 shows the schematic representation of dissolution and

dispersion process. TiO<sub>2</sub> nanoparticles with different concentration (1,3,5, and 10% on the weight of cellulose) were dispersed in cellulose solution. Mixture of Cellulose solution and TiO<sub>2</sub> nanoparticles were stirred at room temperature for 5 min. Prepared cellulose-TiO<sub>2</sub> solution was used for coating.

#### 4.2.3 Padding

The cellulose - TiO<sub>2</sub> solution was applied on the surface of cotton fabric (4g) by roller padding machine (figure 17) at room temperature (15-20°C). The time used for padding was 20 seconds and same time used to treat fabric with solvent (60 % H<sub>2</sub>SO<sub>4</sub>).



Figure 17. Padding machine

Fabric was washed after padding by aqueous solution of 100 g/l Sodium carbonate, followed by water until neutralization. The coated fabrics were dried at 60°C for 30 min and pressed

using an electric iron. The concentration of cellulose added is as shown in Table 1. Starching to cotton fabric was done according to procedure given in US patent no 2,693,042 [140] to compare stiffness property with cellulose coated cotton fabric.

Table 1. Amount of cellulose coating on 4 g of cotton fabric

Sample description	Weight of fabric after coating [g]	Added cellulose-TiO <sub>2</sub> / g of fabric
0 % (Without TiO <sub>2</sub> )	4.2415	0.0603
1 % TiO <sub>2</sub>	4.2355	0.0588
3 % TiO <sub>2</sub>	4.2366	0.0591
5 % TiO <sub>2</sub>	4.2383	0.0595
10 % TiO <sub>2</sub>	4.2392	0.0598

### 4.3 Dyeing with reactive dyes

Dyeing bath was prepared by dissolving NaCl (50 g/l), Na<sub>2</sub>CO<sub>3</sub> (20 g/l) and reactive dye in distilled water. The dyeing was done at 70 °C for 60 min with fabric-liquor ratio 1:50. The dyeing was carried out with 3 %, 9 % and 15 % of dye concentration (%w/w). Then dyed samples were washed with hot (80 °C) water and dried at 70 °C in hot air convection oven for 30 min.

#### 4.3.1 Effect of cellulose coating on dyeing properties

Reflectance of the coated and uncoated fabric samples were measured on spectrophotometer (Datacolor 110TM Switzerland) at  $\lambda_{max}$  and Kubalka–Munk equation was used to determine K/S value of the both fabrics:

$$\frac{K}{S} = \frac{(1 - R_{\lambda_{max}})^2}{2R_{\lambda_{max}}} \quad (10)$$

where K is the coefficient of absorption;  $R_{\lambda}$  is the reflectance of the fabric at peak wavelength and S is the coefficient of scattering;

The relative color strength and color difference between cellulose coated dyed samples and uncoated dyed samples were calculated by using following formula:

$$\text{Relative color strength (\%)} = \frac{\text{K/S of coated sample}}{\text{K/S of uncoated sample}} \times 100 \quad (11)$$

$$\Delta E = \sqrt{(\Delta L)^2 + (\Delta a)^2 + (\Delta b)^2} \quad (12)$$

Where  $\Delta L = L_{\text{Coated}} - L_{\text{unCoated}}$ ;  $\Delta a = a_{\text{Coated}} - a_{\text{unCoated}}$ ;  $\Delta b = b_{\text{Coated}} - b_{\text{unCoated}}$ ; L is lightness, 'a' explain redness or greenness and 'b' indicate yellowness or blueness [56].

#### 4.3.2 Fastness properties

The coated samples were washed according to the standard conditions given in the test method ISO 105-C06 [57] to assess staining of adjacent fabrics and change in the color after washing. Rubbing fastness of both coated and uncoated samples were evaluated according to the test method ISO 105-X12 [58]. The coated fabrics were evaluated for their perspiration fastness using the test method ISO 105-E04 [59].

#### 4.4 Characterization and measurements

##### 4.4.1 Scanning Electron Microscopy (SEM)

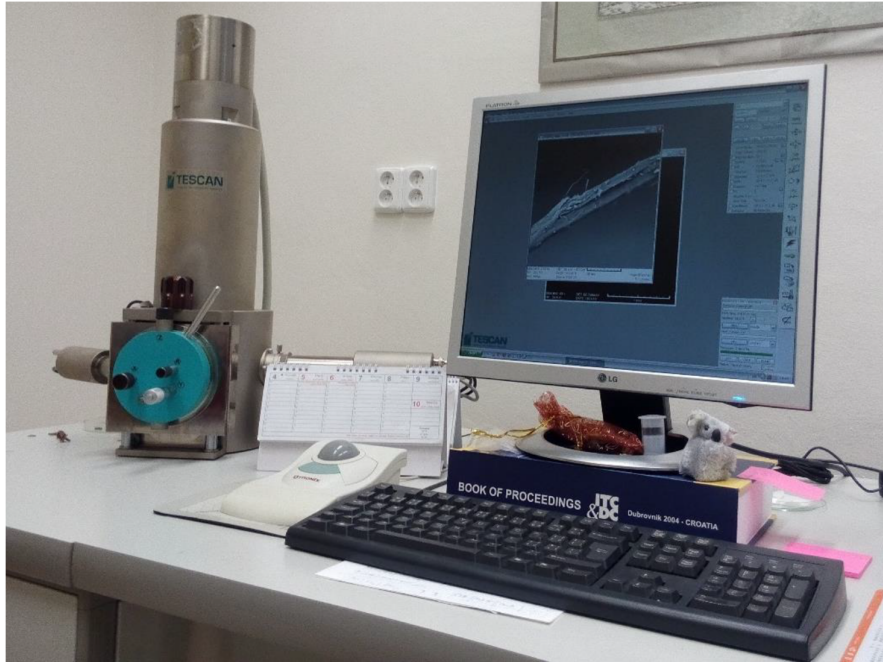


Figure 18. TS5130 Vega-Tescan Scanning Electron Microscope



The surface morphologies of the control, cellulose coated and cellulose-TiO<sub>2</sub> coated cotton fabric surfaces were investigated using a TS5130 Vega-Tescan Scanning Electron Microscope (figure 18) with accelerating voltage of 20kV. The samples were sputter coated with gold to increase the surface conductivity.

#### **4.4.2 Simulation method to calculate amount of cellulose II by x-ray diffraction**

PANalytical X'Pert<sup>3</sup> X-ray powder diffractometer (figure 19) was used to analyze crystal structure of coated and control cotton fabric. The fabric samples were run at angle 8° to 70° in steps of 0.017. Cellulose II was estimated by following AD French's simulation method [50-52]. The published coordinates of the asymmetric units of cellulose I $\beta$  and cellulose II containing crystallographic information file was downloaded from the supplementary material of the AD French paper [50-52].



Figure 19. PANalytical X'Pert<sup>3</sup> X-ray powder diffractometer

The whole contents was copied into a note pad, and  $a = 7.784^\circ \text{ \AA}$  for I $\beta$  unit cell was changed to  $7.906^\circ \text{ \AA}$  for cotton fabric cellulose and saved in .cif file format. The Mercury 3.5.1 program [53] was used to simulate diffraction patterns. The Full Width Half Maximum (FWHM) was

set at  $1.5^\circ 2\theta$  and the CuK $\alpha$  wavelength was set at 1.54056 Å. For the preferred orientation, a March–Dollase factor of 2.0 [54] was applied to the (0 0 1) plane. The pattern of cellulose II at  $9^\circ$  FWHM [51] was used to incorporate amorphous fraction of cellulose.

#### **4.4.3 Mechanical properties**

In order to understand the effect of 60 % H<sub>2</sub>SO<sub>4</sub> solvent on the mechanical properties of cotton fabric, samples with dimensions 15 X 5 cm were tested for the breaking strength, elongation and modulus of control and cellulose-TiO<sub>2</sub> coated fabrics were measured according to ISO 1924-2 [55] standard test method on Testometric M250-2.5 machine (UK). Five number of samples were tested and statistical treatment was done.

#### **4.4.4 Photocatalytic properties**

The Orange II dye and wine were used as a stain for the experiments. Stained samples were irradiated under UV light as a function of time to see the effect of TiO<sub>2</sub> on degradation of stain. Philips TL 6W/05 CE UV tubes (400-320 nm) were used for irradiation of stain. After irradiation, the fabric samples were scanned on the scanner at 300 dpi and the scanned images were analyzed by ‘Image J’ software [141, 142]. ImageJ is an open source Java image processing program inspired by NIH Image [142]. It runs on any computer with a Java 1.8 or later virtual machine. Downloadable distributions are available for Windows, Mac OS X and Linux. ImageJ has a strong, established user base, with thousands of plugins and macros for performing a wide variety of tasks.

ImageJ can display, edit, analyze, process, save and print 8-bit, 16-bit and 32-bit images. It can read many image formats including TIFF, GIF, JPEG, BMP, DICOM, FITS and "raw". It supports "stacks", a series of images that share a single window. It is multithreaded, so time-consuming operations such as image file reading can be performed in parallel with other operations. It can calculate area and pixel value statistics of user-defined selections. It can measure distances and angles. It can create density histograms and line profile plots. It supports standard image processing functions such as contrast manipulation, sharpening, smoothing, edge detection and median filtering [143]. Ten number of samples were analysed for photocatalytic degradation. Blue colour intensity was taken into consideration since it was only changing. Figure 20 shows the process to analyze stain degradation by ImageJ.



#### Procedure of image analysis by ImageJ software

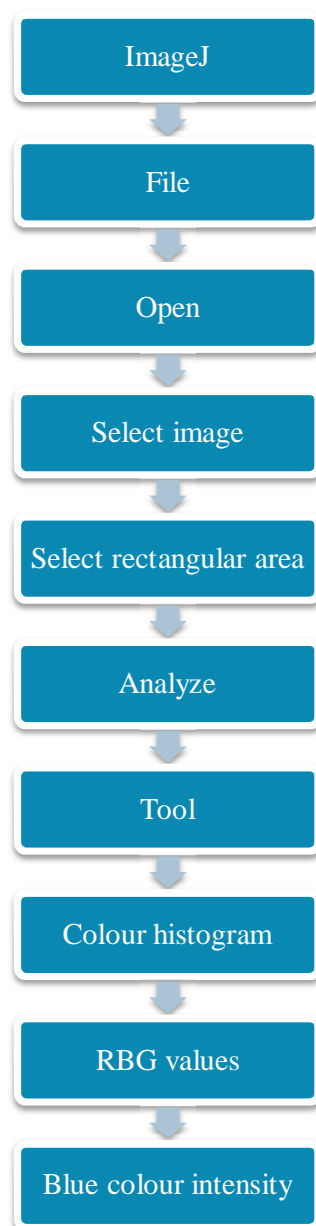


Figure 20. Method to analyze photocatalytic degradation of stain by ImageJ

#### 4.4.5 Stiffness of treated fabric

The bending force of fabric was measured on TH-7 instrument [61]. The device TH-7 (figure 21-a) was developed in Department of Textile Evaluation at Technical University of Liberec by Dr. Ludmila Fridrichova. It was developed by means of innovation of device TH-5 on which

only rectangle samples sized 2.5 cm 5 cm could be measured. The differences between model of device TH-5 and TH-7 and the essential innovations that were realized on the older device TH-5 is given below.

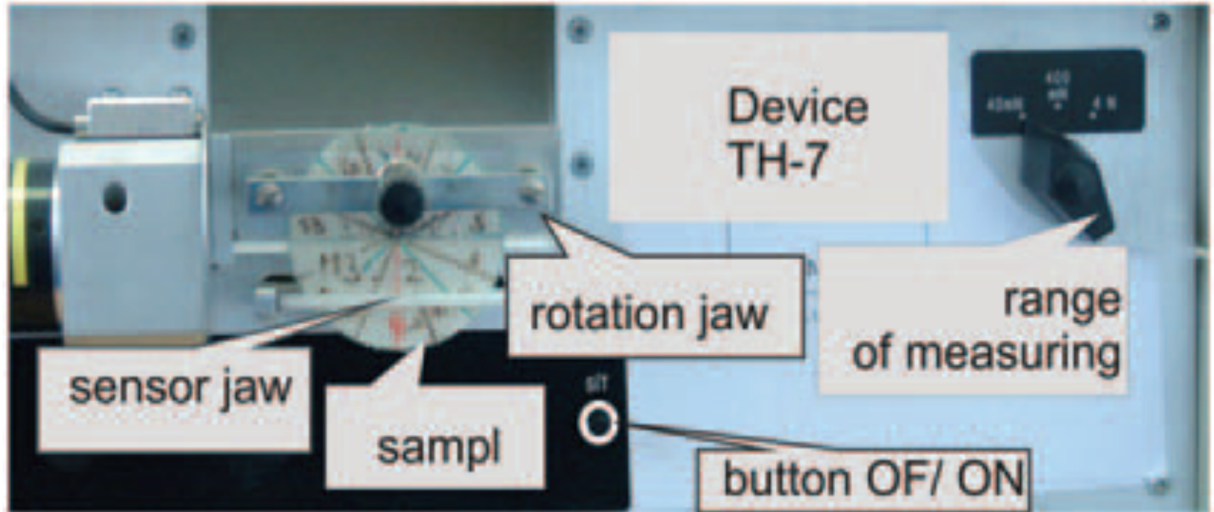


Figure 21(a). Device TH-7 [144].

1. The clamping and sensor jaw was extended so that the device could be used for measuring rectangular, square and circular samples.
2. The revolving clamping jaw was designed so that it could turn in both directions, which enabled one to draw the whole hysteresis loop of bending (figure 21-b).
3. The sensor jaw was adjusted so that the bending power could be scanned in both directions: face– face and back–back. The sensor jaw is U-shaped.
4. There are Teflon tubes on the sensor jaw that reduces the coefficient of friction between the tube and the bent fabric.
5. To control the device and store the measured data, new software was developed. The output of the measuring is a hysteresis loop (curve). The data are stored in a data file (csv) and at the same time in a graphic file (png), as shown in figure 21-b.
6. Device TH-7 also enables one to measure the cyclical strain of the sample. It is possible to set 10 cycles of automatic bending at maximum. The values of every cycle are recorded, as well as the final average value.

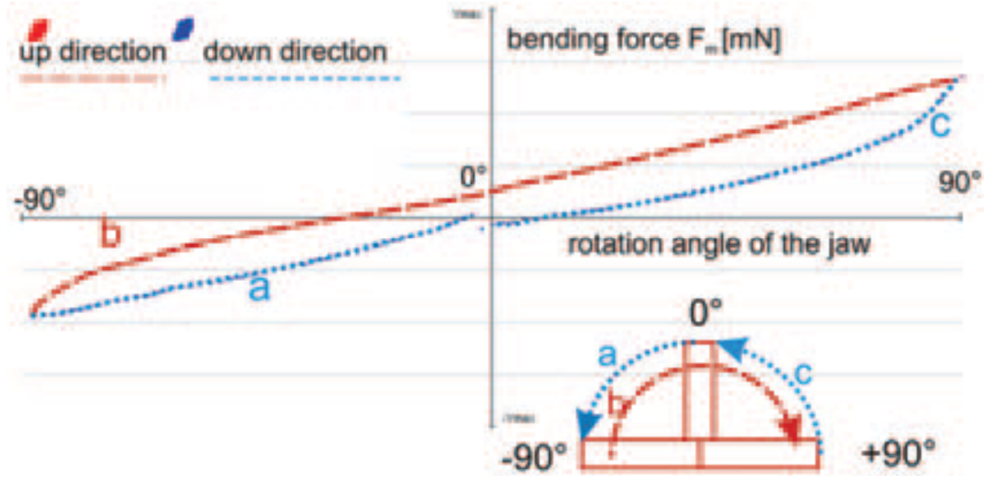


Figure 21 (b). Hysteresis loop of bending from device TH-7 [144].

The device enables the measuring of non-textile materials, for example paper, foils and membranes; however, it was constructed mainly for measuring fabrics. It has three ranges of measured bending force. The range of measuring force of bending is from 40 to 4000 mN. The output from the device is the value of bending force  $F_m$  [mN]. This value can be measured for various sample widths, with 50 mm being the maximum and the minimum being unlimited.

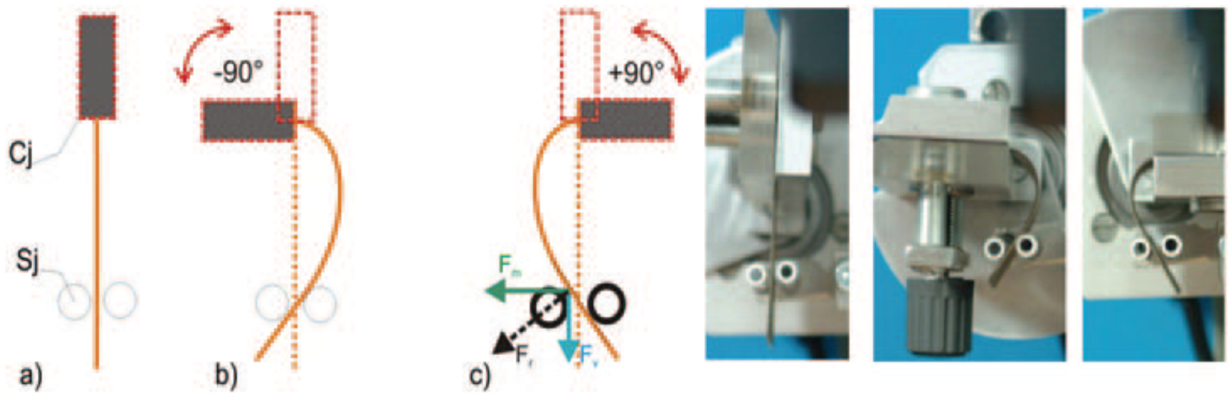


Figure 22. Scheme and photography of bending sample on device TH-7. [144].

The suggested length of the sample is 50 mm; however, textiles of 25 mm minimum length can be measured, too. Materials whose thickness does not exceed 1.5 mm can be bent. The distance between the clamping and the sensor jaws is 14 mm. The scheme and photography of bending the fabric on device TH-7 is given in figure 22 [Cj: clamping jaw; Sj: sensor jaw, it is scanning

bending force ( $F_m = F_h$  horizontal force component);  $F_r$ : resultant force;  $F_v$ : vertical force. (a) Sample in zero position. (b) Sample turned to position +90° face–face. (c) Sample turned to position -90° back–back]. The output value from device TH-5 or TH-7 is bending force  $F_m$ . The calculation of bending moment  $M_o$  [Nm] is described for the older model, device TH-5, according to the standard C<sub>SN</sub> 80 0858, where  $M_o = \frac{1}{4} F_m k$ ,  $k = 0.604$  for samples of 2.5 cm width. There is more information in the article by Naujokaityte et al- [145]. If we want to compare the mutual bending behavior of textiles that were measured only on device TH-7, it is possible to work only with the value of bending force  $F_m$  [Nm], so it is not necessary to convert  $F_m$  to the value of bending rigidity  $B$  [Nm<sup>2</sup> /m], or to the bending moment  $M$  [Nm]. Stiffness was calculated by multiplying bending force to 0.008. Five number of samples were tested and standard deviation was calculated.

#### **4.4.6 Quantitative evaluation of anti-bacterial activity (AATCC–100)**

American Association of Textile Chemists and Colorists (AATCC) standard methods such as AATCC 147 and AATCC100 were used to investigate antibacterial activity of cellulose-TiO<sub>2</sub> coated cotton fabric. Four different bacterial strains, Escherichia coli (EC), Klebsiella pneumonia (KP), Staphylococcus aureus (SA), Methicillin resistant staphylococcus aureus (MRSA) respectively were used.

**AATCC 147:** The sample with dimensions 18x18 mm was wetted in distilled water and placed on moist filter paper (in distilled water). Both sample and filter paper were placed together in petri dish and then dish was closed. After 15 minutes of UV radiation exposure, the sample was placed on blood agar. The blood agar plates were individually inoculated with bacterial stains at a concentration of 10<sup>5</sup> CFU / ml. The samples were cultivated in incubator at 37 °C for 24 hours.

**AATCC100:** The sample wetted in distilled water with the dimension of 18x18 mm was placed on wet filter paper and then together placed in covered petri dish. The sample was placed into sterile container and exposed to UV radiations for 15 minutes. Thereafter 50µl of bacterial stain (inoculums) was applied on the sample and allowed to wick through the sample stack. The inoculated swatches incubated for 24 hours at 37°C; thereafter a neutralizing broth composed of 50ml of saline was added and container was shaken so as to release the inoculums from the

test swatches and into the neutralizing broth. The bacteria present in this liquid was obtained as the percentage reduction [146].

The percentage reduction of bacteria was calculated using the following formula:

$$(B - A) \frac{100}{B} = R \quad (13)$$

Where R is the percentage reduction; A and B are the number of bacteria recovered from the inoculated treated and untreated fabrics.

#### **4.4.7 Evaluation of antifungal properties of coated fabric**

The antifungal properties were measured using the following fungi mixture in aqueous suspension at a concentration of 10<sup>6</sup> CFU/ml: *Penicillium digitatum* (CCM F-382), *Rhizopus stolonifer* (CCM F-445), *Cladosporium sphaerospermum* (CCM F-351), *Chaetomium globosum* (CCM 8156). Three samples of cotton fabric coated with TiO<sub>2</sub>, each with area of about 4 cm<sup>2</sup>, with different concentrations of TiO<sub>2</sub> (0, 1, 3, 5 and 10%) were placed on agar medium [Malt agar, Cadarsky-Envitek, Ltd, Brno, Czech Rep.] and inoculated with a suspension of testing moulds. Incubation of the tested sample was conducted for two weeks at a temperature of 22 ± 3 °C, at daylight (near a window). After the test, evaluation of antifungal properties was done on the basis of visual assessment according to the EN 14119, 2003 Standard [147] by determining degree of mould growth on the surface of fabric samples.

The rating system for mold growth was as follows:

- 0 – no visible growth evaluated microscopically,
- 1 – no visible growth evaluated with the naked eye but clearly visible microscopically,
- 1 – growth visible with naked eye, covering up to 25% of tested surface,
- 2 – growth visible with naked eye, covering up to 50% of tested surface,
- 3 – considerable growth, covering more than 50% of tested surface,
- 4 – Very intense growth, covering all tested surface.

#### **4.4.8 Air and water vapor permeability**

The air permeability of control and coated cotton fabrics was analyzed using a Textest FX instrument according to the ASTM D2986 standard test method. The air permeability was measured at pressure of 200 Pa and range of 3. The measuring principle depends on measurement of the air flow through the fabric under a certain pressure gradient Dp. The water

vapor permeability was analyzed using a Permetest device (Sensora Instruments) with the fast skin model according to the ISO 11092 standard.

#### **4.4.9 Durability of stiffness and photocatalytic properties**

Durability of Cellulose-TiO<sub>2</sub> coated fabrics for stiffness and photocatalytic properties against repeated washing were evaluated by washing TiO<sub>2</sub>-Cellulose coated cotton fabrics according to modified AATCC (American Association of Textiles Chemists & Colorists) test method 61 (2A)-1996 [66]. After washing, samples were analyzed for stiffness and photocatalytic properties. The fabric was washed with 4g per liter (g/l) detergent at 40 °C for 1hr. Washed fabrics were further evaluated for stiffness and stain degradation.



## CHAPTER 5

### RESULTS AND DISCUSSION

#### 5.1 Morphology of cellulose and cellulose-TiO<sub>2</sub> coated cotton fabric

To investigate the change in the surface morphology of the coated cotton fabric, scanning electron microscopy was used to estimate the influence of the modification process on the fabric. These images (figure 23) are of cellulose coated cotton fabric in which coating was done with dissolved pulp in NaOH-urea-thiourea solvent system. Cross sectional and surface images of cellulose-coated and uncoated cotton fabrics are presented in figure 23.

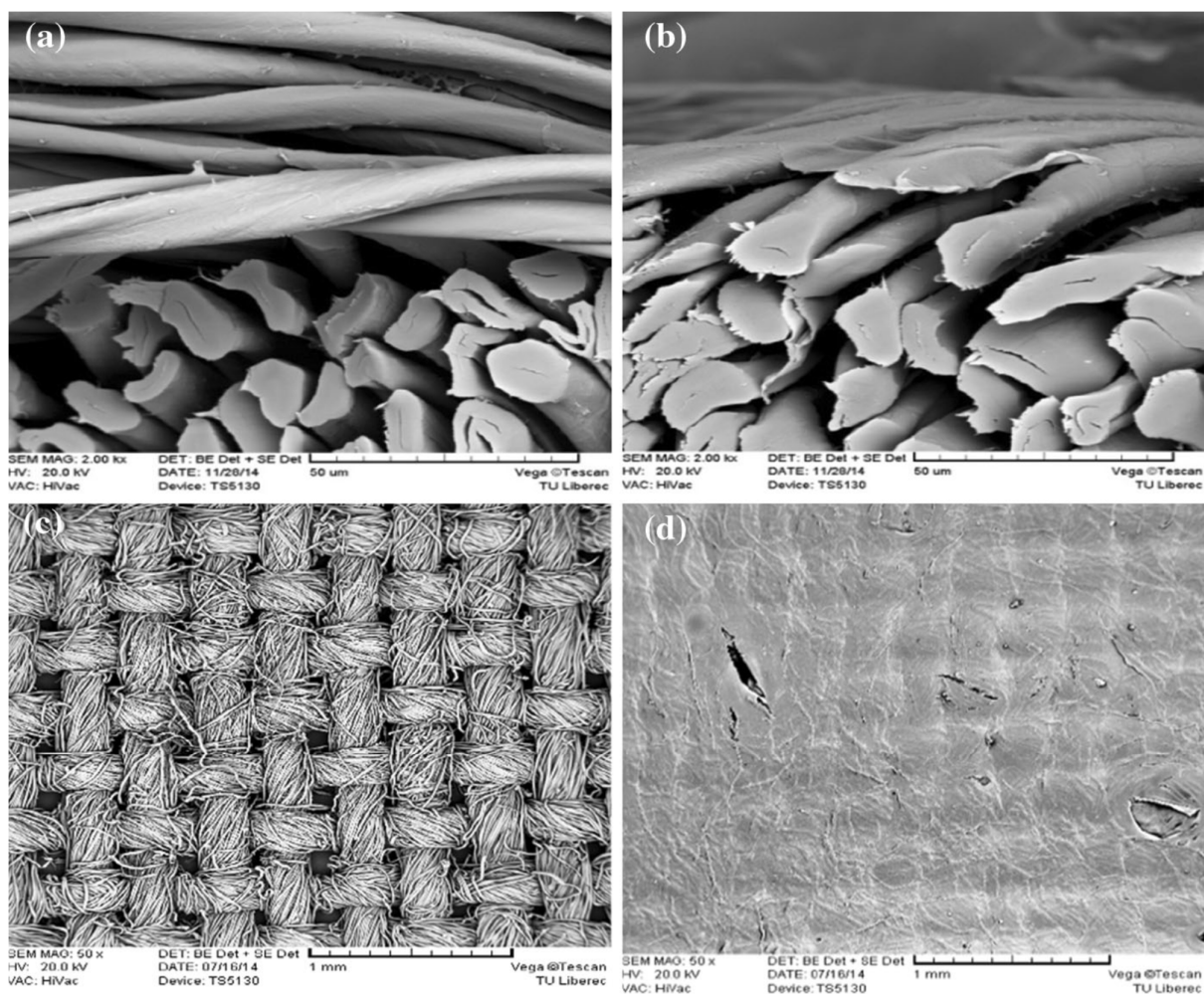


Figure 23. SEM images of (a, c) uncoated cotton fabric and (b, d) cellulose-coated cotton fabric

These micrographs (figure 23) reveal that the applied cellulose formed a film on the surface of the cotton fabric, covering the spaces between yarns. This formed film is attached to the surface of cotton fabric by intermolecular hydrogen bonding. The hydrogen bonds form between coated cellulose and cotton fabric cellulose because strong solvent such as NaOH-urea-thiourea and 60% H<sub>2</sub>SO<sub>4</sub> has been used to dissolve cellulose for coating. Solvent molecules interact with cotton fabric cellulose and try to dissolve and bring both cellulosic phase together. During this process coated cellulose and cotton fabric cellulose form intermolecular hydrogen bonding. This interchain linkage helps coated cellulose to stay attached to fabric.

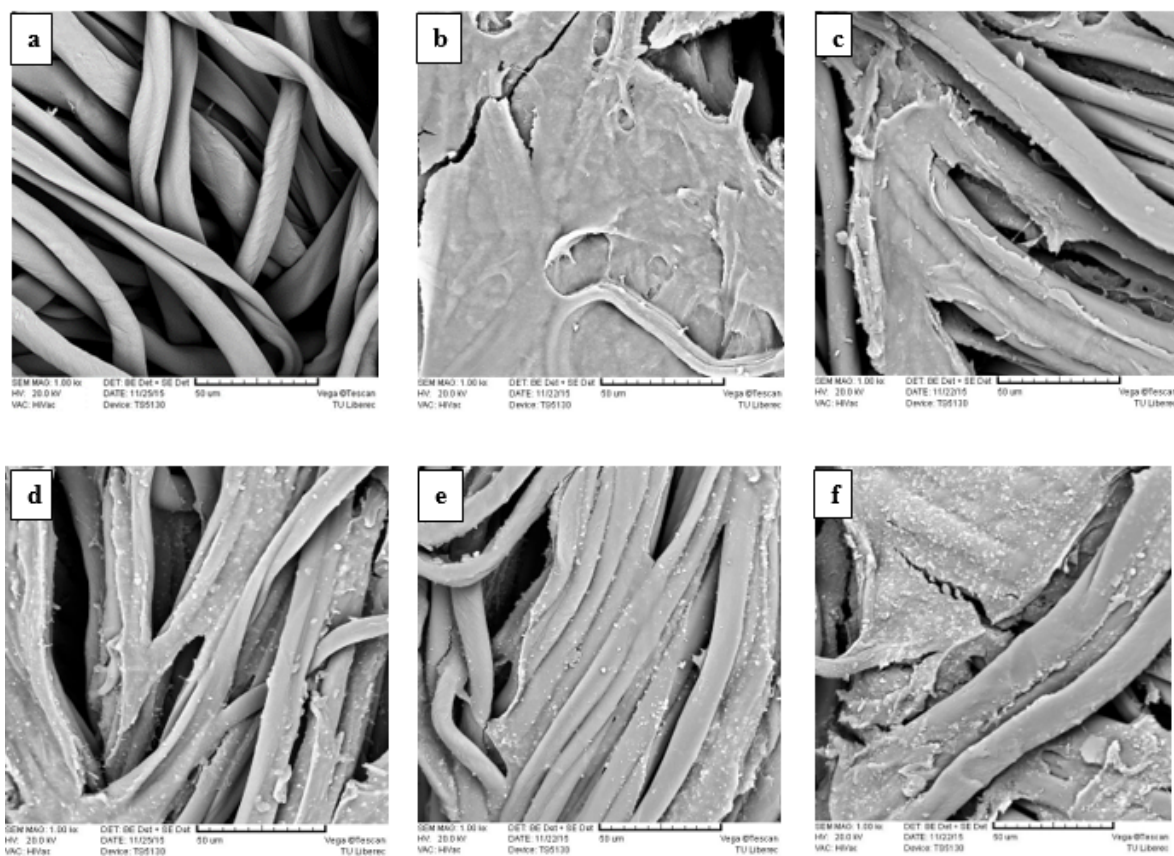


Figure 24. SEM photographs of TiO<sub>2</sub> - cellulose coated cotton fabric a) Control, b) 0% TiO<sub>2</sub>, c) 1 % TiO<sub>2</sub>, d) 3% TiO<sub>2</sub>, e) 5 % TiO<sub>2</sub>, f) 10% TiO<sub>2</sub>.

Figure 24 (a–f) show the morphological changes induced by the coating of cellulose-TiO<sub>2</sub> on the surface of the cotton fabric. It is apparent from the micrographs that coated cellulose forms a thin film on the fiber surface. Figure 24 (c–f) show the white particles on the surface and these white particles in the micrographs confirm that TiO<sub>2</sub> was successfully coated with the cellulose on the surface. Micro-graphs also reveal that coated cellulose holds the TiO<sub>2</sub> particles by



forming the film on fabric surface. Solvent (60% H<sub>2</sub>SO<sub>4</sub>) molecules interact with cotton fabric cellulose therefore forming an interchain linkage between dissolved cellulose and coated cellulose as a result of this linkage, cellulose is not easily washed away by water. It is not possible to detect the interchain linkage by spectroscopic technique because both the molecules are same. X-ray diffraction pattern of solvent treated cotton fabric (figure 40) shows some changes in the structure of cellulose. Cellulose II content increases slightly and proves the interaction between solvent and cotton fabric during coating.

## 5.2 Photocatalytic degradation of orange II under UV light

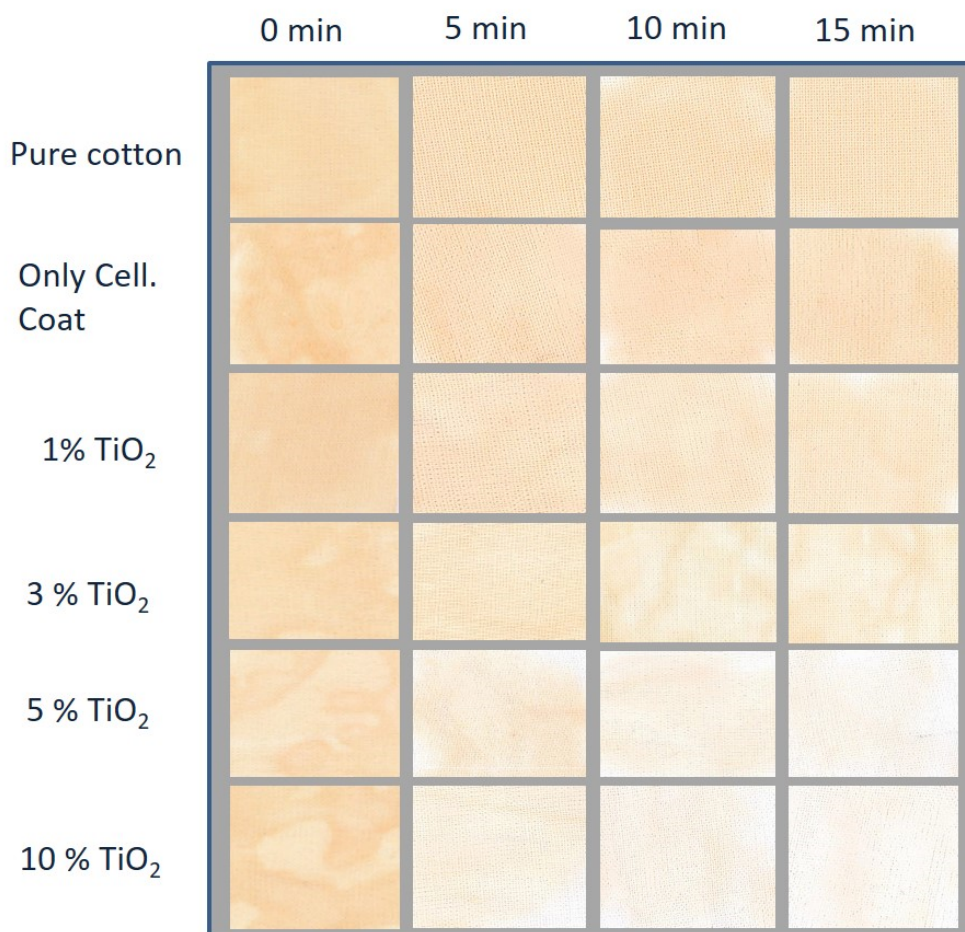


Figure 25. Degradation of Orange II under UV-visible light irradiation on cellulose-TiO<sub>2</sub> coated samples.

Cotton fabrics coated with cellulose-TiO<sub>2</sub> were analyzed for self-cleaning using photocatalytic degradation of orange II dye under UV light irradiation. Figure 25 shows scanned images of TiO<sub>2</sub> coated cotton fabric with various concentrations after irradiation under UV light at different time of intervals. In figure 26, the exponential curves are form of the equation  $B=B_0+(B_{\infty}-B_0)(1-e^{-kt})$ . Here  $B$  is calculated intensity,  $B_0$  is observed highest intensity,  $B_{\infty}$  is the intensity of pure cotton fabric without stain,  $k$  is constant and  $t$  is time. Significant discoloration of orange II dye was observed at 5 and 10 % TiO<sub>2</sub> coated samples. Evaluation of Orange II by ImageJ software is shown in figure 26. ImageJ software measures the intensity of color by using the color histogram tool. Here when sample becomes whiter, the value (counts) of color intensity increases that means it is measuring the whiteness of the sample. It is clear from figure 25 and 26 that degradation rate increases with increasing concentration of TiO<sub>2</sub> and time of irradiation. Coated samples with 1 and 3 % TiO<sub>2</sub> showed some degradation too but low as compared to 5 and 10 % due to low concentration. Figure 26 also shows that degradation of orange II increases with increasing irradiation time and TiO<sub>2</sub> concentration. Undyed control sample gave 249.7 counts whereas the dyed sample gave 186.6 counts and all the samples were compared in this range. All the TiO<sub>2</sub> coated samples show the photocatalytic properties and are therefore capable of stain degradation.

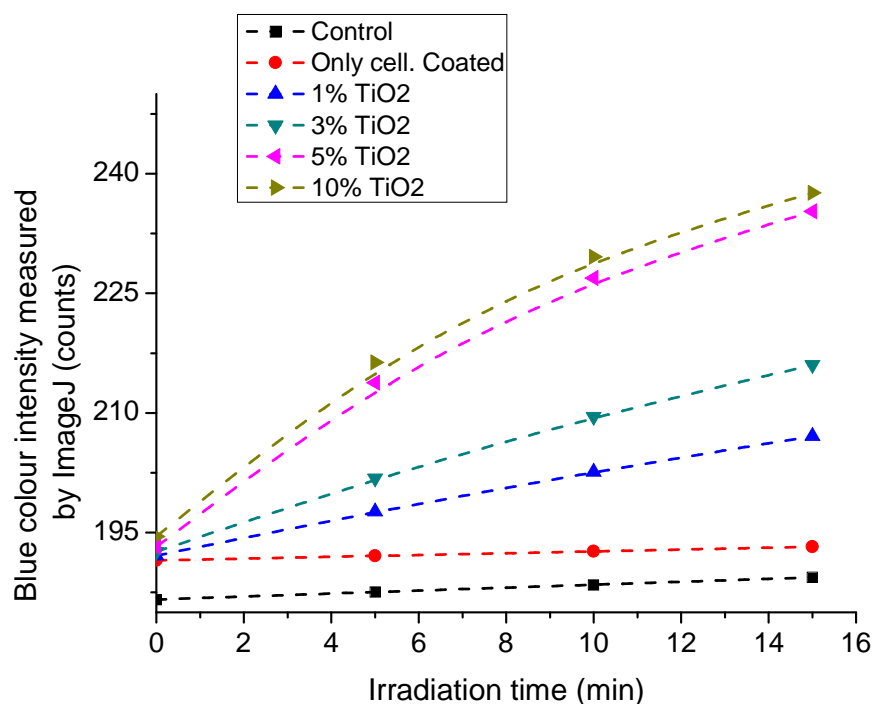


Figure 26. Evaluation of orange II degradation by ImageJ.

### 5.3 Wine stain degradation

The photocatalytic self-cleaning ability of TiO<sub>2</sub>-cellulose coated cotton fabric with red wine stain was observed by irradiating samples under UV light. Irradiated coated cotton fabric samples were scanned on the scanner and then evaluated by using ImageJ software. Figure 27 shows the scanned images of control, only cellulose coated and 1, 3, 5 and 10% TiO<sub>2</sub>-cellulose coated cotton fabric with red wine stain after 15 minutes of irradiation under UV light. It is clear from the figure 27 that red wine stain of 3, 5 and 10% TiO<sub>2</sub>-cellulose coated samples was degraded whereas control, only cellulose coated samples remained unaffected. Due to low concentration of TiO<sub>2</sub> in 1% coating sample shows less degradation of wine stain.

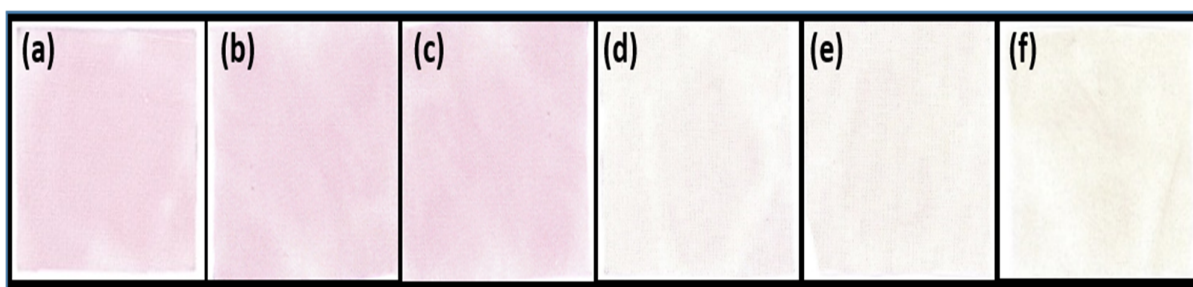


Figure 27. Scanned pictures of (a) Control (b) only cellulose coated and (c) TiO<sub>2</sub>-cellulose coated cotton fabric after irradiation of red wine stain under UV light

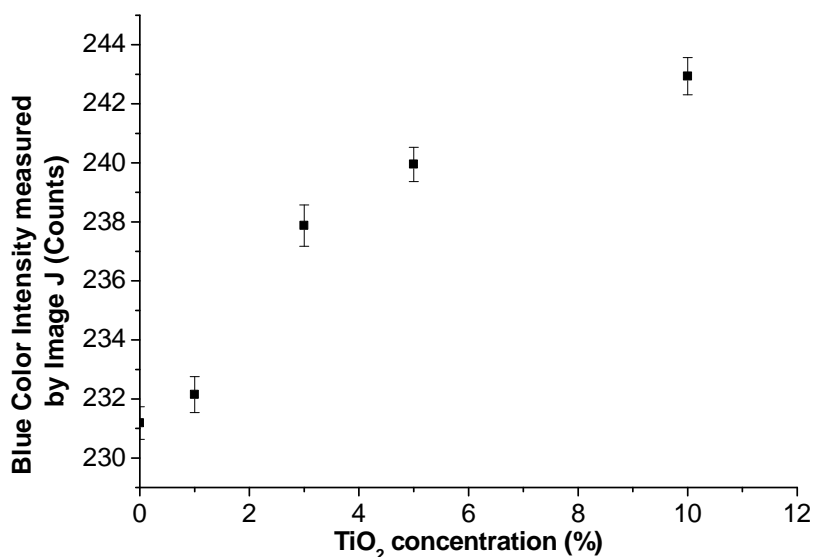


Figure 28. Effect of TiO<sub>2</sub> concentration on wine stain degradation

Effect of TiO<sub>2</sub> concentration on wine stain degradation was evaluated by using ImageJ software. It is observed in figure 28 that degradation of stain increases with increasing

irradiation time and concentration of TiO<sub>2</sub>. Samples coated with 3, 5 and 10% TiO<sub>2</sub> shows significant discoloration of stain after irradiation under UV light for 15 minute. 1% TiO<sub>2</sub> coated cotton fabric shows least amount of degradation after UV light irradiation because of less concentration of TiO<sub>2</sub>. Thus, from these results it is clear that degradation of stain depends on amount of TiO<sub>2</sub> in coating.

#### 5.4 Durability of cellulose-TiO<sub>2</sub> coated cotton fabric for self-cleaning ability

To study the effect of washing on the self-cleaning ability of cellulose-TiO<sub>2</sub> coated cotton fabric, the fabric was washed with 4g per liter (g/l) detergent at 40 °C for 1hr. Figure 29 shows the effect of washing on self-cleaning ability of coated fabrics. In figure 29, the exponential curves are form of the equation  $B=B_0+(B_{\infty}-B_0)(1-e^{-kw})$ . Here  $B$  is calculated intensity,  $B_0$  is observed highest intensity,  $B_{\infty}$  is the intensity of pure cotton fabric without stain,  $k$  is constant and  $w$  is washing cycle. Coated samples with 1, 3 and 5% TiO<sub>2</sub> show very good durability against washing up to 10 cycles.

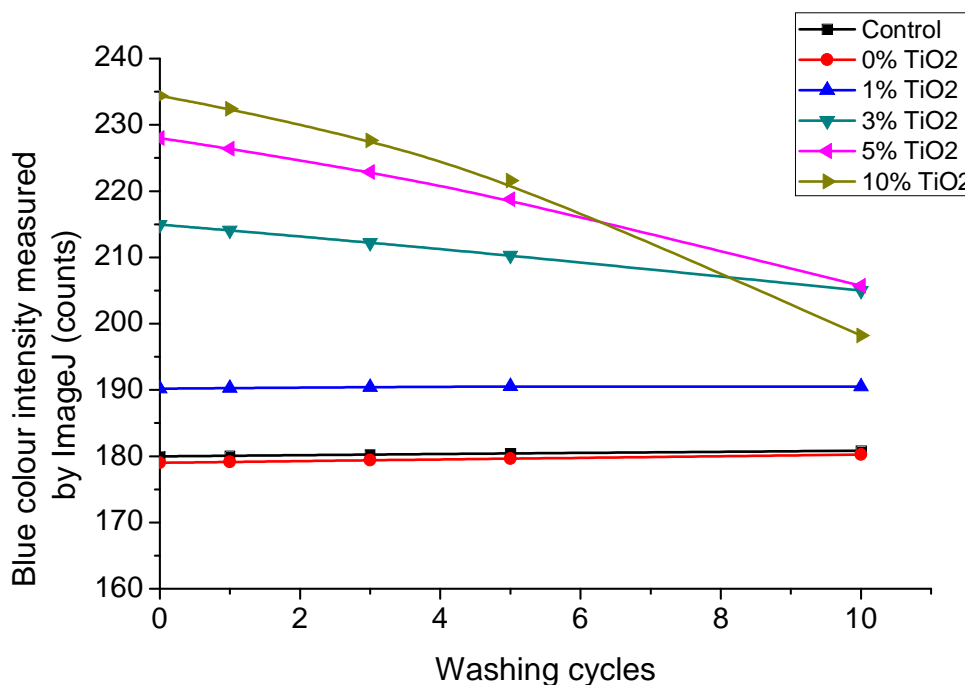


Figure 29. Effect of washing on stain degradation

The sample coated with 10% TiO<sub>2</sub> showed poor durability because TiO<sub>2</sub> was not dispersed homogeneously in cellulose solution due to the higher concentration and is illustrated in the

SEM images (figure 24 f). It is apparent from figure 29 that stain degradation starts decreasing after 1st washing for 3, 5, and 10 % TiO<sub>2</sub> coated cotton fabric, however, the ability to degrade the orange II dye stain still persists upto 10 washing cycles with all cellulose-TiO<sub>2</sub> coated samples. The fabric ability to degrade stain dropping after first cycle of washing because loosely attached cellulose was washed away with water. Therefore, this study confirms that significantly higher level of stain degradation is preserved as compared to uncoated fabric.

### 5.5 Rubbing effect on wine stain degradation

Textile materials frequently go through rubbing so it is necessary to investigate its effect on self-cleaning ability of cellulose-TiO<sub>2</sub> coated cotton fabric. The cellulose-TiO<sub>2</sub> coated cotton fabric was tested against rubbing on abrasion and pilling tester for different cycles such as 0, 5, 10, 50, 100 cycles. Samples coated with 5 and 10% TiO<sub>2</sub> (on the weight of cellulose) shows excellent results against rubbing upto 100 cycles. 3% TiO<sub>2</sub> coated sample shows significant decrease in self-cleaning ability.

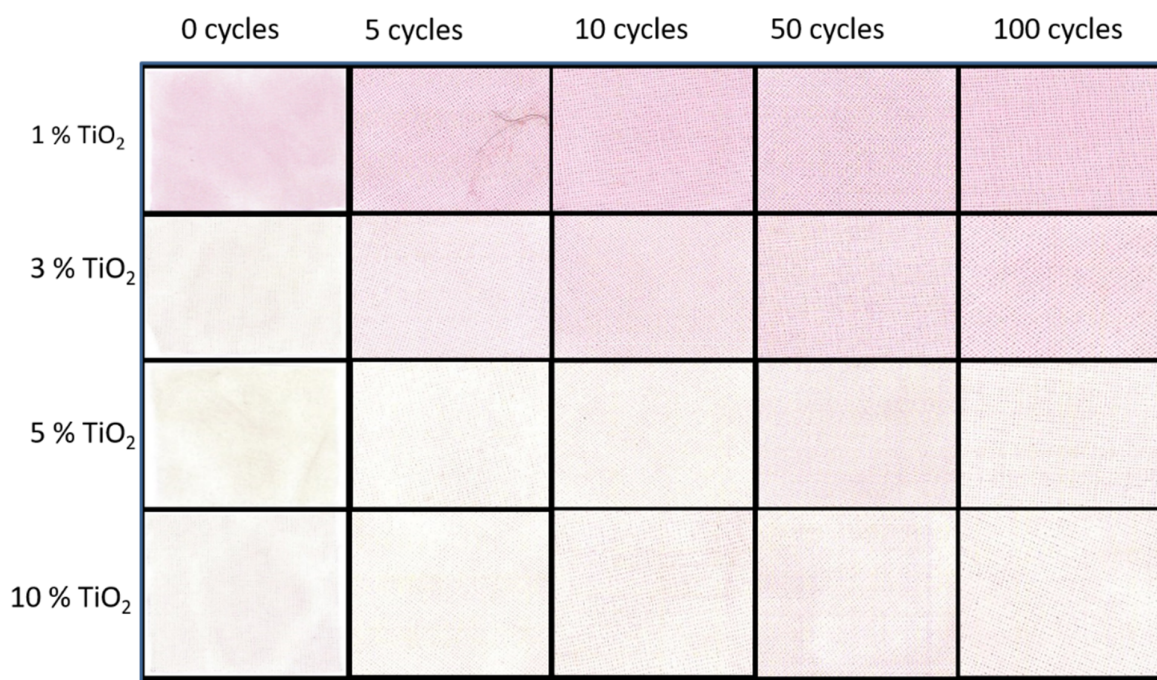


Figure 30. Scanned images of wine stain degradation of rubbed samples after 15 minutes of UV irradiation



The trend show that with increasing concentration of TiO<sub>2</sub> the stability against increasing of coated samples. Figure 30 shows the pictorial images of wine stain degradation after 15 minutes of UV irradiation. Evaluation of wine stain degradation after rubbing 100 cycles by ImageJ is shown in figure 31. The origin lab software was used to plot this graph and B-spline function used to draw curve for smoothness. There is some amount of drop in stain degradation between 1-10 rubbing cycles in all samples but not very significant. This is happening because loosely attached cellulose-TiO<sub>2</sub> going away at initial abrasion. After 10 cycles of rubbing there is no substantial change on wine stain degradation under UV irradiation for 15 min. Trend shows that stain degradation decreases with decreasing concentration of TiO<sub>2</sub> as rubbing cycles increases. Therefore, cellulose-TiO<sub>2</sub> coated cotton fabric is stable against rubbing.

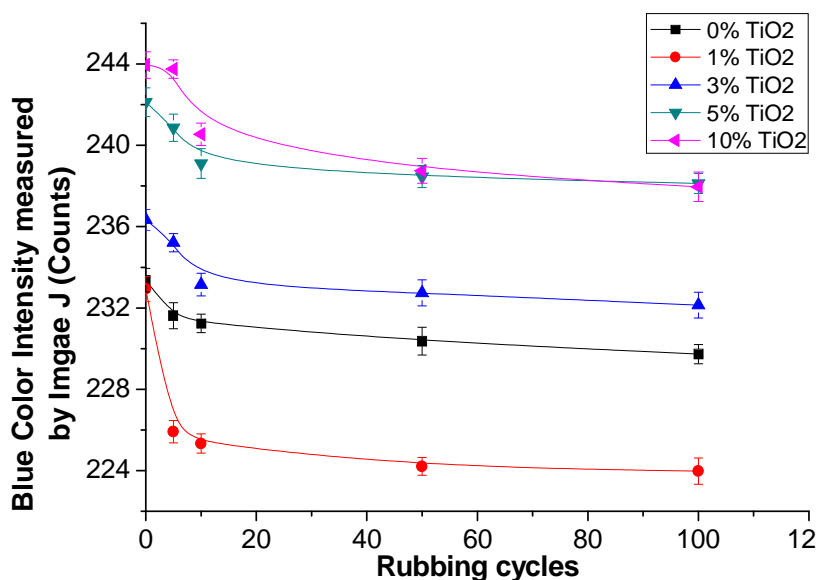


Figure 31. Evaluation of rubbing effect on wine stain degradation after 15 min of UV irradiation by ImageJ

## 5.6 Stiffness

### 5.6.1 Stiffness of cellulose coated cotton fabric in Urea–Thiourea–NaOH solvent system

Different concentrations of cellulose solution were prepared by dissolving cellulose in the Urea–Thiourea–NaOH–Water solvent system. The cellulose concentration was increased up to 5 % by decreasing the water concentration. This solvent can clearly dissolve a maximum of 6

% cellulose, but such 6 % solution has very high viscosity and is difficult to apply to fabric. The prepared cellulose solution was applied on cotton fabric by using roller padding to increase its stiffness permanently. The stiffness of the control as well as coated cotton fabrics was measured using a TH-7 instrument [144]. Figure 32 shows the effect of cellulose coating on the stiffness of the cotton fabric. The cotton fabric with 5 % cellulose coating showed very high stiffness compared with the other samples. From figure 33 it is also clear that the stiffness increased with increasing cellulose concentration. The SEM micrographs in figure 23 reveal that the coated cellulose was attached homogeneously to the fabric surface, which is why the stiffness was high and permanent. The coated cellulose was homogeneously distributed over the fabric surface because, during coating, the solvent molecules try to dissolve the fabric cellulose and link cellulose chains together. It is not easy to prove such linking by spectroscopic methods, because both molecules are the same. However, from the results of SEM imaging and the washing study, it is clear that there is a link between both kinds of cellulose chains, which is why the coated cellulose was not removed by the water during washing.

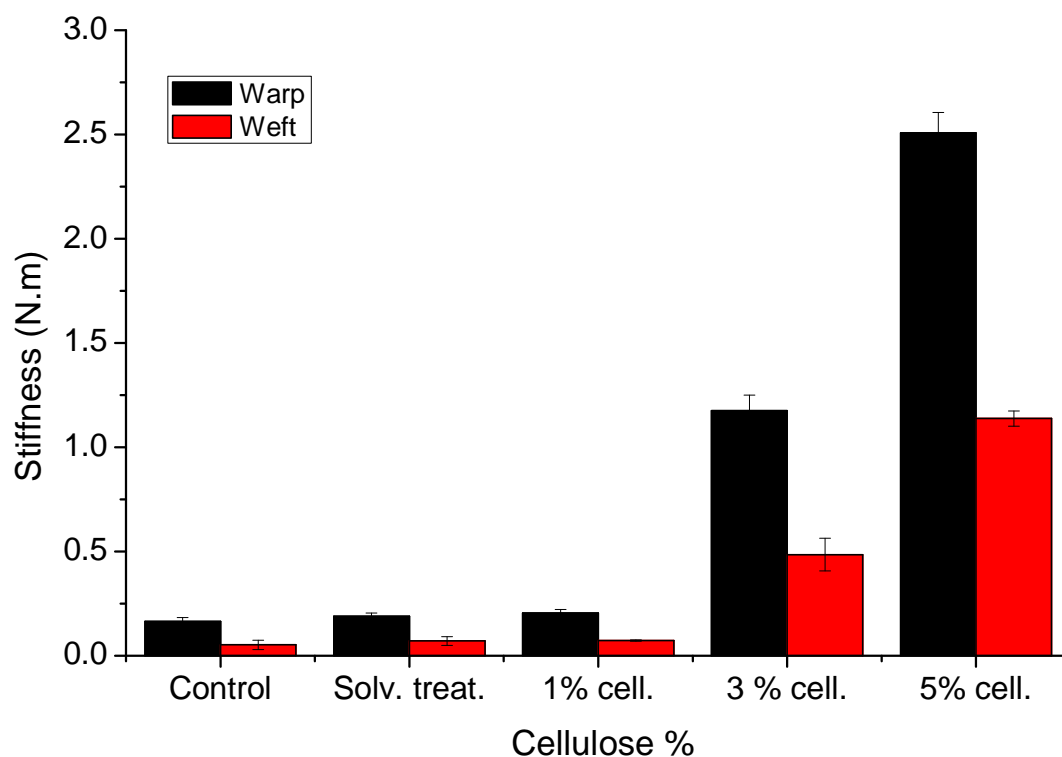


Figure 32. Stiffness of uncoated and coated samples.

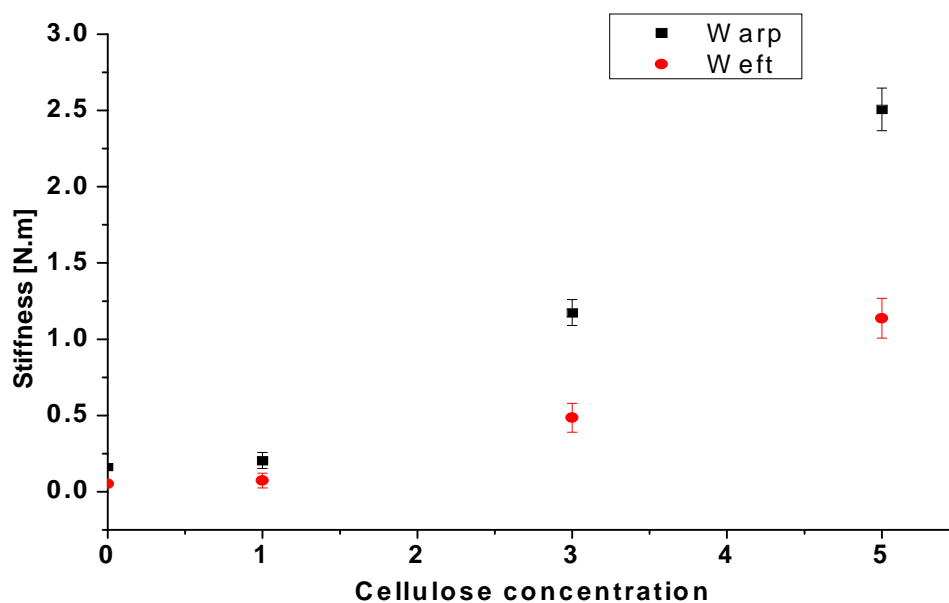


Figure 33. Effect of cellulose concentration on stiffness of cotton fabric

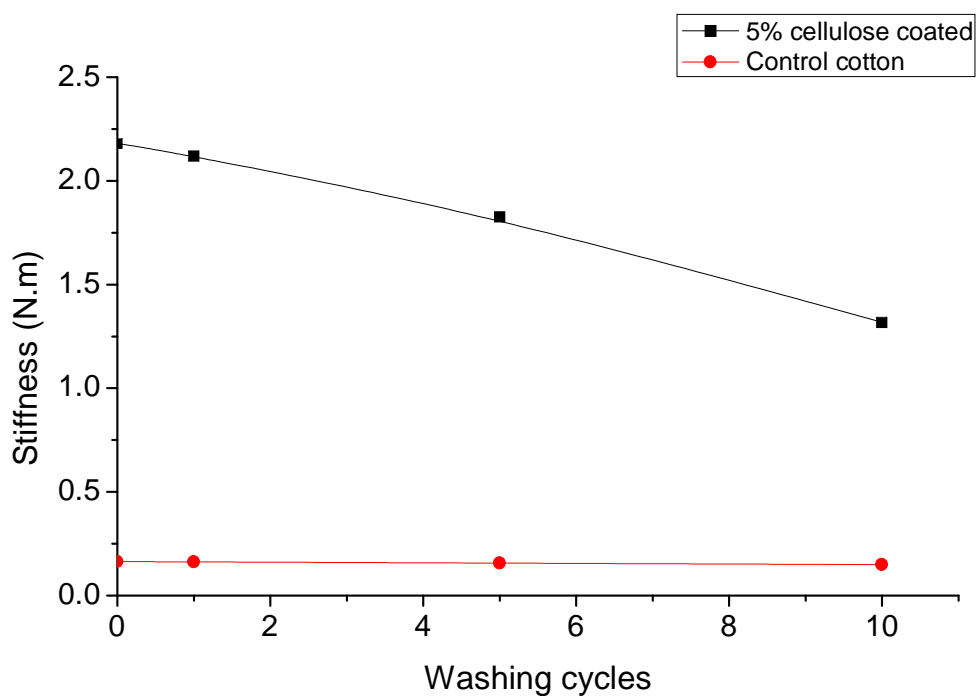


Figure 34. Durability of only cellulose coated cotton fabric against washing



Figure 34 shows the effect of washing on the stiffness of the cotton fabric. In figure 34, the exponential curves are form of the equation  $B=B_0+(B_{\infty}-B_0)(1-e^{-kw})$ . Here  $B$  is calculated stiffness,  $B_0$  is observed highest stiffness in sample,  $B_{\infty}$  is maximum stiffness (3 N.m),  $k$  is constant and  $w$  is washing cycle. This study was carried out with the 5 % cellulose-coated sample. Samples were washed with 4-gpl soap detergent at 40 °C. Figure 34 shows that the stiffness decreased slightly after the first washing, but thereafter there was no drastic change, and the stiffness remained high even after 10 washing cycles. There was no significant drop in stiffness after 5 washing cycles, because the stiffness decreased by only 0.29 N m between 5 and 10 washing cycles. This indicates that there is no need to reapply cellulose solution like starch. This study confirms that the stiffness obtained after applying cellulose to the surface of cotton fabric is permanent.

### 5.6.2 Stiffness of cellulose-TiO<sub>2</sub> coated cotton fabric in 60% Sulfuric acid solution

Stiffness is a special property of the fabric. It is a tendency of the fabric to keep standing without support. The bending force was measured to calculate the stiffness of the fabric on TH-7 instrument. Figure 35 compares the stiffness of control fabric with cellulose-TiO<sub>2</sub> coated cotton fabric. It is clear from figure 35 that the stiffness increases significantly when the cotton fabric is coated with cellulose.

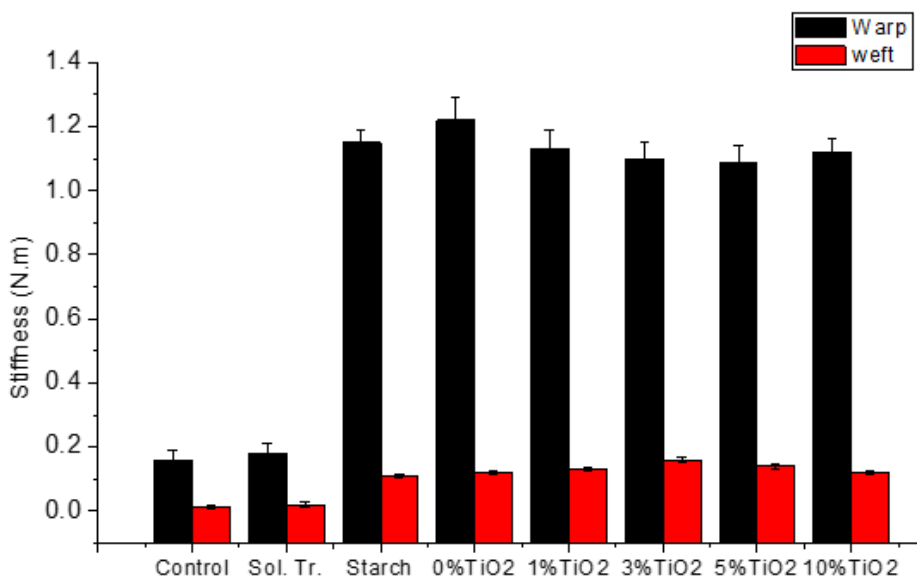


Figure 35. Stiffness of control, Solvent treated (Sol. Tr.), Starched, only cellulose (0% TiO<sub>2</sub>) and cellulose-TiO<sub>2</sub> coated cotton fabric.

The stiffness was slightly decreased when TiO<sub>2</sub> was added to the cellulose solution because viscosity of cellulose solution decreases after mixing TiO<sub>2</sub>. Xu et al explain how viscosity decreases after adding small amount of nanoparticles in to solution [148]. Viscosity decreases after adding TiO<sub>2</sub> in cellulose solution because nanoparticles reduce the polymer chain entanglement. Stiffness of all coated samples was higher than the control cotton fabric sample and comparable to starched sample. Stiffness of coated samples is in the range of 1.07 - 1.22 Nm. Solvent treated cotton fabric shows similar stiffness to control cotton fabric that means there was no effect of solvent treatment on stiffness of cotton fabric. Hence, cellulose coating increases the stiffness of cotton fabric significantly.

### **5.7 Durability stiffness against washing of cellulose-TiO<sub>2</sub> coated cotton fabric**

To study the effect of washing on stiffness of cellulose-TiO<sub>2</sub> coated cotton fabric, the fabric was washed with 4 g/l detergent at 40<sup>0</sup>C for 1 hr. Figure 36 shows the effect of washing on stiffness of coated fabrics. Coated samples with 1, 3 and 5 % TiO<sub>2</sub> show very good durability against washing up to 20 cycles. It is apparent from the figure 36 that stiffness decreased after 1<sup>st</sup> washing. However, the stiffness was stable after first washing with all cellulose-TiO<sub>2</sub> coated samples as compare to starched fabric. The fabric stiffness dropped after first cycle of washing by 0.68 Nm because loosely attached cellulose was washed away with water. There is no significant drop in stiffness after first washing because the stiffness was slightly decreased until after the 20<sup>th</sup> cycle of washing. Therefore, there is no need to reapply cellulose solution unlike starch. This study confirms that significantly higher level of stiffness is preserved as compared to starched fabric.

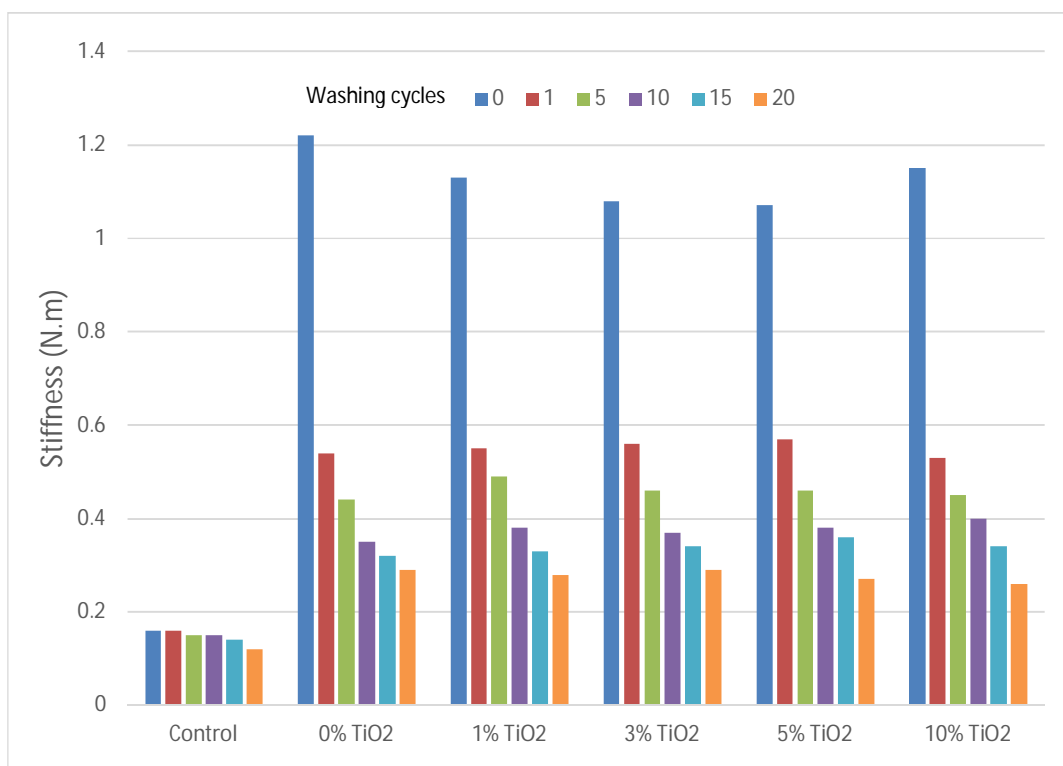


Figure 36. Durability of stiffness against washing

### 5.8 Antibacterial activity of cellulose-TiO<sub>2</sub> coated cotton fabric

Effect of TiO<sub>2</sub> coating on the growth of bacterias such as Escherichia coli G- CCM 2024, Klebsiella pneumoniae G- CCM 2318, Staphylococcus aureus G+ CCM 226 a MRSA (methicillin-resistant Staphylococcus aureus) G+ CCM 4223 were investigated. Figure 37 shows the pictures of bacterial growth on coated and uncoated cotton fabric against S. aureus (figure 37 (a)) and MRSA (figure (b)). Table 2 reflects the observation of bacterial reduction by AATCC 100. Table 2 shows that compact bacteria's were obtained in case of G-ve Escherichia coli (EC) and Klebsiella pneumonia (KP) bacterias. Table 3 gives the percentage reduction/multiplication of the test bacteria (G+ve S. aureus and MRSA) confirmed quantitatively utilizing the AATCC100 method. It is observed that the coating of fabrics with TiO<sub>2</sub>-cellulose had a positive reduction of S. aureus bacteria and MRSA bacteria. The effectiveness of the anti-microbial activity increased with increase in the concentration of the TiO<sub>2</sub> coating.

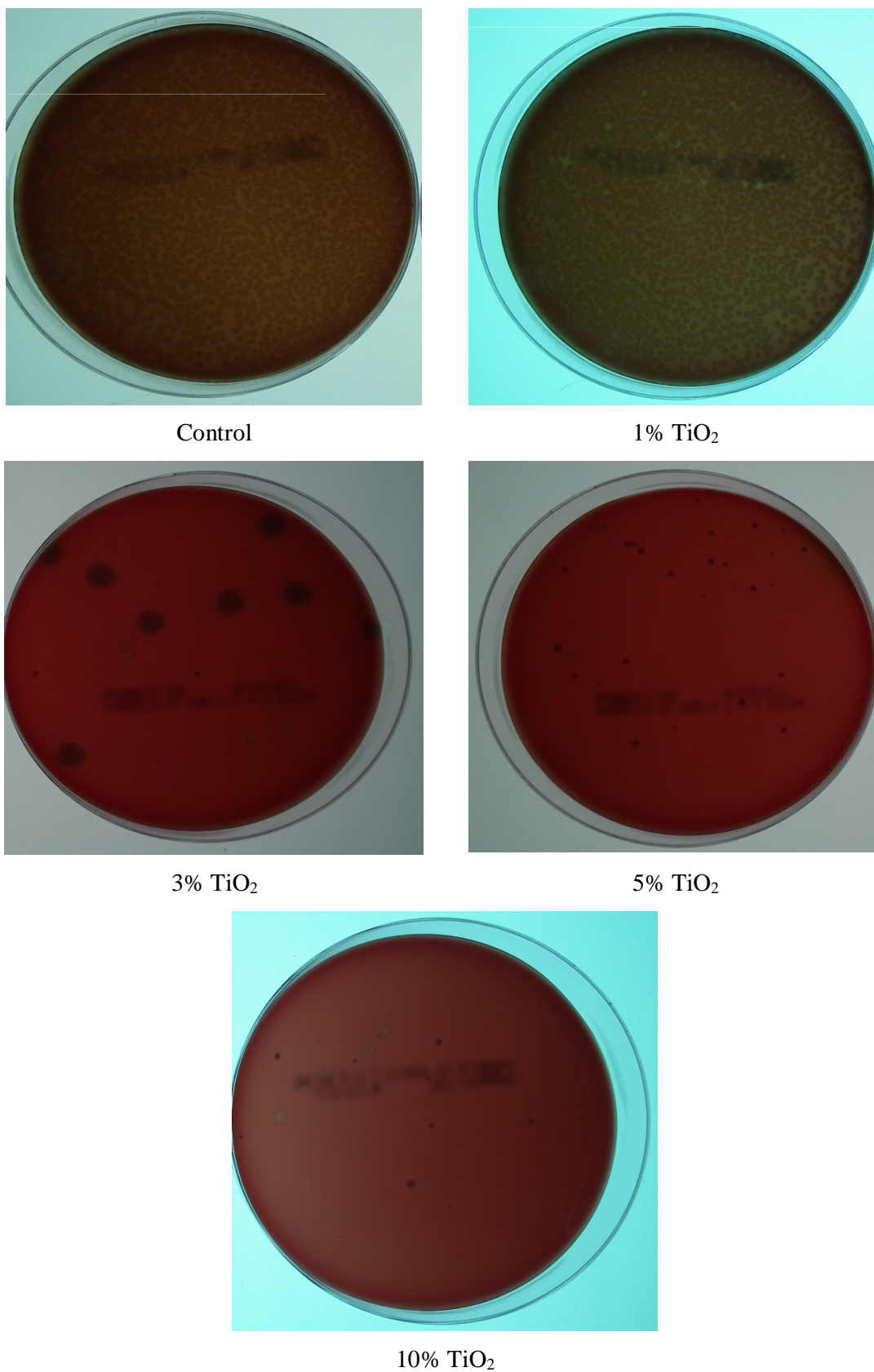


Figure 37. (a) Antibacterial activity against *Staphylococcus aureus* bacteria

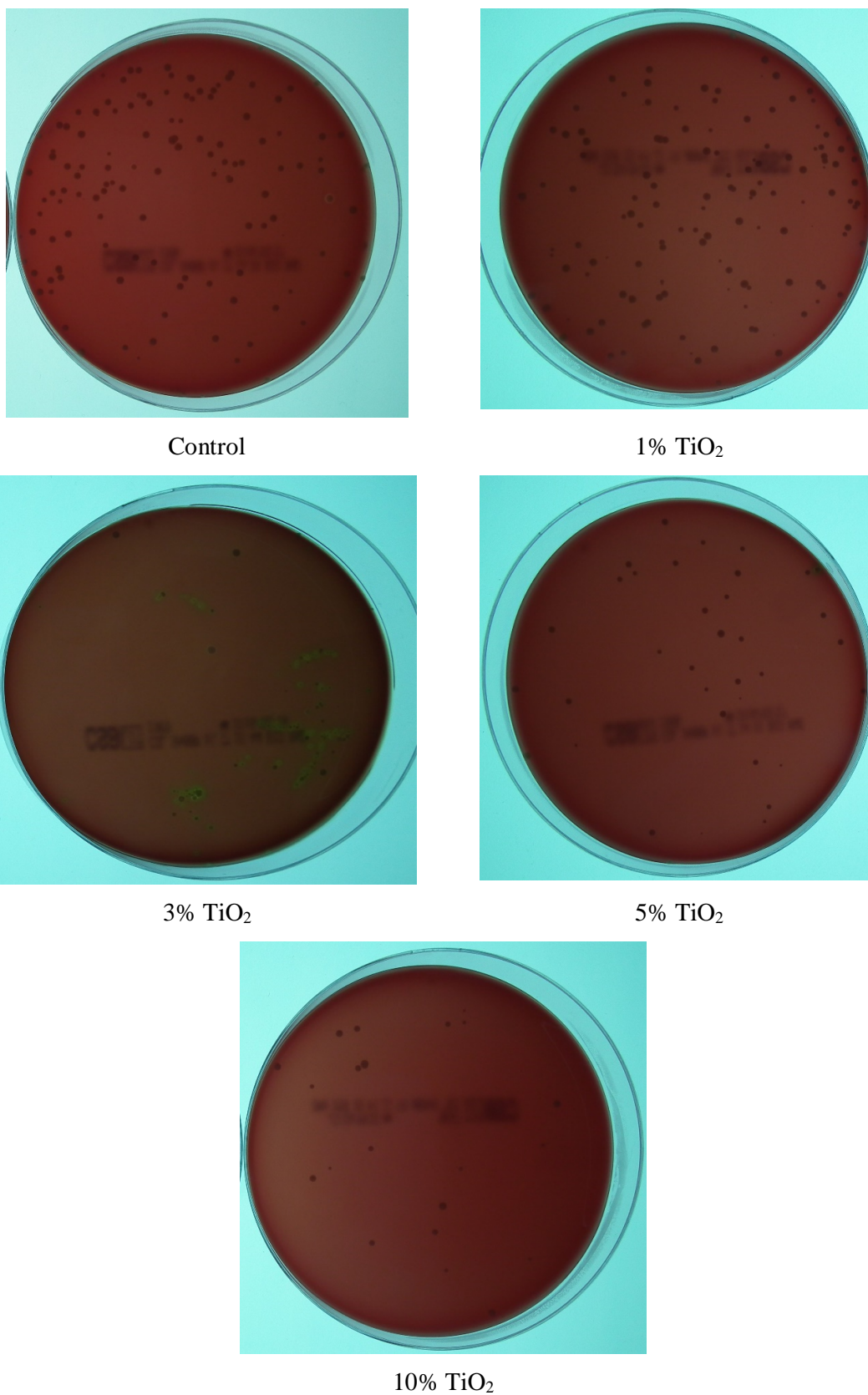


Figure 37. (b) Antibacterial activity against Methicillin-resistant Staphylococcus aureus

Fabrics treated with 1% TiO<sub>2</sub> had the lowest *S. aureus* bacterial reduction. However, with an increase in the concentration of TiO<sub>2</sub>, there was a high jump from 6.3% to 96.7% reduction of *S. aureus* bacteria on 3% TiO<sub>2</sub> treated fabrics. These results confirm that sample coated with 3, 5 and 10% TiO<sub>2</sub>-cellulose show strongest inhibition efficiency against bacteria's. The effectiveness of the anti-microbial activity increased with increase in the concentration of the TiO<sub>2</sub> coating. Fabrics treated with 1% TiO<sub>2</sub> had the lowest *S. aureus* bacterial reduction, however with an increase in the concentration of TiO<sub>2</sub>, there was a high jump from 6.3% to 96.7% reduction of *S. aureus* bacteria on 3% TiO<sub>2</sub> treated fabrics. Therefore, sample coated with 3, 5 and 10% TiO<sub>2</sub>-cellulose show strongest inhibition efficiency against G+ bacteria's and compact bacterias occurred against G- bacterias.

Table 2. Observation of bacterial reduction by AATCC 100

Method: AATCC100	Control	Cellulose coated	1% TiO <sub>2</sub>	3% TiO <sub>2</sub>	5% TiO <sub>2</sub>	10% TiO <sub>2</sub>
<i>Escherichia coli</i> 10 <sup>5</sup> CFU/ml	Compact bacteria occurrence	Compact bacteria occurrence	Compact bacteria occurrence	Compact bacteria occurrence	Compact bacteria occurrence	Compact bacteria occurrence
<i>Klebsiella pneumoniae</i> 10 <sup>5</sup> CFU/ml	Compact bacteria occurrence	Compact bacteria occurrence	Compact bacteria occurrence	Compact bacteria occurrence	Compact bacteria occurrence	Compact bacteria occurrence
<i>Staphylococcus aureus</i> 10 <sup>5</sup> CFU/ml	960	900	68	32	22	17
<i>MRSA</i> 10 <sup>5</sup> CFU/ml	104	120	98	42	34	22

Same samples were analysed according to AATCC147 standard method to investigate antibacterial activity. Unlike AATCC100, the results from AATCC147 (Table 4) shows no effect of cellulose-TiO<sub>2</sub> coating on G-ve bacterias such as *Escherichia coli* (EC) and *Klebsiella pneumonia* (KP). Also there is no effect of coating on G+ve *Staphylococcus aureus* (SA) and Methicillin resistant *staphylococcus aureus* (MRSA).



Table 3. Quantitative evaluation of bacterial reduction

Test Sample	Bacterial Reduction/Multiplication	
	Staphylococcus aureus (SA)	Methicillin-resistant Staphylococcus aureus (MRSA)
Control	-	-
1% TiO <sub>2</sub>	6.3	13.3
3% TiO <sub>2</sub>	96.7	65.0
5% TiO <sub>2</sub>	97.7	68.3
10% TiO <sub>2</sub>	98.2	81.6

Table 4. Evaluation of antibacterial testing by AATCC 147

Method:	Control	Cellulose				
AATCC147	Cotton fabric	coated cotton fabric	1 % TiO <sub>2</sub>	3 % TiO <sub>2</sub>	5 % TiO <sub>2</sub>	10 % TiO <sub>2</sub>
Escherichia coli 10 <sup>5</sup> CFU/ml	No effect	No effect	No effect	No effect	No effect	No effect
Klebsiella pneumoniae 10 <sup>5</sup> CFU/ml	Halo zone not clear Ø 1,74 mm	No effect	No effect	No effect	No effect	No effect
Staphylococcus aureus 10 <sup>5</sup> CFU/ml	Halo zone not clear Ø 4,93 mm	No effect	No effect	No effect	No effect	No effect
MRSA 10 <sup>5</sup> CFU/ml	No effect	No effect	No effect	No effect	No effect	No effect

### 5.9 Evaluation of antifungal activity of cellulose-TiO<sub>2</sub> coated cotton fabric

Antifungal activity of TiO<sub>2</sub> coated cotton fabric was evaluated with mixture of *Penicillium digitatum* (CCM F-382), *Rhizopus stolonifer* (CCM F-445), *Cladosporium sphaerospermum* (CCM F-351), *Chaetomium globosum* (CCM 8156) fungi's in aqueous suspension at a concentration of 10<sup>6</sup> CFU/ml. Figure 38 (a, b, c, d and f) shows the results of antifungal test. The surface of agar in the Petri dishes was completely covered with fungi (filamentous hyphae

forming the mycelium) in the first 4 days. However, the filamentous hyphae (mycelium) started to lose from the surface over the second week.

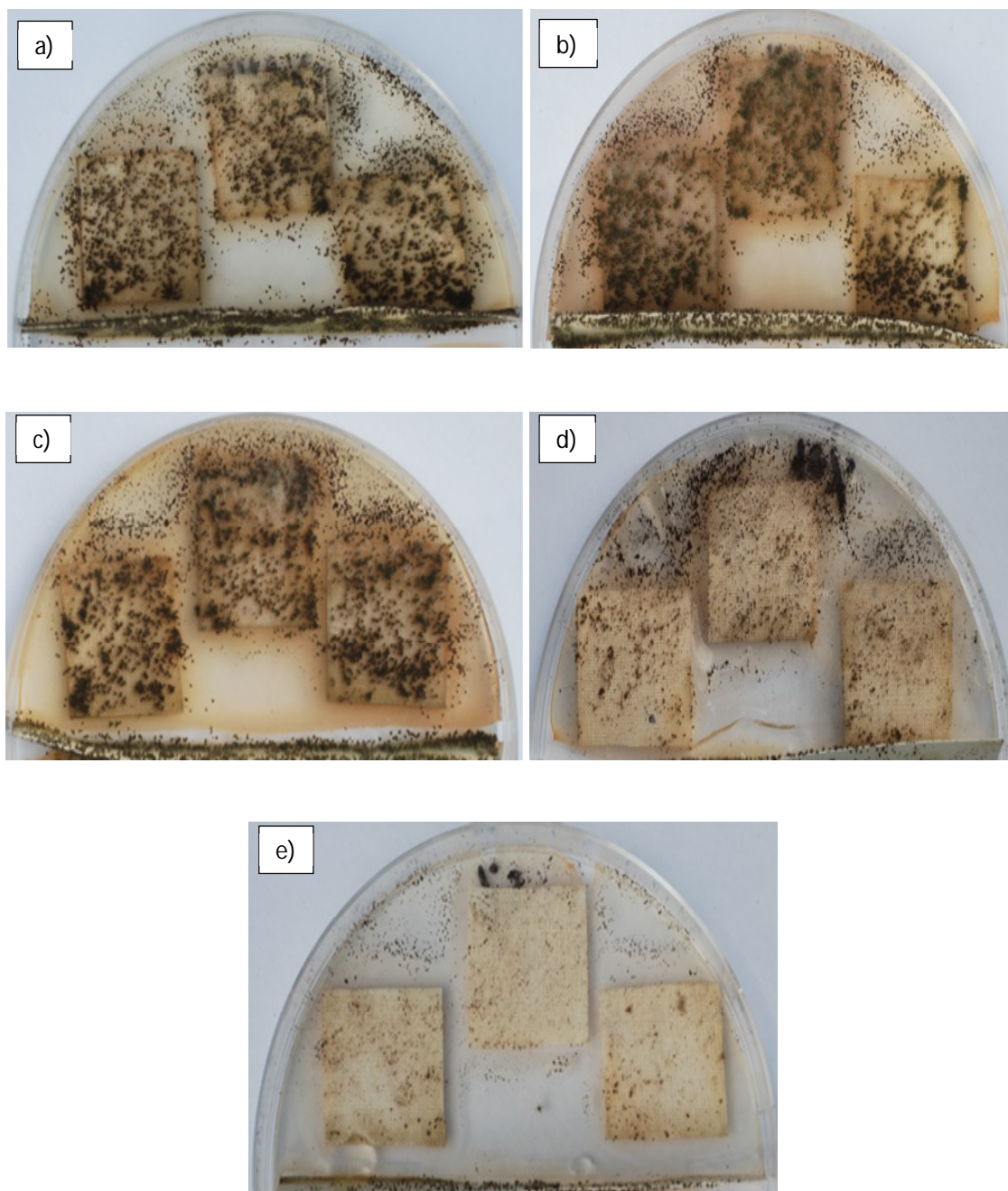


Figure 38. Antifungal activity of (a) Control (b) 1% TiO<sub>2</sub> (c) 3% TiO<sub>2</sub> (d) 5% TiO<sub>2</sub> and (e) 10 % TiO<sub>2</sub> coated cotton fabric



Finally, the samples containing the titanium dioxide of 5 and 10% were most cleared. The reason of this antibacterial activity is photocatalytic effect of TiO<sub>2</sub>, but this effect occurred slowly and later (during the second week of cultivation). The amount of fungi decreased with increasing concentration of TiO<sub>2</sub> from the beginning. Thus, long-term antifungal effect was observed on samples of cotton fabrics coated with TiO<sub>2</sub> at concentration of 5% or higher and according to the EN 14119, 2003 Standard [147] the grow of fungi ranged between degree 2 (high concentration of TiO<sub>2</sub>) and 4 (low concentration of TiO<sub>2</sub>) on the samples.

## **5.10 Investigation the effect of cellulose-TiO<sub>2</sub> coating and strong solvent on cellulose structure by X-ray diffraction patterns**

### **5.10.1 Effect of cellulose-TiO<sub>2</sub> coating and 60% Sulfuric acid on structure of cellulose**

X-ray diffraction patterns were obtained to detect TiO<sub>2</sub> and to investigate the effect of 60 % H<sub>2</sub>SO<sub>4</sub> solvent on cotton fabric. Figure 39 shows the X-ray diffraction patterns of the control and cellulose-TiO<sub>2</sub> coated cotton fabric. The characteristic peak at  $2\theta$  25.4° shows the presence of TiO<sub>2</sub> in 3, 5 and 10 % TiO<sub>2</sub> coated cotton fabric. 1 % TiO<sub>2</sub> coated cotton fabric does not show this peak presumably due to the lower concentration of TiO<sub>2</sub>. It can be seen from figure 39 that the peak height of TiO<sub>2</sub> at 25° increases with increasing concentration of TiO<sub>2</sub>. X-ray diffraction spectra of the control and cellulose-TiO<sub>2</sub> coated cotton fabric exhibited main characteristic diffraction peaks at 14.7°, 16.3°, and 22.4° of cellulose I. The small peak at 12.3° and the bigger shoulder at 20° confirm the presence of cellulose II in both control and the solvent treated samples. The control cotton fabric (figure 40) shows the peak of Cellulose II because of the chemical treatments used during the fabric processing to improve the properties of cotton, such as dimensional stability, reactivity, luster etc. The amount of cellulose II was estimated by simulation method [149-151]. The 'a' value ( $I\beta$  unit cell) was adjusted to 0.7906 nm from 0.7784 nm, because less perfectly ordered cotton cellulose.

The basic idea of this simulation is to fit combined x-ray diffraction patterns of cellulose I, II and amorphous fractions obtained from Mercury 3.0 program with diffraction pattern of treated sample to quantify cellulose fractions. Diffraction intensities, output by the Mercury program from the Cambridge Crystallographic Data Centre, have several uses including comparisons with experimental data. Calculated intensities from different polymorphs can be added in varying proportions using a spreadsheet program to simulate patterns such as those from partially mercerized cellulose or various composites.

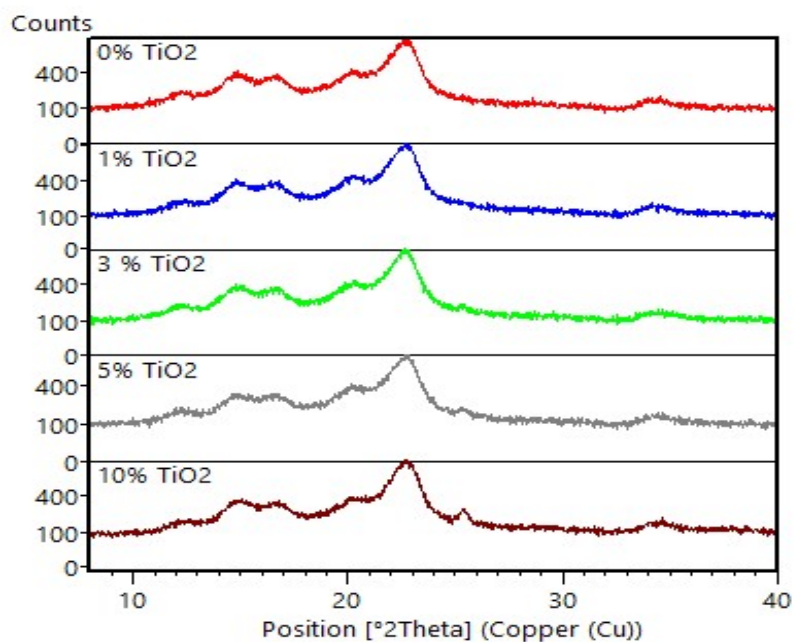


Figure 39. X-ray diffraction patterns of cellulose-TiO<sub>2</sub> coated cotton fabric

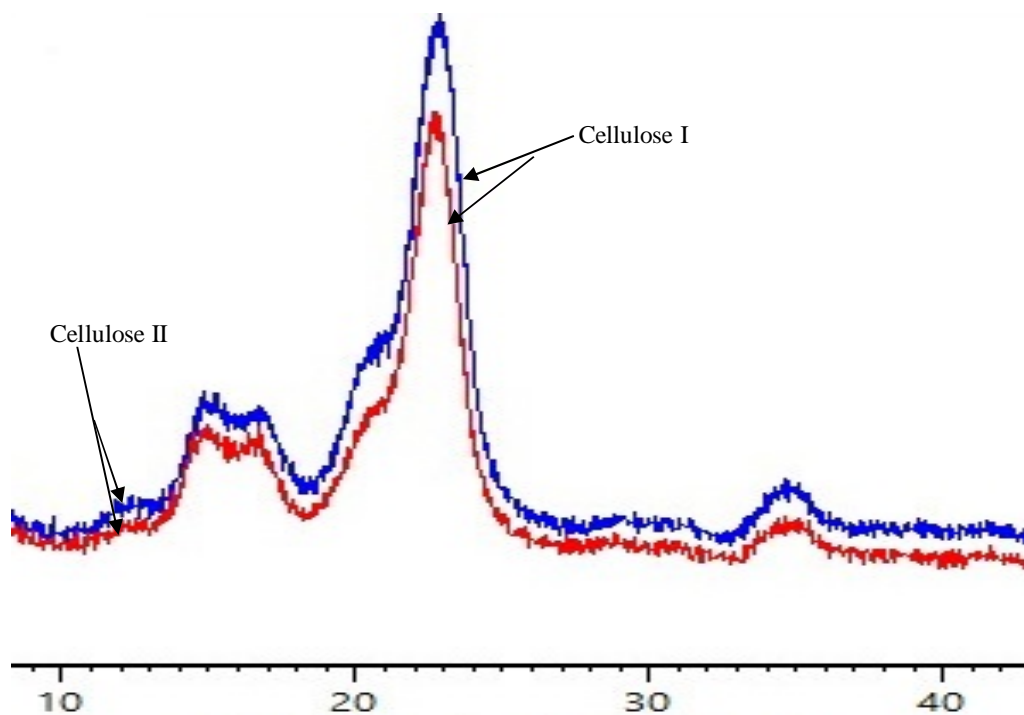


Figure 40. Diffraction pattern of Control (red curve) and solvent (without cellulose) treated (blue curve) cotton fabric

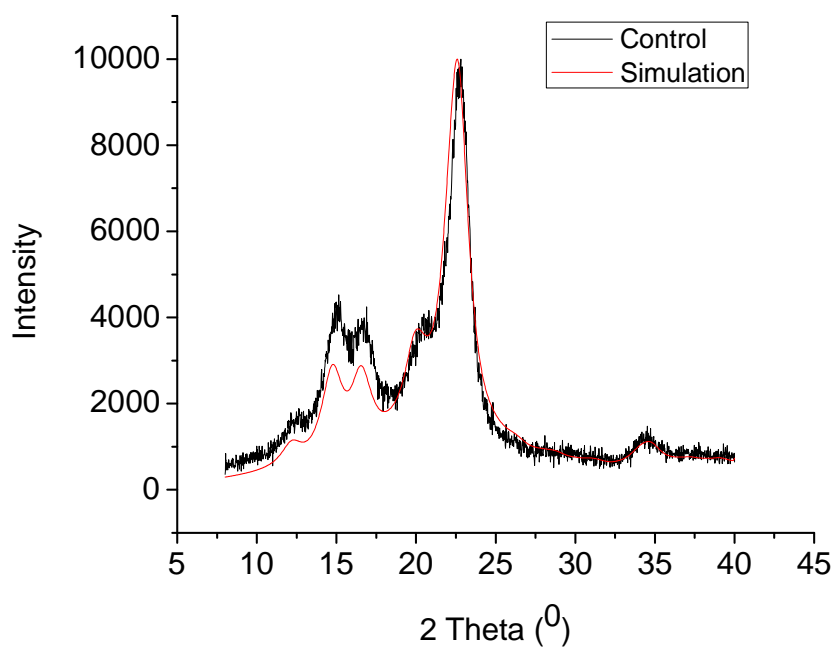


Figure 41. Diffraction pattern of control cotton fabric fitted with simulated pattern

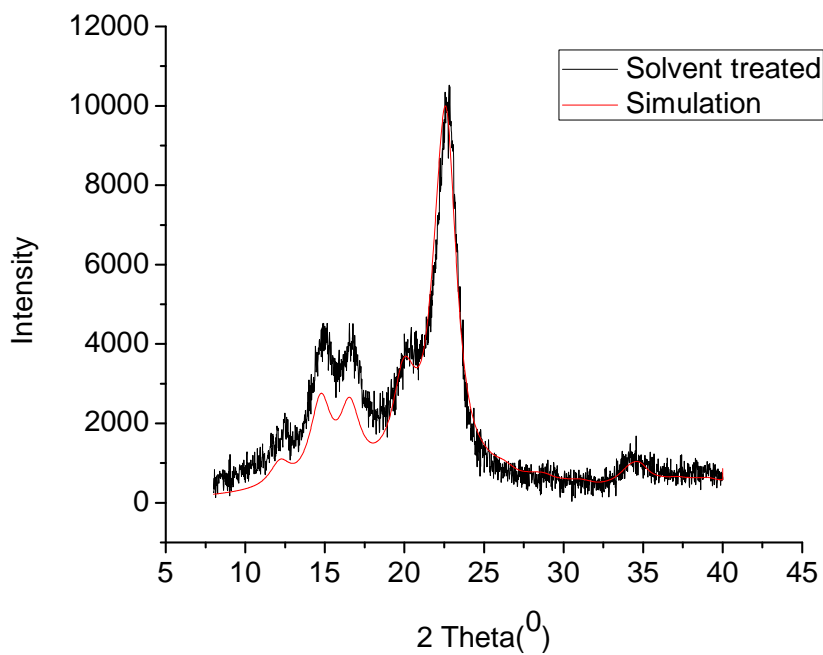


Figure 42. Diffraction pattern of 60 % H<sub>2</sub>SO<sub>4</sub> treated cotton fabric fitted with simulated pattern.

Amorphous cellulose significantly influences the diffraction pattern and that is why it was included in the simulation. To incorporate amorphous fraction into the simulation, the diffraction pattern of Cellulose II at 9 deg. FWHM was used [150]. Figure 41 and 42 are the diffraction patterns of 60 % H<sub>2</sub>SO<sub>4</sub> solvent treated and control cotton fabrics respectively fitted with corresponding simulated pattern. Table 5 shows the composition of cellulose in 60% H<sub>2</sub>SO<sub>4</sub> solvent treated and control cotton fabric. Solvent (60 % H<sub>2</sub>SO<sub>4</sub>) treated cotton fabric shows 22.2 % cellulose II, which is slightly higher than the control sample (16.9 %), that means there is an effect of the solvent on cotton fabric during coating. The effect of solvent on structure of cotton fabric was negligible because the treatment time was of 20 sec duration at room temperature which was the same conditions used for cellulose coating.

### **5.10.2 Effect of NaOH-Urea-Thiourea-Water solvent system on cellulose structure**

The effect of the urea–thiourea–NaOH–water solvent system on the cotton fabric was analyzed using X-ray diffraction analysis. Figure 43 shows an overlay of the X-ray diffraction spectra of the original (black) and regenerated (red) cellulose pulp, while figure 44 shows an overlay of the X-ray diffraction spectra of control (black) and urea–thiourea–NaOH–water-treated (red) cotton fabric. In figure 43, the characteristic peak of cellulose I at 16.20° is missing for the regenerated pulp cellulose while the peaks at 12.3° and 21.20° show that the structure of the pulp cellulose has been converted from cellulose I to II. The X-ray diffraction spectra and overlapping peak resolution of the control and solvent-treated cotton fabric show main characteristic diffraction peaks at 14.7°, 16.3°, and 22.4° for cellulose I. The small peak at 12.3° and larger shoulder at 20° show the presence of cellulose II in both samples (figure 44) with slightly more in the solvent-treated (red curve) sample. The control cotton fabric showed peak of cellulose II because of the chemical treatments used during fabric processing to improve properties of cotton such as its dimensional stability, reactivity, luster, etc. [152]. The amount of cellulose II was estimated by the simulation method [149-151]. The 'a' value was adjusted to 0.7906 nm because of the less perfectly ordered cotton cellulose. Amorphous cellulose significantly influenced the diffraction pattern and was therefore included in the simulation. The diffraction pattern of cellulose II with FWHM of 9° was used for amorphous cellulose [150] in the simulation. Figures 45 and 46 show the diffraction pattern of the control and solvent-treated cotton fabrics, respectively, fit with the corresponding simulated pattern.

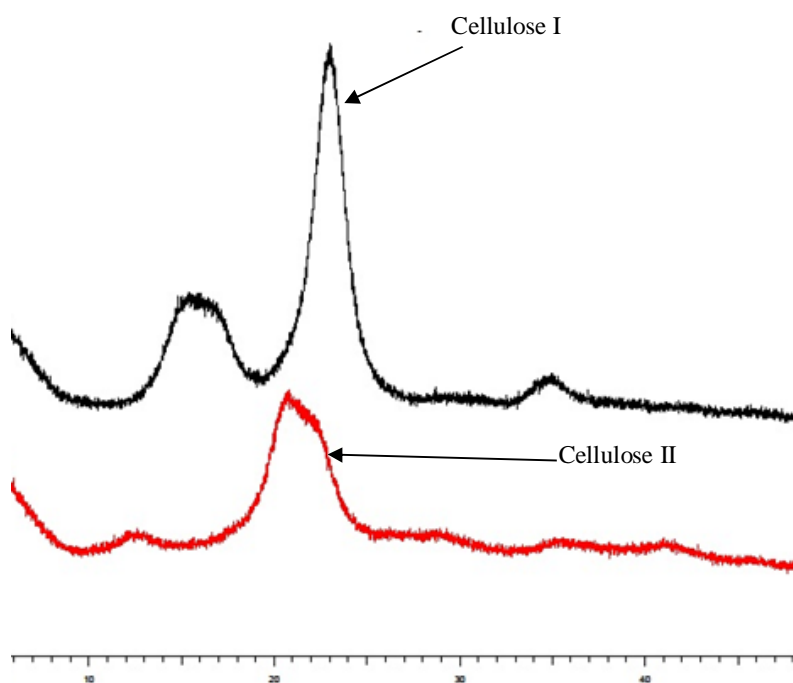


Figure 43. X-ray diffraction pattern and analysis of original (Black) and regenerated (Red) cellulose pulp.

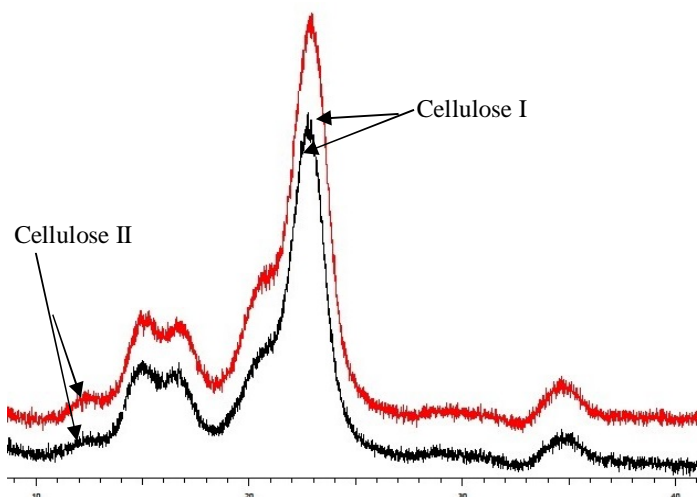


Figure 44. X-ray diffraction pattern and analysis of control (black) and solvent treated cotton fabric (Red).

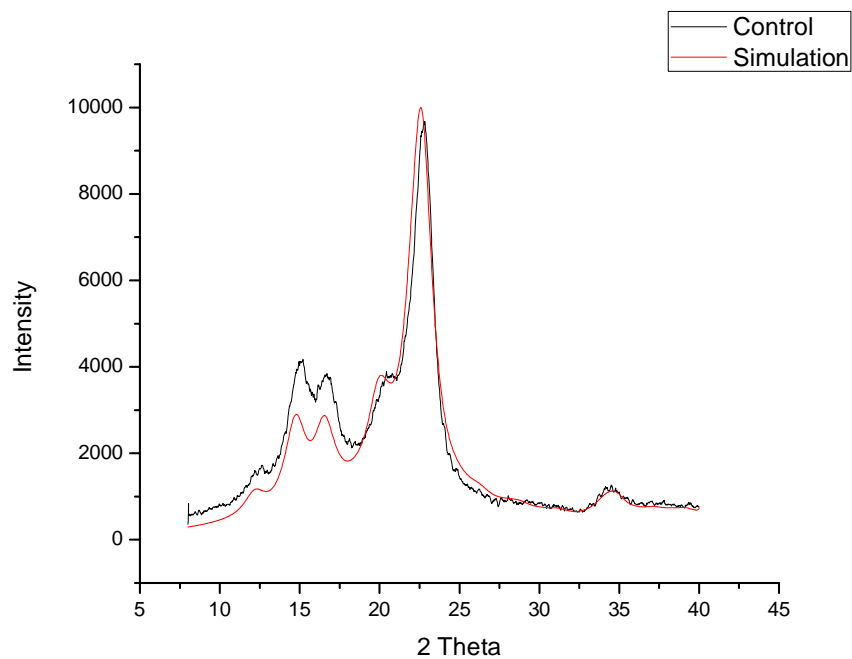


Figure 45. Diffraction pattern of control cotton fabric fitted with simulated pattern.

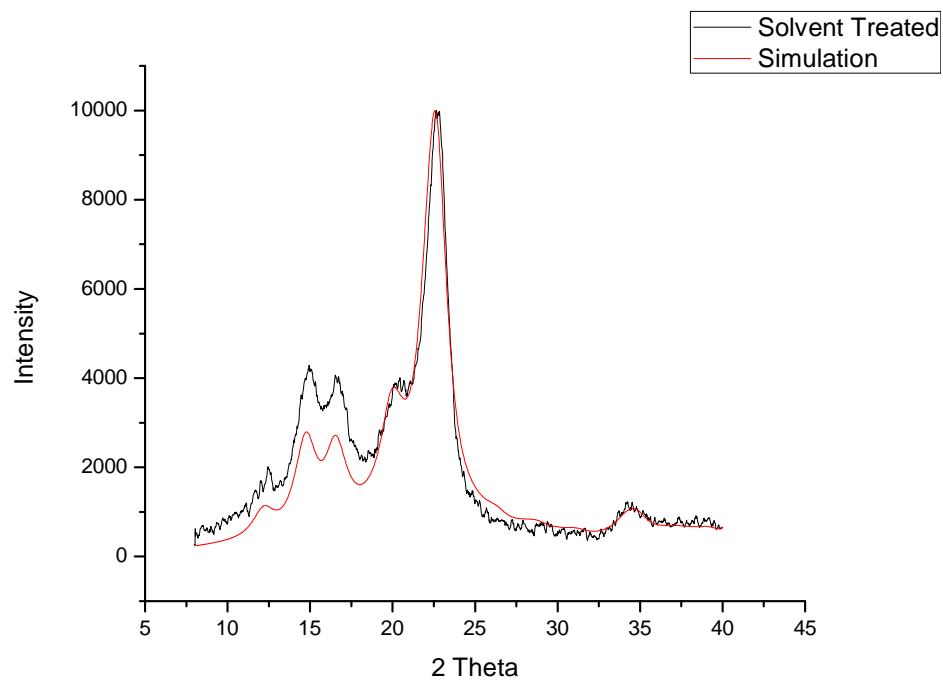


Figure 46. Diffraction pattern of solvent treated cotton fabric fitted with simulated pattern.

Table 5 presents the composition of cellulose in the control and solvent-treated cotton fabric. Solvent-treated cotton fabric showed a slightly greater amount of cellulose II (21.5 %) compared with the control sample (16.9 %), indicating a solvent effect on the cotton fabric during coating. The effect of the urea–thiourea–NaOH–water solvent system on the structure of the cotton fabric was small because the treatment time was just 20 second at room temperature, with the same conditions used for cellulose coating.

Table 5. Estimation of cellulose fractions

Sample description	Cellulose I [%]	Cellulose II [%]	Amorphous cellulose [%]
Control cotton fabric	47.5	16.9	35.6
NaOH-Urea-Thiourea-Water	45.2	21.5	33.3
60 % H <sub>2</sub> SO <sub>4</sub> treated cotton fabric	44.7	22.2	33.1

### 5.11 Colour strength and related parameter

The K/S value of the dyed fabric was directly proportional to the amount of dye present in the fabric. The relative color strength (%) and K/S values of the cellulose-coated dyed samples are presented in Table 6 from which it is clear that the K/S values of the cellulose-coated dyed fabrics were lower than for control dyed samples. Dye uptake decreased as the cellulose concentration was increased, as reflected in the observed values. Reactive Blue 49 dye showed better dyeability than Reactive Red 240 or Reactive Yellow 95. The lower K/S values for the cellulose-coated cotton fabrics are related to the applied cellulose. The possible cause of this decrease is that the coated pulp cellulose was mercerized after dissolution, reducing dye uptake by the fabric because it was on the surface. Table 6 shows that the relative color strength (%) of the dyed samples decreased with increasing cellulose concentration for each shade % of the dye. These results further indicate that the cellulose coating decreased the dye uptake by the coated cotton fabric.

Table 6. Spectrophotometric analysis of dyed sample

Dye Content [% owf]	Dye	Cellulose concentration [%]	L*	a*	b*	$\Delta E$	K/S	Standard Deviation [ $\sigma$ ] K/S	C.I. (Half size) K/S	Relative color strength [%]
3	Reactive Red 240	Control	53.22	61.15	2.25	0	7.29	0.65	0.81	100
		1	59.33	62.21	2.75	6.22	2.54	0.38	0.47	34.87
		3	61.34	62.98	3.23	8.38	2.36	0.25	0.31	32.45
		5	63.75	63.26	3.56	10.81	2.25	0.32	0.40	30.97
	Reactive Yellow 95	Control	81.51	16.63	66.91	0	8.15	0.45	0.56	100
		1	82.59	17.26	67.49	1.37	3.74	0.85	1.05	45.98
		3	82.87	15.14	61.93	5.37	3.07	0.63	0.78	37.72
		5	84.32	21.28	73.46	8.51	3.21	0.56	0.70	39.45
	Reactive Blue 49	Control	24.91	-3.89	-18.1	0	20.47	0.25	0.31	100
		1	25.12	-3.45	-17.18	1.04	13.72	1.32	1.64	67.03
		3	27.25	-2.77	-15.99	3.34	13.3	1.25	1.55	64.98
		5	28.32	-2.45	-15.58	4.47	12.49	1.71	2.12	61.04
9	Reactive Red 240	Control	42.17	59.55	13.72	0	20.75	0.61	0.76	100
		1	47.26	61.1	5.66	9.65	12.14	1.98	2.46	58.51
		3	48.37	61.85	5.72	10.37	8.79	1.59	1.97	42.36
		5	49.98	62.12	5.85	11.38	7.7	1.92	2.38	37.15
	Reactive Yellow 95	Control	73.32	15.53	69.91	0	21.73	0.31	0.38	100
		1	75.59	16.26	67.49	3.39	13.67	0.92	1.14	62.92
		3	80.87	16.64	66.93	8.19	12.1	1.45	1.80	55.69
		5	82.32	17.12	62.46	11.79	8.71	2.1	2.61	40.09
	Reactive Blue 49	Control	16.11	-4.22	-15.1	0	26.63	1.21	1.50	100
		1	16.92	-3.35	-14.68	1.26	23.28	1.82	2.26	87.41
		3	17.25	-3.67	-14.09	1.61	22.59	1.61	2.00	84.83
		5	18.32	-3.75	-13.78	2.61	17.12	1.77	2.20	64.31
15	Reactive Red 240	Control	37.94	57.92	14.72	0	24.91	1.10	1.37	100
		1	46.1	58.1	5.56	12.26	13.46	1.55	1.92	54.05
		3	47.21	58.98	5.61	13.04	12.4	1.20	1.49	48.32
		5	47.42	59.23	5.67	13.17	9.14	1.65	2.05	36.7
	Reactive Yellow 95	Control	69.32	14.63	66.91	0	25.74	0.85	1.05	100
		1	72.52	17.26	59.49	8.49	16.13	1.62	2.01	62.67
		3	74.38	15.14	58.93	9.46	15.46	1.23	1.53	60.05
		5	75.13	21.28	59.46	11.55	11.71	1.10	1.37	45.48
	Reactive Blue 49	Control	12.11	-5.45	-13.01	0	29.68	0.52	0.65	100
		1	15.02	-4.55	-12.88	3.04	25.6	0.95	1.18	86.26
		3	15.95	-4.87	-12.19	3.96	24.78	1.09	1.35	83.49
		5	16.41	-3.95	-11.78	4.71	18.69	1.32	1.64	62.99



The Commission Internationale de l'Eclairage (CIE) Lab system was used to determine the color parameters and color variation, where L\* indicates the darkness–lightness value with 0 to 100 representing black to white, the a\* value goes from negative (green) to positive (red), and the b\* value goes from negative (blue) to positive (yellow);  $\Delta E$  gives the total color difference. High L\* values indicate that the dyed coated sample was lighter than the uncoated sample. Reactive Blue 49 dye showed lower L\* values (Table 6) than Reactive Red 240 or Reactive Yellow 95. However, the L\* value increased with increasing cellulose concentration, meaning that all the coated samples were brighter compared with uncoated cotton fabric. The color difference values ( $\Delta E$ ) are presented in Table 6, showing that there was a significant color difference between the uncoated and coated cotton fabric samples with different cellulose concentrations, even though both samples were dyed with the same dye concentration. The  $\Delta E$  values for the samples dyed with Reactive Blue 49 were better than for the other two dyes used for dyeing. Hence, Reactive Blue 49 showed better dyeability of coated cotton fabric compared with Reactive Red 240 or Reactive Yellow 95.  $\Delta E$  for Reactive Blue 49 dyed samples are better than other two dyes which was used for dyeing. Hence the Reactive Blue 49 has better dyeability to coated cotton fabric as compare to Reactive Red 240 and Reactive Yellow 95.

### **5.12 Evaluation of fastness properties**

During the use of textiles, they are frequently put through washing, rubbing & perspiration, therefore durability of coated cotton fabric to these conditions is very important and that's why it was evaluated and given in Table 7. Washing and rubbing fastness was evaluated for all the three types of dyed fabric. Washing fastness of cellulose coated cotton fabric for staining with adjacent fabrics (wool and cotton) for all dyed fabrics are excellent (4–5) & for change in color are also fine (2-3). Ratings against rubbing for cellulose coated cotton fabrics are good, 4 at dry rubbing and 3 at wet rubbing conditions. Thus, there is no significant impact of cellulose coating on washing and rubbing fastness properties of cotton fabric. Perspiration fastness at acidic & alkaline condition in terms of gray scale ratings for cellulose coated and uncoated samples are given in Table 8. The gray scale ratings in the case of cellulose coated dyed samples for change in color are 2-3 at both acidic and alkaline, that means dyed samples are sensitive towards pH. Rating 4-5 for staining with wool as adjacent fabrics are excellent and with cotton as adjacent fabric are also good. Perspiration fastness was observed for all three kind of dyed samples and almost ratings are similar to all dyed samples. Hence the perspiration fastness after coating cellulose on the surface of cotton fabric remain good.

Table 7. Washing and Rubbing Fastness properties assessment of dyed samples

Dye Content [% owf]	Dye	Cellulose Content [%]	Wash Fastness		Rubbing Fastness	
			Evaluation of change in color	Evaluation of staining		Evaluation of staining
				Cotton	Wool	
3	Reactive Red 240	Control	2-3	4-5	4-5	4-5
		1	2-3	4-5	4-5	4-5
		3	2-3	4-5	4-5	4-5
		5	2-3	4-5	4-5	3
	Reactive Yellow 95	Control	2-3	4-5	4-5	4-5
		1	2-3	4-5	4-5	4-5
		3	2-3	4-5	4-5	4-5
		5	2-3	4-5	4-5	3
	Reactive Blue 49	Control	2-3	4-5	4-5	4-5
		1	2-3	4-5	4-5	4-5
		3	2-3	4-5	4-5	4-5
		5	2-3	4-5	4-5	3
9	Reactive Red 240	Control	2-3	4-5	4-5	4-5
		1	2-3	4-5	4-5	4-5
		3	2-3	4-5	4-5	4-5
		5	2	4-5	4-5	3
	Reactive Yellow 95	Control	2-3	4-5	4-5	4-5
		1	2-3	4-5	4-5	4-5
		3	2-3	4-5	4-5	4-5
		5	2	4-5	4-5	3
	Reactive Blue 49	Control	2-3	4-5	4-5	4-5
		1	2-3	4-5	4-5	4-5
		3	2-3	4-5	4-5	4-5
		5	2	4-5	4-5	3
15	Reactive Red 240	Control	2-3	4-5	4-5	4
		1	2-3	4-5	4-5	4
		3	2	4-5	4-5	4
		5	2	4-5	4-5	3-4
	Reactive Yellow 95	Control	2-3	4-5	4-5	4
		1	2-3	4-5	4-5	4
		3	2-3	4-5	4-5	4
		5	2	4-5	4-5	3-4
	Reactive Blue 49	Control	2-3	4-5	4-5	4
		1	2-3	4-5	4-5	4
		3	2-3	4-5	4-5	4
		5	2	4-5	4-5	3-4

Table 8. Perspiration Fastness assessment of dyed samples

Dye Content [% owf ]	Dye	Cellulose Content [%]	Perspiration Fastness					
			Evaluation of change in color		Evaluation of staining			
			Acidic	Alkaline	Acidic		Alkaline	
					With wool	With cotton	With wool	With cotton
3	Reactive Red 240	Control	2-3	2-3	4-5	4-5	4-5	3-4
		1	2-3	2-3	4-5	4-5	4-5	3-4
		3	2-3	2-3	4-5	4-5	4-5	3-4
		5	2-3	2-3	4-5	4-5	4-5	3-4
	Reactive Yellow 95	Control	2-3	2-3	4-5	4-5	4-5	3-4
		1	2-3	2-3	4-5	4-5	4-5	3-4
		3	2-3	2-3	4-5	4-5	4-5	3-4
		5	2-3	2-3	4-5	4-5	4-5	3-4
	Reactive Blue 49	Control	2-3	2-3	4-5	4-5	4-5	3-4
		1	2-3	2-3	4-5	4-5	4-5	3-4
		3	2-3	2-3	4-5	4-5	4-5	3-4
		5	2-3	2-3	4-5	4-5	4-5	3-4
9	Reactive Red 240	Control	2-3	2-3	4-5	3-4	4-5	3-4
		1	2-3	2-3	4-5	3-4	4-5	3-4
		3	2-3	2-3	4-5	3-4	4-5	3-4
		5	2-3	2-3	4-5	3-4	4-5	3-4
	Reactive Yellow 95	Control	2-3	2-3	4-5	3-4	4-5	3-4
		1	2-3	2-3	4-5	3-4	4-5	3-4
		3	2-3	2-3	4-5	3-4	4-5	3-4
		5	2-3	2-3	4-5	3-4	4-5	3-4
	Reactive Blue 49	Control	2-3	2-3	4-5	3-4	4-5	3-4
		1	2-3	2-3	4-5	3-4	4-5	3-4
		3	2-3	2-3	4-5	3-4	4-5	3-4
		5	2-3	2-3	4-5	3-4	4-5	3
15	Reactive Red 240	Control	2-3	2-3	4-5	3-4	4-5	3-4
		1	2-3	2-3	4-5	3-4	4-5	3-4
		3	2-3	2-3	4-5	3-4	4-5	3-4
		5	2-3	2-3	4-5	3-4	4-5	3
	Reactive Yellow 95	Control	2-3	2-3	4-5	3-4	4-5	3-4
		1	2-3	2-3	4-5	3-4	4-5	3-4
		3	2-3	2-3	4-5	3-4	4-5	3
		5	2-3	2-3	4-5	3-4	4-5	3
	Reactive Blue 49	Control	2-3	2-3	4-5	3-4	4-5	3-4
		1	2-3	2-3	4-5	3-4	4-5	3-4
		3	2-3	2-3	4-5	3-4	4-5	3
		5	2-3	2-3	4-5	3-4	4	3

#### 4.13 Mechanical properties

Breaking strength of cotton and cellulose-TiO<sub>2</sub> coated fabric was measured on Testometric M250 - 2.5 instrument. Breaking strength of coated and the uncoated cotton fabric is shown in figure 47. It is clear from figure 47 that the tensile strength increased after coating of cellulose-TiO<sub>2</sub> on the surface of the cotton fabric. The breaking strength of cellulose-TiO<sub>2</sub> coated fabric is increased by 65-83 N. The strength of coated fabric was increased because coated cellulose attaches on the surface in the form of thin layer and this attached cellulose provides additional strength to cotton fabric. Tensile strength was not decreased even though strong solvent was used for coating because while coating solvent does not interact strongly with cotton cellulose and was confirmed by analyzing X-ray diffraction patterns of solvent treated cotton fabric. Table 9 shows modulus and % elongation of coated and uncoated cotton fabric. Results show that modulus and elongation increases after cellulose coating. It also confirms that only cellulose coating increases the strength, elongation and modulus of cotton fabric. Hence the added strength due to cellulose made the fibrous material withstand more load with increase in elongation.

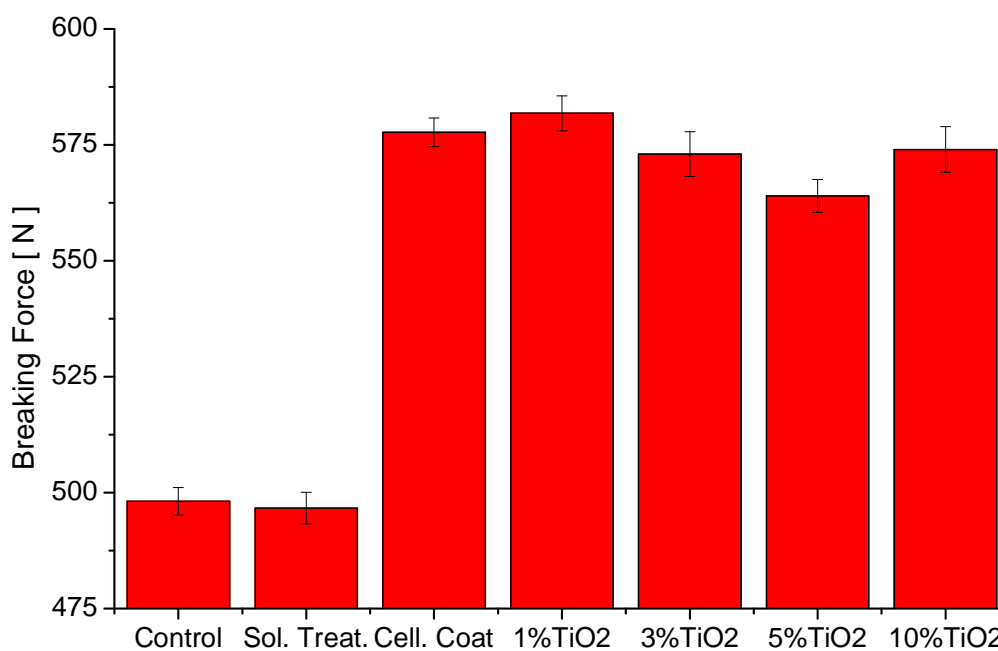


Figure 47. Breaking strength of control, Solvent treated (Sol. Treat.) and coated cotton fabrics.

Table 9. Mechanical properties

Sample description	Modulus (E) [Mpa]	Elongation [%]
Control	121.73	6.23
Solvent treated	121.37	7.33
Only cellulose coated	141.18	8.19
1% TiO <sub>2</sub> coated	142.17	8.23
3% TiO <sub>2</sub> coated	140.03	7.99
5% TiO <sub>2</sub> coated	137.83	7.40
10 % TiO <sub>2</sub> coated	140.27	8.39

#### 5.14 Air and water vapor permeability

Air and water vapor permeability are the important comfort properties of textiles. It is necessary to analyze the effect of coating on comfort properties of textiles. Figure 48 shows the effect of cellulose coating on air (figure 48 (a)) and water vapor permeability (figure 48 (b)) of the cotton fabric.

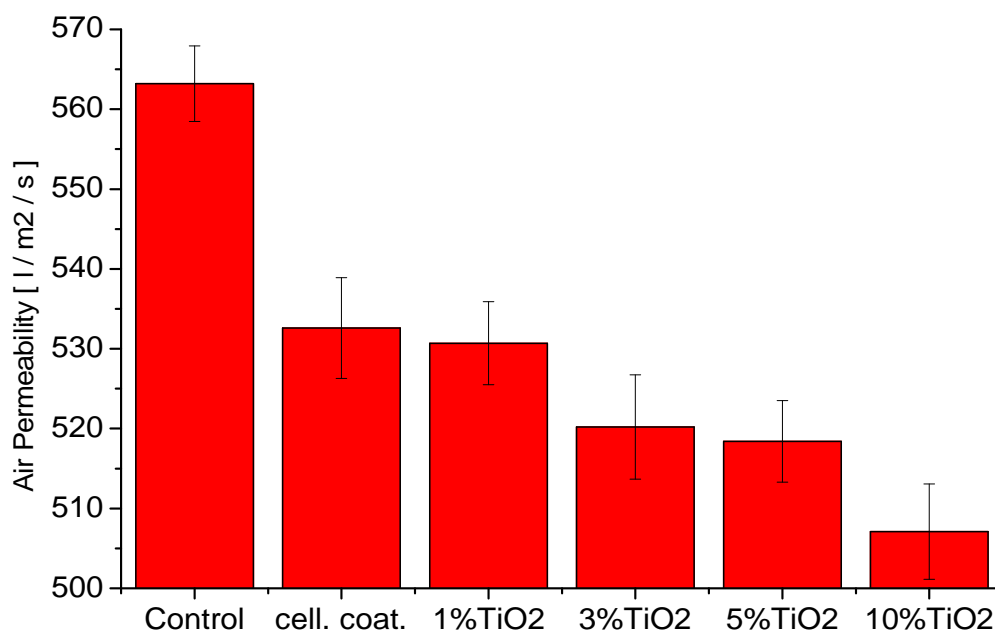


Figure 48. (a) Effect of cellulose-TiO<sub>2</sub> coating on air permeability of cotton fabric

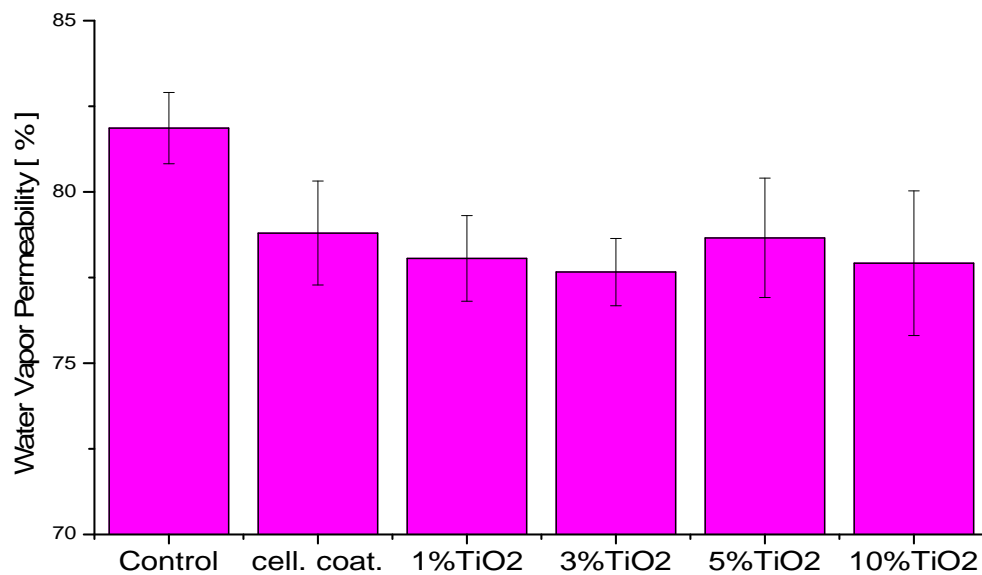


Figure 48. (b) Effect of cellulose coating on water vapor permeability of cotton fabric

Air permeability of cotton fabric was decreased by 32.5 to 56.1  $l/m^2/s$ . However, there was no significant deterioration of air permeability. Water vapor permeability was also slightly decreased (3.94 %) but is acceptable. 10% TiO<sub>2</sub> showed lower air and water vapor permeability as compared to other samples. Cellulose forms a thin film on the surface of the cotton fabric and covers the space between two yarns, which is the main cause that permeability was decreased slightly after cellulose coating. From the results, it can be concluded that there is no significant drop in both air and water vapor permeability after cellulose-TiO<sub>2</sub> coating on the surface of the cotton fabric.

## CHAPTER 6

### CONCLUSIONS

This study has produced new route to make cotton fabric self-cleaning, antibacterial, antifungal and highly stiff. Cellulose-TiO<sub>2</sub> nanoparticles were coated on the surface of cotton fabric by using roller padding. Novel method was developed for quantification of cellulose fractions by simulating X-ray diffraction patterns to investigate the effect of strong solvent during coating on cotton fabric. Degradation of Orange II dye under UV light was evaluated by using “Image J” software. Effect of cellulose coating on dyeing, color fastness, perspiration fastness, rubbing fastness and washing fastness was studied by using three reactive dyes. Antibacterial activity was analysed with four different bacterias such as Escherichia coli, Klebsiella pneumonia, Staphylococcus aureus and Methicillin resistant staphylococcus aureus. The following findings were drawn from the results;

#### 6.1 SEM and X-ray diffraction

Surface morphology showed that coated cellulose is attached to cotton fibres and this is due to interchain linkage between coated cellulose molecules and cotton fabric cellulose molecules of cotton fabric by intermolecular hydrogen bonding. Since both the molecules are same and both have hydrogen bonding, it is difficult to prove by using spectroscopic measurements. However, SEM pictures and washing study confirms that coated cellulose is strongly attached to cotton fabric. Coated cellulose forms thin film on the surface of cotton fabric and it holds the TiO<sub>2</sub> nanoparticles. Presence of characteristic peak of TiO<sub>2</sub> at 25.4° in x-ray diffraction pattern of cellulose-TiO<sub>2</sub> coated cotton fabric confirms successful coating process. Since strong solvent is used for this study, the effect of solvent on cotton fabric has been studied by developing simulation model based on X-ray diffraction patterns. According to simulation amount of cellulose II was increased slightly after solvent treatment.

#### 6.2 Photocatalytic Self-cleaning

Degradation of orange II dye was increased with increasing TiO<sub>2</sub> concentration and irradiation time. Wine stain degradation evaluation proved that cotton fabric coated TiO<sub>2</sub> and cellulose is capable for self-cleaning. The samples coated with 1, 3 and 5% TiO<sub>2</sub> were stable against washing up to 10 washing cycles for both self-cleaning and stiffness properties. However, 10% TiO<sub>2</sub> coated sample does not show similar stability against washing due to poor dispersion of

TiO<sub>2</sub> in cellulose solution. We, therefore claim that cellulose-TiO<sub>2</sub> coating makes cotton fabric self-cleaning.

### **6.3 Stiffness**

Dissolved cellulose can be coated on cotton fabric to improve its stiffness permanently. Stiffness of cellulose coated cotton fabric increased with increasing cellulose concentration. Only coated cellulose is responsible to increase stiffness so there is no effect of TiO<sub>2</sub> on stiffness of cotton fabric. Stiffness of cotton fabric can be controlled by changing cellulose concentration while coating according to requirement. The washing study confirmed that the stiffness of the cellulose-coated cotton fabric was permanent.

### **6.4 Antibacterial and Antifungal activity**

Samples coated with TiO<sub>2</sub> showed significant reduction of Staphylococcus aureus and Methicillin-resistant Staphylococcus aureus bacteria under UV light. Samples coated with more than 3% TiO<sub>2</sub> showed strongest inhibition efficiency against these bacteria's. Antifungal testing results showed that the photo-catalytic activity of titanium dioxide nanoparticles allows a disinfection of cotton fabric from fungal colonization. The antibacterial, self-cleaning, and antifungal properties of coated samples were increased with increasing amount of titanium dioxide. Therefore, we claim that Nano TiO<sub>2</sub>-cellulose coating makes cotton fabric self-cleaning, antibacterial and antifungal.

### **6.5 Mechanical and comfort Properties**

Coated cellulose provides additional strength to cotton fabric and hence tensile strength increased significantly after cellulose coating on the surface of cotton fabric. The comfort properties like air and water vapour permeability were hardly affected.

### **6.6 Dyeing**

Reactive Blue 49 dye showed better dyeability towards the coated cotton fabric compared with Reactive Red 240 or Reactive Yellow 95 dye. However, the decrease in the *K/S* values indicates that cellulose coating decreased the dye uptake by the fabric. The *L\** value increased in the case of cellulose-coated samples, meaning that cellulose coating increased the lightness of the cotton fabric. The fastness properties of both control and coated cotton fabrics against washing, rubbing, and perspiration were similar and good.



## CHAPTER 7

### APPLICATIONS AND FUTURE WORK

#### 7.0. Prologue

After the success of this coating method, it has opened new doors to coat nanoparticles on the surface of cotton fabric for various applications such as flame retardant, thermoregulatory, antifungal, antibacterial, self-cleaning etc. This chapter introduces to the reader the proposed application of cellulose-TiO<sub>2</sub> nanoparticles coated cotton fabric.

#### 7.1 Self-cleaning applications

This coating method can be commercialised to make cotton fabric self-cleaning. This method can be used in suiting, shirting, women wear etc. kind of garments for self-cleaning. The limitation of this method is, it need UV light to work as a self-cleaning and antibacterial. However, it works under normal light for antifungal application.



Figure 49. Cellulose-TiO<sub>2</sub> coated cotton fabric self-cleaning applications

#### 7.2 Stiffness application

This method easily can replace traditional starching method to make cotton fabric stiff permanently. Materials used for this method are not very expensive that is why this method is quite feasible and easy to commercialise. Cellulose coated cotton fabric can be used in garments such as mens's shirts, collar, sleeves, girls peticoates, ruffels. Some examples of application are shown in figure 50.



Figure 50. Stiff fabric applications.

### **7.3 Antibacterial and antifungal**

Cellulose-TiO<sub>2</sub> coated cotton fabric could be used for antibacterial and antifungal applications. Figure 51 shows some example of antibacterial and antifungal application. This coated fabric can be used in bed sheets, towel, undergarments products.



Figure 51. Antibacterial and antifungal applications of cellulose-TiO<sub>2</sub> coated cotton fabric.

#### 7.4 Future work

This work has endeavored to introduce new route to coat functional nanoparticles with cellulose on cotton fabric to the scientific community. Due to the scope of the task, the following is recommended for follow-up work.

1. Coating of Nano-clay with cellulose for fire retardant application.
2. Coating of copper nanoparticles for antimicrobial application.
3. Investigation the durability of cellulose-TiO<sub>2</sub> coated cotton fabric against UV light.
4. Investigation of superoxide radicals effect on mechanical properties of cotton fabric.

## REFERENCES

1. Ali, S., et al., *Cationic starch (Q-TAC) pre-treatment of cotton fabric: influence on dyeing with reactive dye*. Carbohydr Polym, 2015. **117**: p. 271-8.
2. Abidi, N., L. Cabrales, and E. Hequet, *Functionalization of a cotton fabric surface with titania nanosols: applications for self-cleaning and UV-protection properties*. ACS Appl Mater Interfaces, 2009. **1**(10): p. 2141-6.
3. Bae, G.Y., et al., *Superhydrophobicity of cotton fabrics treated with silica nanoparticles and water-repellent agent*. J Colloid Interface Sci, 2009. **337**(1): p. 170-5.
4. Boxun Leng, et al., *Superoleophobic Cotton Textiles*. Langmuir, 2009. **25**: p. 2456-2460.
5. Gupta, D. and M.L. Gulrajani, *Self cleaning finishes for textiles*. 2015: p. 257-281.
6. Meilert, K.T., D. Laub, and J. Kiwi, *Photocatalytic self-cleaning of modified cotton textiles by TiO<sub>2</sub> clusters attached by chemical spacers*. Journal of Molecular Catalysis A: Chemical, 2005. **237**(1-2): p. 101-108.
7. Daoud, W.A., J.H. Xin, and Y.-H. Zhang, *Surface functionalization of cellulose fibers with titanium dioxide nanoparticles and their combined bactericidal activities*. Surface Science, 2005. **599**(1-3): p. 69-75.
8. Wu, D. and M. Long, *Realizing visible-light-induced self-cleaning property of cotton through coating N-TiO<sub>2</sub> film and loading AgI particles*. ACS Appl Mater Interfaces, 2011. **3**(12): p. 4770-4.
9. Xu, F., et al., *A self-stiffness finishing for cotton fabric with N-methylmorpholine-N-oxide*. Cellulose, 2015. **22**(4): p. 2837-2844.
10. Nazari, A., et al., *Self-cleaning properties of bleached and cationized cotton using nanoTiO<sub>2</sub>: A statistical approach*. Carbohydrate Polymers, 2011. **83**(3): p. 1119-1127.
11. Xu, B., et al., *Self-cleaning cotton fabrics via combination of photocatalytic TiO<sub>2</sub> and superhydrophobic SiO<sub>2</sub>*. Surface and Coatings Technology, 2015. **262**: p. 70-76.
12. El-Rafie, H.M., et al., *Antibacterial and anti-inflammatory finishing of cotton by microencapsulation using three marine organisms*. International Journal of Biological Macromolecules, 2016. **86**: p. 59-64.

13. Shaheen, T.I., et al., *Durable antibacterial and UV protections of in situ synthesized zinc oxide nanoparticles onto cotton fabrics*. International Journal of Biological Macromolecules, 2016. **83**: p. 426-432.
14. Borkow, G. and J. Gabbay, *Biocidal textiles can help fight nosocomial infections*. Med Hypotheses, 2008. **70**(5): p. 990-4.
15. Kang, C.K., et al., *Antibacterial cotton fibers treated with silver nanoparticles and quaternary ammonium salts*. Carbohydr Polym, 2016. **151**: p. 1012-8.
16. Joost, U., et al., *Photocatalytic antibacterial activity of nano-TiO<sub>2</sub> (anatase)-based thin films: effects on Escherichia coli cells and fatty acids*. J Photochem Photobiol B, 2015. **142**: p. 178-85.
17. Banerjee, S., D.D. Dionysiou, and S.C. Pillai, *Self-cleaning applications of TiO<sub>2</sub> by photo-induced hydrophilicity and photocatalysis*. Applied Catalysis B: Environmental, 2015. **176-177**: p. 396-428.
18. Saif, M., et al., *Synthesis of highly active thin film based on TiO<sub>2</sub> nanomaterial for self-cleaning application*. Spectrochimica Acta Part A: Molecular and Biomolecular Spectroscopy, 2013. **112**: p. 46-51.
19. Shan, A.Y., T.I.M. Ghazi, and S.A. Rashid, *Immobilisation of titanium dioxide onto supporting materials in heterogeneous photocatalysis: A review*. Applied Catalysis A: General, 2010. **389**(1-2): p. 1-8.
20. Afzal, S., W.A. Daoud, and S.J. Langford, *Photostable self-cleaning cotton by a copper(II) porphyrin/TiO<sub>2</sub> visible-light photocatalytic system*. ACS Appl Mater Interfaces, 2013. **5**(11): p. 4753-9.
21. Styliidi, M., *Visible light-induced photocatalytic degradation of Acid Orange 7 in aqueous TiO<sub>2</sub> suspensions*. Applied Catalysis B: Environmental, 2004. **47**(3): p. 189-201.
22. Ryu, J., et al., *Photocatalytic nanocomposite thin films of TiO<sub>2</sub>-β-calcium phosphate by aerosol-deposition*. Catalysis Communications, 2009. **10**(5): p. 596-599.
23. Khataee, A.R., V. Vatanpour, and A.R. Amani Ghadim, *Decolorization of C.I. Acid Blue 9 solution by UV/Nano-TiO<sub>2</sub>, Fenton, Fenton-like, electro-Fenton and electrocoagulation processes: a comparative study*. J Hazard Mater, 2009. **161**(2-3): p. 1225-33.
24. Andronic, L. and A. Duta, *The influence of TiO<sub>2</sub> powder and film on the photodegradation of methyl orange*. Materials Chemistry and Physics, 2008. **112**(3): p. 1078-1082.



25. He, H.Y., *Comparison Study of Photocatalytic Properties of SrTiO<sub>3</sub> and TiO<sub>2</sub> Powders in Decomposition of Methyl Orange*. International Journal of Environmental Research 2009. **3**(1): p. 57-60.
26. Mai, F.D., et al., *Fabrication of porous TiO<sub>2</sub> film on Ti foil by hydrothermal process and its photocatalytic efficiency and mechanisms with ethyl violet dye*. J Hazard Mater, 2010. **177**(1-3): p. 864-75.
27. Wu, C.H., *Photodegradation of C.I. Reactive Red 2 in UV/TiO<sub>2</sub>-based systems: effects of ultrasound irradiation*. J Hazard Mater, 2009. **167**(1-3): p. 434-9.
28. Cappelletti, G., et al., *Photodegradation of Pollutants in Air: Enhanced Properties of Nano-TiO<sub>2</sub> Prepared by Ultrasound*. Nanoscale Res Lett, 2008. **4**(2): p. 97-105.
29. Jiang, X., et al., *Cotton fabric coated with nano TiO<sub>2</sub>-acrylate copolymer for photocatalytic self-cleaning by in-situ suspension polymerization*. Applied Surface Science, 2011. **257**(20): p. 8451-8456.
30. Doganli, G., et al., *Functionalization of cotton fabric with nanosized TiO<sub>2</sub> coating for self-cleaning and antibacterial property enhancement*. Journal of Coatings Technology and Research, 2015.
31. Peterson, E. and T. Dantzig, *Stiffness in fabrics produced by different starches and starch mixtures, and a quantitative method for evaluating stiffness*, in *Technical Bulletin* No. 108. 1929. p. 33.
32. Chen, Y., W.H. Kampen, and B.J. Collier, *Evaluation of CPI Starch for Laundry Application*. Textile Chemist & Colorist, 1998. **30**(11): p. 25-30.
33. Mukerjea, R., G. Slocum, and J.F. Robyt, *Determination of the maximum water solubility of eight native starches and the solubility of their acidic-methanol and -ethanol modified analogues*. Carbohydr Res, 2007. **342**(1): p. 103-10.
34. Yuan, Z., et al., *Fabrication of cellulose self-assemblies and high-strength ordered cellulose films*. Carbohydr Polym, 2015. **117**: p. 414-21.
35. Feese, E., et al., *Photobactericidal Porphyrin-Cellulose Nanocrystals: Synthesis, Characterization, and Antimicrobial Properties*. Biomacromolecules, 2011. **12**(10): p. 3528-3539.
36. Hashemikia, S., et al., *A novel cotton fabric with anti-bacterial and drug delivery properties using SBA-15-NH<sub>2</sub>/polysiloxane hybrid containing tetracycline*. Materials Science and Engineering: C, 2016. **59**: p. 429-437.

37. Wang, C., et al., *Cotton fabric with plasma pretreatment and ZnO/Carboxymethyl chitosan composite finishing for durable UV resistance and antibacterial property*. Carbohydrate Polymers, 2016. **138**: p. 106-113.
38. Khajavi, R. and A. Berendjchi, *Effect of dicarboxylic acid chain length on the self-cleaning property of Nano-TiO<sub>2</sub>-coated cotton fabrics*. ACS Appl Mater Interfaces, 2014. **6**(21): p. 18795-9.
39. Wu, D., et al., *Photocatalytic self-cleaning properties of cotton fabrics functionalized with p-BiOI/n-TiO<sub>2</sub> heterojunction*. Surface and Coatings Technology, 2014. **258**: p. 672-676.
40. Molgaard, S.L., et al., *Cellulose-nanofiber/polygalacturonic acid coatings with high oxygen barrier and targeted release properties*. Carbohydr Polym, 2014. **114**: p. 179-82.
41. Raeisi, M., et al., *Effect of carboxymethyl cellulose-based coatings incorporated with Zataria multiflora Boiss. essential oil and grape seed extract on the shelf life of rainbow trout fillets*. LWT - Food Science and Technology, 2015. **64**(2): p. 898-904.
42. Imran, M., et al., *Cellulose derivative based active coatings: Effects of nisin and plasticizer on physico-chemical and antimicrobial properties of hydroxypropyl methylcellulose films*. Carbohydrate Polymers, 2010. **81**(2): p. 219-225.
43. Grüneberger, F., et al., *Nanofibrillated cellulose in wood coatings: Dispersion and stabilization of ZnO as UV absorber*. Progress in Organic Coatings, 2015. **87**: p. 112-121.
44. Lavoine, N., I. Desloges, and J. Bras, *Microfibrillated cellulose coatings as new release systems for active packaging*. Carbohydr Polym, 2014. **103**: p. 528-37.
45. Klemm, D., et al., *Cellulose: fascinating biopolymer and sustainable raw material*. Angew Chem Int Ed Engl, 2005. **44**(22): p. 3358-93.
46. Ioelovich, M., *Study of Cellulose Interaction with Concentrated Solutions of Sulfuric Acid*. ISRN Chemical Engineering, 2012. **2012**: p. 1-7.
47. Gupta, K.M. and J. Jiang, *Cellulose dissolution and regeneration in ionic liquids: A computational perspective*. Chemical Engineering Science, 2015. **121**: p. 180-189.
48. Kimura, A., N. Nagasawa, and M. Taguchi, *Cellulose gels produced in room temperature ionic liquids by ionizing radiation*. Radiation Physics and Chemistry, 2014. **103**: p. 216-221.
49. Gao, Q., X. Shen, and X. Lu, *Regenerated bacterial cellulose fibers prepared by the NMMO·H<sub>2</sub>O process*. Carbohydrate Polymers, 2011. **83**(3): p. 1253-1256.

50. Shen, L., E. Worrell, and M.K. Patel, *Environmental impact assessment of man-made cellulose fibres*. Resources, Conservation and Recycling, 2010. **55**(2): p. 260-274.
51. Dupont, A.-L., *Cellulose in lithium chloride/N,N-dimethylacetamide, optimisation of a dissolution method using paper substrates and stability of the solutions*. Polymer, 2003. **44**(15): p. 4117-4126.
52. Jin, H., C. Zha, and L. Gu, *Direct dissolution of cellulose in NaOH/thiourea/urea aqueous solution*. Carbohydr Res, 2007. **342**(6): p. 851-8.
53. Australian, G., *The Biology of Gossypium hirsutum L. and Gossypium barbadense L. (cotton)*. Department of health and ageing office of the gene technology regulator, 2008. **2**: p. <http://www.ogtr.gov.au>.
54. <https://oecotextiles.wordpress.com/category/fibers/cotton-fibers/>.
55. Gao, A., et al., *Preparation of multi-functional cellulose containing huge conjugated system and its UV-protective and antibacterial property*. Carbohydr Polym, 2014. **114**: p. 392-8.
56. Ge, B., et al., *A graphene coated cotton for oil/water separation*. Composites Science and Technology, 2014. **102**: p. 100-105.
57. Jur, J.S., et al., *Atomic Layer Deposition of Conductive Coatings on Cotton, Paper, and Synthetic Fibers: Conductivity Analysis and Functional Chemical Sensing Using "All-Fiber" Capacitors*. Advanced Functional Materials, 2011. **21**(11): p. 1993-2002.
58. Bi, H., et al., *Carbon fiber aerogel made from raw cotton: a novel, efficient and recyclable sorbent for oils and organic solvents*. Adv Mater, 2013. **25**(41): p. 5916-21.
59. Dobircan, L., et al., *Wheat flour thermoplastic matrix reinforced by waste cotton fibre: Agro-green-composites*. Composites Part A: Applied Science and Manufacturing, 2009. **40**(4): p. 329-334.
60. Gan, L., et al., *Graphene nanoribbon coated flexible and conductive cotton fabric*. Composites Science and Technology, 2015. **117**: p. 208-214.
61. Nilghaz, A., et al., *Flexible microfluidic cloth-based analytical devices using a low-cost wax patterning technique*. Lab Chip, 2012. **12**(1): p. 209-18.
62. Zhukovskiy, M., et al., *Nanowire-functionalized cotton textiles*. ACS Appl Mater Interfaces, 2014. **6**(4): p. 2262-9.
63. <https://www.slideshare.net/ashmkumar/nano-finishes-in-textiles>. 2007.
64. Ensikat, H.J., et al., *Superhydrophobicity in perfection: the outstanding properties of the lotus leaf*. Beilstein J Nanotechnol, 2011. **2**: p. 152-61.



65. Zhang, M., et al., *Lotus effect in wetting and self-cleaning*. Biotribology, 2016. **5**: p. 31-43.
66. <https://futureprospects.wordpress.com/2010/05/17/the-lotus-effect/>.
67. Bhushan, B. and M. Nosonovsky, *Lotus Effect*, in *Encyclopedia of Nanotechnology*, B. Bhushan, Editor. 2012, Springer Netherlands: Dordrecht. p. 1224-1233.
68. Yamamoto, M., et al., *Theoretical Explanation of the Lotus Effect: Superhydrophobic Property Changes by Removal of Nanostructures from the Surface of a Lotus Leaf*. Langmuir, 2015. **31**(26): p. 7355-7363.
69. Yuranova, T., et al., *Self-cleaning cotton textiles surfaces modified by photoactive SiO<sub>2</sub>/TiO<sub>2</sub> coating*. Journal of Molecular Catalysis A: Chemical, 2006. **244**(1-2): p. 160-167.
70. Andrew Mills and S.-K. Lee, *A web-based overview of semiconductor photochemistry-based current commercial applications*. Journal of Photochemistry and Photobiology A: Chemistry, 2002. **152**: p. 233-247.
71. Mohammad, H., et al., *Anti-biofilm activity and synergism of novel thiazole compounds with glycopeptide antibiotics against multidrug-resistant staphylococci*. J Antibiot (Tokyo), 2015. **68**(4): p. 259-66.
72. Yuan, G. and R. Cranston, *Recent Advances in Antimicrobial Treatments of Textiles*. Textile Research Journal, 2008. **78**(1): p. 60-72.
73. Gillet, Y., et al., *Association between Staphylococcus aureus strains carrying gene for Panton-Valentine leukocidin and highly lethal necrotising pneumonia in young immunocompetent patients*. The Lancet, 2002. **359**(9308): p. 753-759.
74. David, M.Z. and R.S. Daum, *Community-associated methicillin-resistant Staphylococcus aureus: epidemiology and clinical consequences of an emerging epidemic*. Clin Microbiol Rev, 2010. **23**(3): p. 616-87.
75. Locke, J.B., et al., *Elevated linezolid resistance in clinical cfr-positive Staphylococcus aureus isolates is associated with co-occurring mutations in ribosomal protein L3*. Antimicrob Agents Chemother, 2010. **54**(12): p. 5352-5.
76. Thangamani, S., et al., *Antibacterial activity and mechanism of action of auranofin against multi-drug resistant bacterial pathogens*. Sci Rep, 2016. **6**: p. 22571.
77. Zhang, F., et al., *Application of silver nanoparticles to cotton fabric as an antibacterial textile finish*. Fibers and Polymers, 2009. **10**(4): p. 496-501.

78. Perelshtein, I., et al., *Sonochemical coating of silver nanoparticles on textile fabrics (nylon, polyester and cotton) and their antibacterial activity*. Nanotechnology, 2008. **19**(24): p. 245705.
79. Mishra, R., et al., *The production, characterization and applications of nanoparticles in the textile industry*. Textile Progress, 2014. **46**(2): p. 133-226.
80. Chen, S., et al., *Environmentally friendly antibacterial cotton textiles finished with siloxane sulfopropylbetaine*. ACS Appl Mater Interfaces, 2011. **3**(4): p. 1154-62.
81. Zhilong Shi, K. G. Neoh, and E.T. Kang, *Antibacterial and Adsorption Characteristics of Activated Carbon Functionalized with Quaternary Ammonium Moieties*. Industrial and Engineering Chemistry Research, 2007. **46**(2): p. 439-445.
82. Kawabata, A. and J.A. Taylor, *The effect of reactive dyes upon the uptake and antibacterial efficacy of poly(hexamethylene biguanide) on cotton. Part 3: Reduction in the antibacterial efficacy of poly(hexamethylene biguanide) on cotton, dyed with bis(monochlorotriazinyl) reactive dyes*. Carbohydrate Polymers, 2007. **67**(3): p. 375-389.
83. Ren, X., et al., *Antimicrobial efficacy and light stability of N-halamine siloxanes bound to cotton*. Cellulose, 2008. **15**(4): p. 593-598.
84. El-Shafei, A.M., et al., *Antibacterial activity of cationically modified cotton fabric with carboxymethyl chitosan*. Journal of Applied Polymer Science, 2008. **110**(3): p. 1289-1296.
85. Yu-Bin Chang, et al., *A study on chitosan modification of polyester fabrics by atmospheric pressure plasma and its antibacterial effects*. Fibers and Polymers, 2008. **9**(3): p. 307-311.
86. Orhan, M., D. Kut, and C. Gunesoglu, *Improving the antibacterial activity of cotton fabrics finished with triclosan by the use of 1,2,3,4-butanetetracarboxylic acid and citric acid*. Journal of Applied Polymer Science, 2009. **111**(3): p. 1344-1352.
87. Simoncic, B. and B. Tomsic, *Structures of Novel Antimicrobial Agents for Textiles - A Review*. Textile Research Journal, 2010. **80**(16): p. 1721-1737.
88. Russell, A.D., *Bacterial adaptation and resistance to antiseptics, disinfectants and preservatives is not a new phenomenon*. J Hosp Infect, 2004. **57**(2): p. 97-104.
89. Xiao fei liu, et al., *Antibacterial action of chitosan and carboxymethylated chitosan*. Journal of Applied Polymer Science, 2001. **79**: p. 1324-1335.

90. Darbari, S., et al., *Investigating the antifungal activity of TiO<sub>2</sub> nanoparticles deposited on branched carbon nanotube arrays*. Journal of Physics D: Applied Physics, 2011. **44**(24): p. 245401.
91. Gittard, S.D., et al., *Antifungal Textiles Formed Using Silver Deposition in Supercritical Carbon Dioxide*. Journal of Materials Engineering and Performance, 2009. **19**(3): p. 368-373.
92. Simona Strnad, et al., *Antifungal activity assessment of cotton fabrics using image processing and analysis*. FIBRES & TEXTILES in Eastern Europe 2010. **18**(83): p. 86-90.
93. Zyska, B., *A short history of investigations of microbial biodeterioration in Poland, 1875–2002*. International Biodeterioration & Biodegradation, 2004. **53**(3): p. 145-150.
94. Anita Pal, Rakesh Kumar, and Y.C. Tripathi, *Antifungal activity of natural colourant from melia composita bark and its application in functional textile finishing*. International Journal of Pharmacy and Pharmaceutical Sciences, 2016. **8**(5): p. 387-391.
95. Xu, W., et al., *Synthesis of cationic core-shell fluorine-containing polyacrylate soap-free latex and its application on cotton substrate*. Fibers and Polymers, 2013. **14**(6): p. 895-903.
96. Pablo del Pino, Scott G. Mitchell, and B. Pelaz, *Design and Characterization of Functional Nanoparticles for Enhanced Bio-performance*. Methods in Molecular Biology 2013. **1051**: p. 165-207.
97. Palza, H., *Antimicrobial polymers with metal nanoparticles*. Int J Mol Sci, 2015. **16**(1): p. 2099-116.
98. Weir, A., et al., *Titanium Dioxide Nanoparticles in Food and Personal Care Products*. Environmental science & technology, 2012. **46**(4): p. 2242-2250.
99. Nolan, N.T., M.K. Seery, and S.C. Pillai, *Spectroscopic Investigation of the Anatase-to-Rutile Transformation of Sol–Gel-Synthesized TiO<sub>2</sub> Photocatalysts*. The Journal of Physical Chemistry C, 2009. **113**(36): p. 16151-16157.
100. <http://ruby.colorado.edu/~smyth/min/tio2.html>.
101. Yi Hu, H.-L. Tsai, and C.-L. Huang, *Effect of brookite phase on the anatase–rutile transition in titania nanoparticles*. Journal of the European Ceramic Society, 2003. **23**: p. 691-696.
102. Auvinen, S., et al., *Refractive Index Functions of TiO<sub>2</sub> Nanoparticles*. The Journal of Physical Chemistry C, 2013. **117**(7): p. 3503-3512.

103. foundation, T.w., *Uses of titanium dioxide*. RSC Advances p. 1-5.
104. Pelaez, M., et al., *A review on the visible light active titanium dioxide photocatalysts for environmental applications*. Applied Catalysis B: Environmental, 2012. **125**: p. 331-349.
105. Wang, R., et al., *Light-induced amphiphilic surfaces*. Nature, 1997. **388**(6641): p. 431-432.
106. Akira Nakajima, et al., *Effect of repeated photo-illumination on the wettability*. Journal of Photochemistry and Photobiology A: Chemistry 2001. **146**: p. 129-132.
107. Akira Nakajima, et al., *Photoinduced Amphiphilic Surface on Polycrystalline*. Langmuir, 2000. **16**: p. 7048-7050.
108. Zhang, R., et al., *Antifouling membranes for sustainable water purification: strategies and mechanisms*. Chem Soc Rev, 2016. **45**(21): p. 5888-5924.
109. Matsunaga, T. and M. Okochi, *TiO<sub>2</sub>-mediated photochemical disinfection of escherichia coli using optical fibers*. Environmental Science and Technology, 1995. **29**: p. 501-505.
110. Koizumi, Y. and M. Taya, *Kinetic evaluation of biocidal activity of titanium dioxide against phage MS2 considering interaction between the phage and photocatalyst particles*. Biochemical Engineering Journal, 202. **12**: p. 107-116.
111. Park, D., et al., *Inactivation efficiency and mechanism of UV-TiO<sub>2</sub> photocatalysis against murine norovirus using a solidified agar matrix*. Int J Food Microbiol, 2016. **238**: p. 256-264.
112. Gentile, G.J. and M.M. Fidalgo de Cortalezzi, *Enhanced retention of bacteria by TiO<sub>2</sub> nanoparticles in saturated porous media*. J Contam Hydrol, 2016. **191**: p. 66-75.
113. De Filipo, G., et al., *Gellan gum/titanium dioxide nanoparticle hybrid hydrogels for the cleaning and disinfection of parchment*. International Biodeterioration & Biodegradation, 2015. **103**: p. 51-58.
114. Kühn, K.P., et al., *Disinfection of surfaces by photocatalytic oxidation with titanium dioxide and UVA light*. Chemosphere, 2003. **53**(1): p. 71-77.
115. Maness, P.-c., et al., *Bactericidal activity of photocatalytic TiO<sub>2</sub> reaction toward an understanding of its killing mechanism*. Applied and Environmental Microbiology, 1999. **65**: p. 4094-4098.
116. Xu, Q., et al., *Facile synthesis of casein-based TiO<sub>2</sub> nanocomposite for self-cleaning and high covering coatings: Insights from TiO<sub>2</sub> dosage*. Progress in Organic Coatings, 2016. **99**: p. 223-229.

117. Long, M., et al., *Photocatalytic self-cleaning cotton fabrics with platinum (IV) chloride modified TiO<sub>2</sub> and N-TiO<sub>2</sub> coatings*. Applied Surface Science, 2016. **386**: p. 434-441.
118. Sangchay, W., *The Self-cleaning and Photocatalytic Properties of TiO<sub>2</sub> Doped with SnO<sub>2</sub> Thin Films Preparation by Sol-gel Method*. Energy Procedia, 2016. **89**: p. 170-176.
119. Wijesena, R.N., et al., *Slightly carbomethylated cotton supported TiO<sub>2</sub> nanoparticles as self-cleaning fabrics*. Journal of Molecular Catalysis A: Chemical, 2015. **398**: p. 107-114.
120. Gupta, D. and M.L. Gulrajani, *8 - Self cleaning finishes for textiles A2 - Paul, Roshan*, in *Functional Finishes for Textiles*. 2015, Woodhead Publishing. p. 257-281.
121. Smits, M., et al., *Photocatalytic degradation of soot deposition: Self-cleaning effect on titanium dioxide coated cementitious materials*. Chemical Engineering Journal, 2013. **222**: p. 411-418.
122. A. Bule'on a, et al., *Starch granules: structure and biosynthesis*. International Journal of Biological Macromolecules, 1998. **23**: p. 85-112.
123. W Vorwerg, S Radosta, and E. Leibnitz, *Study of a preparative-scale process for the production of amylose*. 2002. **47**(2): p. 181-189.
124. Jeng-Yune Li and A.-I. Yeh, *Relationships between thermal, rheological characteristics and swelling power for various starches*. Journal of Food Engineering, 2001. **50**(3): p. 141-148.
125. Copeland, L., et al., *Form and functionality of starch*. Food Hydrocolloids, 2009. **23**(6): p. 1527-1534.
126. George W. Huber , Sara Iborra , and A. Corma, *Synthesis of Transportation Fuels from Biomass: Chemistry, Catalysts, and Engineering*. Chemical Reviews 2006. **106**: p. 4044-4098.
127. Carlson, T.R., T.P. Vispute, and G.W. Huber, *Green gasoline by catalytic fast pyrolysis of solid biomass derived compounds*. ChemSusChem, 2008. **1**(5): p. 397-400.
128. Fukaya, Y., et al., *Cellulose dissolution with polar ionic liquids under mild conditions: required factors for anions*. Green Chem., 2008. **10**(1): p. 44-46.
129. Bobleter, O., *Hydrothermal degradation of polymers derived from plants*. Progress in Polymer Science, 1994. **19**(5): p. 797-841.
130. Meng, Y., Z. Pang, and C. Dong, *Enhancing cellulose dissolution in ionic liquid by solid acid addition*. Carbohydrate Polymers, 2017. **163**: p. 317-323.
131. *hyatt*. 1880, Google Patents.

132. Liebert, T., *Cellulose Solvents – Remarkable History, Bright Future*. 2010. **1033**: p. 3-54.
133. Y.-H. Percival Zhang , et al., *A Transition from Cellulose Swelling to Cellulose Dissolution by o-Phosphoric Acid: Evidence from Enzymatic Hydrolysis and Supramolecular Structure*. *Biomacromolecules*, 2006. **7**: p. 644-648.
134. Jiang, F., A.R. Esker, and M. Roman, *Acid-Catalyzed and Solvolytic Desulfation of H<sub>2</sub>SO<sub>4</sub>-Hydrolyzed Cellulose Nanocrystals*. *Langmuir*, 2010. **26**(23): p. 17919-17925.
135. Hasani, M., et al., *Cationic surface functionalization of cellulose nanocrystals*. *Soft Matter*, 2008. **4**(11): p. 2238-2244.
136. Kumar, A., et al., *Characterization of Cellulose Nanocrystals Produced by Acid-Hydrolysis from Sugarcane Bagasse as Agro-Waste*. *Journal of Materials Physics and Chemistry*, 2014. **2**(1): p. 1-8.
137. Sofla, M.R.K., et al., *A comparison of cellulose nanocrystals and cellulose nanofibres extracted from bagasse using acid and ball milling methods*. *Advances in Natural Sciences: Nanoscience and Nanotechnology*, 2016. **7**(3): p. 035004.
138. Mascheroni, E., et al., *Comparison of cellulose nanocrystals obtained by sulfuric acid hydrolysis and ammonium persulfate, to be used as coating on flexible food-packaging materials*. *Cellulose*, 2016. **23**(1): p. 779-793.
139. Dumanli, A.G., et al., *Digital Color in Cellulose Nanocrystal Films*. *ACS Applied Materials & Interfaces*, 2014. **6**(15): p. 12302-12306.
140. Ingvar, V.J., *Method of starching fabrics*. 1954, Google Patents.
141. Tang, X.N., et al., *Digitally quantifying cerebral hemorrhage using Photoshop and Image J*. *J Neurosci Methods*, 2010. **190**(2): p. 240-3.
142. Schneider, C.A., W.S. Rasband, and K.W. Eliceiri, *NIH Image to ImageJ: 25 years of image analysis*. *Nat Meth*, 2012. **9**(7): p. 671-675.
143. <https://imagej.nih.gov/ij/docs/index.html>.
144. Fridrichová, L., *A new method of measuring the bending rigidity of fabrics and its application to the determination of their anisotropy*. *Textile Research Journal*, 2013. **83**(9): p. 883-892.
145. Naujokaitytė L, Strazdiene E, and F. L, *Comparative Analysis of Fabrics' Bending Behavior Testing Methods*. *Journal Textile Clothing and Technology* 2007. **6**: p. 343-349.

146. Wiegand, C., et al., *In vitro assessment of the antimicrobial activity of wound dressings: influence of the test method selected and impact of the pH*. J Mater Sci Mater Med, 2015. **26**(1): p. 5343.
147. ISO, *Testing of textiles. Evaluation of the action of microfungi*. 2003.
148. Xu, M., et al., *How to decrease the viscosity of suspension with the second fluid and nanoparticles?* Sci Rep, 2013. **3**: p. 3137.
149. French, A.D., *Idealized powder diffraction patterns for cellulose polymorphs*. Cellulose, 2013. **21**(2): p. 885-896.
150. Nam, S., et al., *Segal crystallinity index revisited by the simulation of X-ray diffraction patterns of cotton cellulose Ibeta and cellulose II*. Carbohydr Polym, 2016. **135**: p. 1-9.
151. Yue, Y., et al., *Characterization of cellulose I/II hybrid fibers isolated from energycane bagasse during the delignification process: Morphology, crystallinity and percentage estimation*. Carbohydr Polym, 2015. **133**: p. 438-47.
152. Cook, J.G., *Handbook of Textile Fibres, Natural fibers*. 1984, Merrow, Cambridge: Woodhead Publishing. 240.



## LIST OF RELATED PUBLICATIONS IN IMPACT FACTOR JOURNALS

- **Kale B.M.**, Wiener J., Militky J., Rwawiire S., Mishra R., Jacob I.K., Wang Y. Coating of Cellulose-TiO<sub>2</sub> nanoparticles on cotton fabric for Photo-catalytic self-cleaning and permanent stiffness, Carbohydrate polymers, 2016, 150:107–113.  
[Impact factor = 4.21]
- **Kale B.M.**, Wiener J., Militky J., Mishra R., Rwawiire S., Jabbar A. Dyeing and stiffness characteristics of cellulose coated cotton Fabric, Cellulose, 2016, 23:981-992.  
[Impact factor = 3.19]
- **Kale B.M.**, Wiener J., Militky J., Maqsood S.H. Effect of Cellulose Coating on Properties of Cotton Fabric, Materials Science Forum, 2016, 860:81-84.  
[Impact factor = 0.28]
- **Kale B.M.**, Wiener J., Rwawiire S., Militky J., Development of Photocatalytic Self-Cleaning Cotton Fabric, Material Science Forum, 2016, 866:171-175.  
[Impact factor = 0.28]
- **Kale B.M.**, Wiener J., Militky J., Rwawiire S., Jabbar A., Multifunctional cotton fabric with Nano TiO<sub>2</sub> loaded cellulose, Carbohydrate polymers, under review- CARBPOL-D-16-03418.  
[Impact factor = 4.21]

## INTERNATIONAL CONFERENCES

1. **Kale B.M.**, Wiener J., Rwawiire S., Militky J. Development of Photocatalytic Self-Cleaning Cotton Fabric, ICCEMS 2016, Singapore.
2. **Kale B. M.**, Wiener J., Rwawiire S., Militky J. Antibacterial and Self-cleaning Cotton Fabric by Nano TiO<sub>2</sub>-cellulose Coating, Nanocon, 2016, Brno, Czech Republic
3. **Kale B. M.**, Vijay B., Wiener J., Militky J., Ludmilla F. Novel method to improve stiffness of cotton fabric permanently, ICNF, 2015, Azores, Portugal.
4. **Kale B.M.**, Wiener J., Militky J. Use of cellulose solution as a stiffener for cotton fabric, ICTN, 2014, IIT Delhi, India.
5. **Kale B.M.**, Wiener J., Militky J. Novel method to produce high stiffness cotton fabric, Strutex, 2014, Liberec, Czech Republic.